

University of Alberta

Comparison of Recoverable Reserves Estimation Techniques

by

Deepak Bhandari



A thesis submitted to the Faculty of Graduate Studies and Research
in partial fulfillment of the requirements for the degree of

Master of Science
in
Mining Engineering

Department of Civil and Environmental Engineering

Edmonton, Alberta, Canada

Fall 2007



Library and
Archives Canada

Bibliothèque et
Archives Canada

Published Heritage
Branch

Direction du
Patrimoine de l'édition

395 Wellington Street
Ottawa ON K1A 0N4
Canada

395, rue Wellington
Ottawa ON K1A 0N4
Canada

Your file *Votre référence*
ISBN: 978-0-494-33200-9
Our file *Notre référence*
ISBN: 978-0-494-33200-9

NOTICE:

The author has granted a non-exclusive license allowing Library and Archives Canada to reproduce, publish, archive, preserve, conserve, communicate to the public by telecommunication or on the Internet, loan, distribute and sell theses worldwide, for commercial or non-commercial purposes, in microform, paper, electronic and/or any other formats.

The author retains copyright ownership and moral rights in this thesis. Neither the thesis nor substantial extracts from it may be printed or otherwise reproduced without the author's permission.

AVIS:

L'auteur a accordé une licence non exclusive permettant à la Bibliothèque et Archives Canada de reproduire, publier, archiver, sauvegarder, conserver, transmettre au public par télécommunication ou par l'Internet, prêter, distribuer et vendre des thèses partout dans le monde, à des fins commerciales ou autres, sur support microforme, papier, électronique et/ou autres formats.

L'auteur conserve la propriété du droit d'auteur et des droits moraux qui protègent cette thèse. Ni la thèse ni des extraits substantiels de celle-ci ne doivent être imprimés ou autrement reproduits sans son autorisation.

In compliance with the Canadian Privacy Act some supporting forms may have been removed from this thesis.

Conformément à la loi canadienne sur la protection de la vie privée, quelques formulaires secondaires ont été enlevés de cette thèse.

While these forms may be included in the document page count, their removal does not represent any loss of content from the thesis.

Bien que ces formulaires aient inclus dans la pagination, il n'y aura aucun contenu manquant.


Canada

Abstract

Quantity and grade of recoverable reserves must be known before execution of any mining project. There are different geostatistical techniques available for the estimation of recoverable reserves, based on the type of information available about the domain of interest. These different geostatistical methods have their own drawbacks, benefits and applicability.

This thesis reviews some of the widely used techniques for recoverable reserves estimation, i.e. ordinary kriging, indicator kriging and simulation (SGS). The thesis includes the application and comparison of panel-wise estimation results of these methods to the setup reference results. The comparison of these methods is based on bias and different error criterions (mean error, mean squared error and mean absolute error). The results show simulation (SGS) as better estimation technique than ordinary kriging and indicator kriging techniques if the data (blasthole and exploration data) are unbiased.

Acknowledgements

I would like to extend my thanks and appreciation to the members of the **Centre for Computational Geostatistics (CCG)** at the University of Alberta for providing a cosmopolitan and friendly environment for learning and knowledge sharing. I would especially like to express my gratitude to **Dr. Clayton V. Deutsch** for his motivation and guidance as a Guru.

I dedicate this thesis to my family. To my father **Ashok Kumar Bhandari**, mother **Sita Bhandari** and wife **Soniya** for their love and encouragement that keep me focus over my goals. To my brother **Amit** and sister **Jyoti** for their moral support.

I am also thankful to the **Placer Dome** for providing the data used in Chapter 4 and allowed the results to be published.

Finally, I would like to thank all others who have touched my life and helped form the person I am today.

Table of Contents

1 Introduction	1
1.1 Background.	3
1.2 Stationarity and Spatial Variability.	4
1.3 Volume Variance Relation.	5
1.4 Estimation Methods.	7
1.4.1 Discrete Gaussian Method.	7
1.4.2 Ordinary Kriging.	7
1.4.3 Indicator Kriging.	9
1.4.4 Simulation.	9
1.5 Goodness of Prediction.	10
1.5.1 Cross Validation.	10
1.5.2 Accuracy Plot.	11
1.6 Thesis Outline.	11
2 Methodology	12
1.1 Comparative Study.	13
1.2 Reference Results.	13
1.3 Calculation of Ore Grade and Quantity for Panels.	13
1.4 Comparison.	18
3 Comparative Case Study – A Synthetic Example	20
3.1 Data.	20
3.2 Parameters and Criterion for Comparative Study.	22
3.3 Variography Analysis.	23
3.4 Reference Results.	25
3.5 Change of Support.	26
3.6 Ordinary Kriging.	27
3.7 Indicator Kriging.	29
3.8 Simulation.	30
3.9 Comparison.	33
4 Comparative Case Study – A Real Data Example	38
4.1 Data.	38
4.2 Parameters and Criterion for Comparative Study.	43
4.3 Variography Analysis.	44
4.4 Reference Results.	48
4.5 Ordinary Kriging.	49
4.6 Indicator Kriging.	51

4.7 Simulation.	53
4.8 Comparison.	56
5 Conclusion and Future Work	67
5.1 Conclusion.	67
5.2 Future Work.. . . .	68
Bibliography	69
Appendix I	71
Appendix II	73
Appendix III	76
Appendix IV	80

List of Tables

3.1	Proportion/quantity comparison.	34
3.2	Grade comparison.	34
4.1	Ore-tonnage Comparison.	58
4.2	Gold equivalent grade Comparison.	58
4.3	Gold quantity (Kg) Comparison.	58
4.4	Gold grade Comparison.	58
4.5	Silver quantity (Kg) Comparison.	58
4.6	Silver grade Comparison.	58

List of Figures

1.1	Selective mining unit (SMU) in a panel.	2
1.2	Selective mining unit (SMU) selection.	3
1.3	Variance decreases as the volume increases due to the averaging out of high and low values.	5
1.4	Schematic diagram of accuracy plot.	11
2.1	Schematic scatter-plot of the true versus estimates.	12
2.2	Schematic diagram for calculating grade and quantity of ore for a panel. . .	17
2.3	Schematic diagram of ore grade and quantity comparison at panel scale on scatter-plot.	18
3.1	Synthetic data at 1m × 1m spacing.	21
3.2	Sampled blasthole data from synthetic data.	21
3.3	Sampled exploration data from synthetic data.	21
3.4	QQ-plot between blasthole data and exploration data distribution.	22
3.5	Cell declustering of exploration data.	22
3.6	Variogram map for blasthole data.	23
3.7	Variogram map for exploration data (a) original data (b) normal scored data..	23
3.8	Reference model at 5m × 5m grid interval..	25
3.9	Cross validation results for ordinary kriging of blasthole data for reference results.	26
3.10	Grade-tonnage comparison for discrete Gaussian model and ordinary kriging models (a) Ordinary kriging with 9 data (b) Ordinary kriging with 3 data. . .	26
3.11	Ordinary kriging estimates at 5m × 5m grid interval.	27
3.12	Cross validation results for ordinary kriging of exploration data.	27
3.13	Ordinary kriging estimates at 5m × 5m grid interval.	28
3.14	Cross validation results for ordinary kriging of exploration data.	28
3.15	Ordinary kriging estimates at 5m × 5m grid interval.	29
3.16	Cross validation results for ordinary kriging of exploration data.	29
3.17	Indicator kriging estimates at 5m × 5m grid interval.	30
3.18	Accuracy plot from cross validation results of indicator kriging using exploration data.	30
3.19	Block-averaged 50 realizations statistics and plotted one of the realizations. .	31
3.20	Reproduction of variograms from 50 realizations generated by SGS at 1m × 1m grid interval. (a) principal direction (b) perpendicular direction. . .	31
3.21	Reproduction of histograms from 50 realizations generated by SGS at 1m × 1m grid interval.	31
3.22	Block-averaged 50 realizations statistics and plotted one of the realizations. .	32

3.23	Reproduction of variograms from 50 realizations generated by SGS at 1m × 1m grid interval. (a) principal direction (b) perpendicular direction.	32
3.24	Reproduction of histograms from 50 realizations generated by SGS at 1m × 1m grid interval.	32
3.25	Comparison of ordinary kriging (Case 1) with reference results (a) proportion (b) grade.	35
3.26	Comparison of ordinary kriging (Case 2) with reference results (a) proportion (b) grade.	35
3.27	Comparison of ordinary kriging (Case 3) with reference results (a) proportion (b) grade.	35
3.28	Comparison of indicator kriging with reference results (a) proportion (b) grade.	36
3.29	Comparison of SGS (Case 1) with reference results (a) proportion (b) grade.	36
3.30	Comparison of SGS (Case 2) with reference results (a) proportion (b) grade.	36
3.31	Error variograms for ordinary kriging comparison with reference results (a) proportion (b) grade.	37
3.32	Error variograms for indicatory kriging comparison with reference results (a) proportion (b) grade.	37
3.33	Error variograms for SGS comparison with reference results (a) proportion (b) grade.	37
4.1	Location of blasthole (light dots) and exploration data (dark dots) (a) all the data (b) exploration data with a constrained search of 7m from blast hole data.	39
4.2	Histogram plots of gold and silver grades of blasthole data.	39
4.3	Cell declustering of gold and silver grades of blasthole data with a cell size of 25m.	39
4.4	Histogram plots of gold and silver grades of exploration data.	40
4.5	Cell declustering of gold (cell size 195m) and silver grades (cell size 295m) of exploration data.	40
4.6	Histogram plots of exploration data that are in close proximity (7m radius) of blasthole data for both gold and silver grades.	41
4.7	Cell-declustering of gold (cell size 182m) and silver grades (cell size 197.5m) of exploration data that are in close proximity (7m radius) of blasthole data.	41
4.8 (a)	QQ-plot of all blasthole and exploration data.	42
4.8 (b)	QQ-plot of all blasthole data and exploration data that are in close proximity (7m radius) of blast-hole data.	42
4.9	Variogram maps for real data. (a) gold blasthole data (b) silver blasthole data (c) gold exploration data (d) silver exploration data (e) normal scored gold exploration data (f) normal scored silver exploration data.	47
4.10	Reference model at SMU scale for (a) gold and (b) silver.	48
4.11	Cross validation results of ordinary kriging used to setup the reference models.	49
4.12	Relation between variance and number of data for ordinary kriging estimation. (a) gold and (b) silver grade estimation.	49

4.13	Ordinary kriging at SMU scale using exploration data for (a) gold and (b) silver grade estimation.	50
4.14	Cross validation results of ordinary kriging estimation using exploration data.	51
4.15	Indicator kriging at SMU scale using exploration data for (a) gold and (b) silver grade estimation.	52
4.16	Accuracy plot from cross validation results of indicator kriging.	52
4.17	Variogram and histogram reproduction of 25 simulated realizations (Case 1) (a) gold (b) silver.	54
4.18	Variogram and histogram reproduction of 25 simulated realizations (Case 2) (a) gold (b) silver.	55
4.19	Scatter-plot comparison of ordinary kriging and reference results at panel scale (ore quantity, gold equivalent grade, gold and silver quantities, gold and silver grades).	59
4.20	Error variograms for ordinary kriging.	60
4.21	Scatter-plot comparison of indicator kriging and reference results at panel scale (ore quantity, gold equivalent grade, gold and silver quantities, gold and silver grades).	61
4.22	Error variograms for indicator kriging.	62
4.23	Scatter-plot comparison of SGS (Case 1) and reference results at panel scale (ore quantity, gold equivalent grade, gold and silver quantities, gold and silver grades).	63
4.24	Error variograms for SGS (Case 1)..	64
4.25	Scatter-plot comparison of SGS (Case 2) and reference results at panel scale (ore quantity, gold equivalent grade, gold and silver quantity, gold and silver grade)..	65
4.26	Error variograms for SGS (Case 2)..	66

List of Symbols and Abbreviations

\cdot	point support volume
\forall	whatever
A	domain/deposit support volume
BLUE	best linear unbiased estimator
cdf	cumulative distribution function
$Cov(0)$	covariance function at zero lag
$Cov(\mathbf{h})$	covariance function at lag \mathbf{h}
$Cov\{z, z^*\}$	covariance between z and z^*
CV	coefficient of variation
$D^2(v, V)$	dispersion variance of smaller blocks v within larger blocks V
$E\{Z\}$	expected value or mean of Z
$\exp(\mathbf{h})$	exponential semivariogram model, a function of separation vector \mathbf{h}
$F(\mathbf{u}; z)$	cumulative distribution function of random variable $Z(\mathbf{u})$
f	variance correction factor
$\gamma(\mathbf{h})$	semivariogram function at lag \mathbf{h}
$\bar{\gamma}(V, v)$	average variogram between domains V and v
$G_V^*(z_c)$	panel grade at cutoff grade z_c
\mathbf{h}	distance vector
λ_j	weight assigned to sample j
MAE	mean absolute error
ME	mean error
MSE	mean squared error
m	mean value
μ	lagrange parameter
$P_V^*(z_c)$	proportion of ore in a panel above cutoff grade z_c
Q-Q plot	quantile-quantile plot
$Q_V(z_c)$	quantity of metal above cutoff grade z_c
$R(\mathbf{u})$	random residual at \mathbf{u}
rf	recovery factor
σ^2	variance
SGS	sequential Gaussian simulation
SMU	selective mining unit
s	specific gravity
$sph(\mathbf{h})$	spherical semivariogram model, a function of separation vector \mathbf{h}

$T_V^*(z_c)$	ore quantity-tonnage in a panel above cutoff grade z_c
\mathbf{u}	location in space
V	large block support volume/panel volume
$Var\{Z\}$	variance of Z
v	small block support volume/SMU volume
$Z(\mathbf{u})$	random variable at location \mathbf{u}
z	true/reference value
z^*	estimated value
z_c	cutoff value

Chapter 1

Introduction

Mining is a primary industry, where the ore is taken out from the earth crust. Economy is the most important parameter for any industry to survive, therefore extraction of ore from the deposit economically is known as mining. The mining is divided in five phases (1) reconnaissance & prospecting, (2) exploration, (3) development, (4) exploitation and (5) reclamation. The site selection, general survey and preliminary samples of ore and rocks are collected in the first phase. The detailed exploration using core drilling, core logging and assaying is done in the second phase. Using these exploration data, the recoverable ore reserves estimation is done. The decisions of feasibility and investments are taken on the basis of these two steps and the economics of calculated reserves. The development of the deposit to extract the ore is done in the third phase, conventionally by drilling and blasting techniques. The blasthole data information is collected in the third and the fourth phases of mining. Finally reclamation is done after the exhaustion of the ore deposit or simultaneously with the fourth phase.

The calculation of recoverable reserves is one of the most critical factors in economic evaluation and investment decision making in the mining industry. There are various geostatistical techniques available to estimate recoverable reserves. These techniques give estimates of grade at the locations of interest using data and technical parameters. Different estimation techniques give different estimates. These reserve estimates are based on prediction of the physical characteristics of a mineral deposit through analysis of the data, modeling the size, shape and grade of the deposit. The sample information consists of [2]:

- physical samples from trenching, pitting, channel sampling and detailed exploration drilling,
- measurement of the grade of mineral in the samples by assaying or other measures,
- direct observations from geological/structural mapping and drill core logging, and
- secondary information such as seismic, other physical contents in the samples etc.

Collection and compilation of geological and assay information goes on during reconnaissance, prospecting and detailed exploration of the area of interest. The

geological information includes mainly the information about geological features, formation of deposit, host rock, extent of mineralization, zones for detailed exploration, type of drilling for exploration. The assay information includes typically the grade of samples collected especially from core logging, location and size of the collected samples.

While collecting sample data from the field and core logging, it is likely that some samples will have very high assay values and some will have very low assay values. This causes a distribution of high variance when the samples are at point scale or very small scale. When compositing, high grades are averaged with low or medium grade material causing the variance to go down. So, the distribution of grades in a deposit is sensitive to the size of samples.

The physical limit of the deposit A is generally defined on the basis of available geological information and legal issues related to land, environment and public.

The selection of reserves estimation technique is critical and subjective, depending on the available information, physical characteristics of the deposit, the variability of grade distribution, the amount of money and time available for estimation. Different estimation techniques have their own assumptions and constraint criterions.

The estimated reserve models are either deterministic or probabilistic type [14]. Deterministic models have a single estimate for location of interest. In the case of probabilistic models we get a set of possible values with corresponding probabilities. These possible values quantify uncertainty at the location of interest.

In estimated models, selective mining unit (SMU) is a common term used. A selective mining unit (SMU) is the smallest practical unit of volume selected at the time of mining [1]. It can also be defined as the smallest production unit, where ore and waste classification is possible. The SMU is usually considered as a rectangular volume for ease in numerical computations (Figure 1.1) and work in the field. The size of SMU has an impact on the variability of the grade distribution. Small SMUs give more variability in grade distribution, whereas large SMUs give less variability in grade distribution.

In an open pit operation, the SMU could be the volume of influence of two to four blastholes [1]. SMU size is not necessarily the same in reserves estimation as when mining. During mining, the important criterion for SMU size selection is the size of equipment used for excavation, size and shape of the ore body, whereas in reserves estimation the important criterion for SMU size selection is the accuracy in assessment of the estimates.

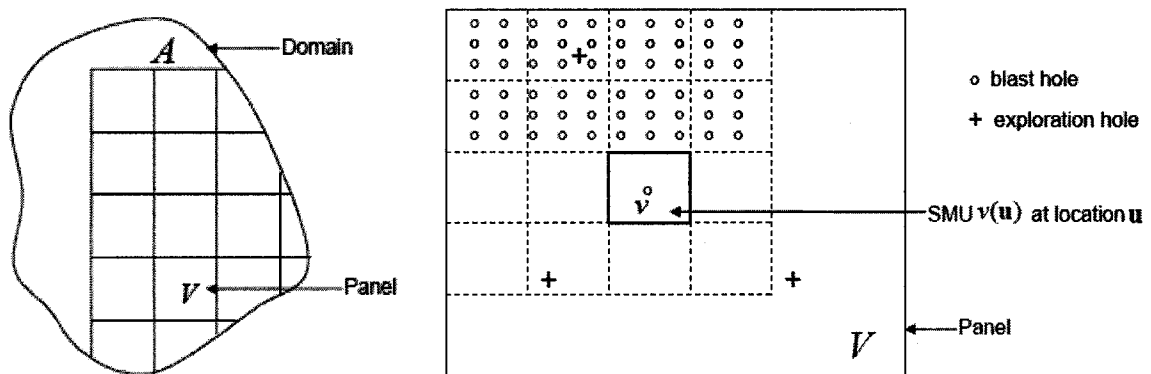


Figure 1.1: Selective mining unit (SMU) in a panel [1].

In both open pit and underground mining operations the whole domain A is divided in panels V for development and exploitation of the ore deposit. The panel size can be decided by the production capacity, type of equipments and demand. For ease in boundary definition, computation and work, panel shape is taken as rectangular. The panel size can be taken as the excavation of a month to a quarter of the year. The domain (A) consists of panels (V) and panel consists of SMUs (v) ($v \subset V \subset A$).

While considering selectivity of mining, the SMU size has an impact on total cost of production. Total mining cost is a function of the ore processing cost, the mining cost and the SMU size (Figure 1.2). As the SMU size increases the overall cost of mining should decrease and the ore processing cost should increase.

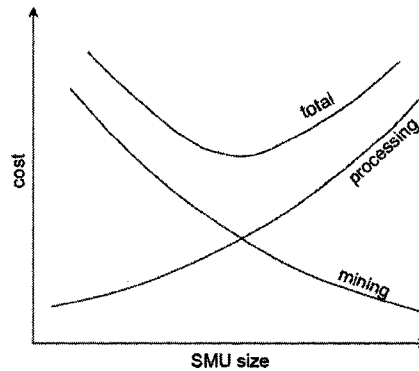


Figure 1.2: Selective mining unit (SMU) selection (redrawn from Deutsch, 2000)

The economical viability of the ore produced is a key parameter for any deposit. The assessed quantity of ore and waste within the deposit must be known to evaluate this parameter. The notion of cutoff grade (z_c) is used to define the minimum grade that separates ore from waste. The cutoff grade can be defined as a technical and economic limit (in terms of grade) with the available technology at that time below which the feed (raw ore) can not be processed as a useful entity economically. Cutoff grade is dependent on the available technology and market demand [16].

1.1 Background

Methods for reserves estimation can be divided in to (a) geometric methods that are done manually on plans or section, (b) interpolation methods such as inverse distance weighting and different kriging approaches, and (c) simulation [2]. As computational speed is increasing, interpolation methods and simulation are becoming popular for reserves estimation. The estimation methods will be discussed in detail in section 1.3.

Statistical approaches for panel-wise reserves estimation were proposed by Krige (1951) and Sichel (1952) [1]. These proposed techniques were developed formally by Matheron (1962) in the form of geostatistics, the application of which is wide spread in mining and beyond [1]. There are many case studies for different types of deposits for global grade and tonnage comparisons for different estimation methods. In a study of ordinary kriging and indicator kriging on a manganese ore deposit concluded that there is practically no significant difference in the grade estimate produced from both the methods [15].

Kriging has an inherent property of smoothing the estimates over the area of interest. To overcome the smoothing effect, simulation was developed. Simulation has the benefit of generating a number of realizations and assessing of uncertainty. Mine planning is difficult in case of multiple realizations. Techniques to deal with uncertainty are being developed [7].

The estimates for any estimation technique are typically established using exploration data as known samples. While mining, the blast hole data information and visual inspection plays vital role in the ore grade and waste decision making. The established exploration data model helps while taking decision on investment at large scale and in the long term production plans but in routine operation the decision of sending the blasted/excavated rock to ore processing plant or waste dump is typically done using blasthole information and visual judgment. Blasthole data are used for establishing the model for short term (daily/weekly/monthly) decision making.

Recoverable reserve is a function of the mining method, economics and support size. Global reserves are calculated before mining, in exploration and feasibility stages. The whole domain of interest (A) is taken in to account for ore grade and quantity calculations at global scale. As a mine is planned and excavated in panels (V) so, local recoverable reserves are calculated at larger blocks called panels. The quantity of ore and waste within a panel depends on physical characteristics of SMUs (v) within that panel. Recoverable reserves in a panel relates to the proportion (tonnage) and average grade of those SMUs that are selected as ore within any given panel. The estimates at SMU scale within the panel are considered for calculation of grade and quantity of ore in that panel. Applying an acceptable cutoff grade, the quantity above cutoff grade is considered ore and below cutoff grade it is considered as waste.

1.2 Stationarity and Spatial Variability

The uncertainty in the true grade at an unsampled location $z(\mathbf{u}) \in A$ can be modeled using cumulative distribution function (cdf) of a random variable $Z(\mathbf{u})$, where \mathbf{u} is the coordinate location vector. The cdf can be written as:

$$F(\mathbf{u}; z) = Prob\{Z(\mathbf{u}) \leq z\} \in [0,1] \quad (1.1)$$

The set of random variables over the area of interest is called a random function $\{Z(\mathbf{u}), \mathbf{u} \in A\}$. Stationarity is the property of the random function model that states the invariance of cdf and moments by translation over the domain A . The geostatistical inference of the unsampled locations needs the sample data to be pooled together under the decision of stationarity. The first order of stationarity assumes that the mean of the variable of interest is constant throughout the domain A . The second order of stationarity assumes that the variance of data and covariance between data are constant throughout the domain A . The stationary covariance is defined as [4]:

$$Cov(\mathbf{h}) = E\{Z(\mathbf{u} + \mathbf{h})Z(\mathbf{u})\} - E\{Z(\mathbf{u})\}E\{Z(\mathbf{u} + \mathbf{h})\} \quad (1.2)$$

The covariance with zero lag distance $Cov(0)$ is the variance σ^2 .

$$\sigma^2 = Cov(0) = E\{[Z(\mathbf{u})]^2\} - [E\{Z(\mathbf{u})\}]^2 \quad (1.3)$$

The spatial variability must be quantified for geostatistical modeling. Variogram $2\gamma(\mathbf{h})$ is used as a quantitative measure for spatial variability. The variogram also assumes the second order of stationarity throughout the domain A . The variogram can be defined as the expected squared difference between two sample values separated by a lag vector \mathbf{h} .

$$2\gamma(\mathbf{h}) = E\{[Z(\mathbf{u}) - Z(\mathbf{u} + \mathbf{h})]^2\} \quad (1.4)$$

For calculation and estimation purposes we use $\gamma(\mathbf{h})$ known as semivariogram. Combining equation 1.2, 1.3 and 1.4 gives a relationship as:

$$\gamma(\mathbf{h}) = Cov(0) - Cov(\mathbf{h}) \quad (1.5)$$

It is always advisable to look at the plotted data and variogram map before calculating and fitting the directional variogram. This can help in selecting the lag and direction of continuity for the variogram calculation.

1.3 Volume Variance Relation

In practice, mining is done considering different block sizes. Exploration data are at point scale. The block size has an impact on the grade distribution. The variance of grade distribution decreases as the volume increases due to averaging out of high and low values (Figure 1.3). The internal dilution of the deposit at different block sizes can be modeled using geostatistical tools for volume-variance correction. Common methods used for volume-variance correction includes affine correction, indirect lognormal correction and discrete Gaussian method. These methods correct the distribution of grade sampled at point scale in to an SMU block size distribution.

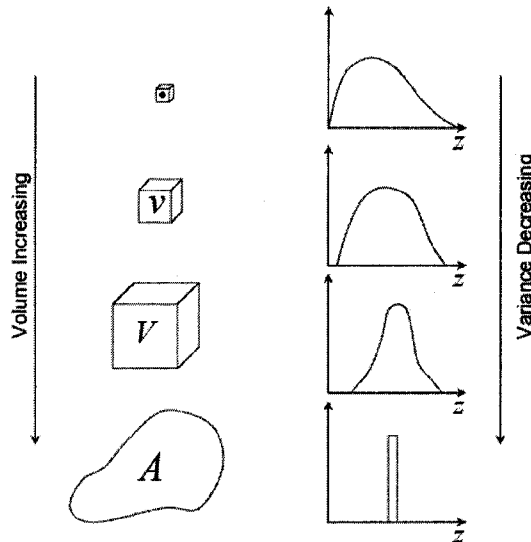


Figure 1.3: Variance decreases as the volume increases due to the averaging out of high and low values (redrawn from Deutsch, 2000)

Gammabar

The average variogram, also called gammabar, is used as a measure of variability between two support volumes chosen arbitrarily. It is the mean or average of variogram pairs, where the head of variogram describes the block $V(\mathbf{u})$ and tail describes the block $v(\mathbf{u}')$. \mathbf{u} and \mathbf{u}' are location vectors. The gammabar values can be calculated as [1, 3]:

$$\bar{\gamma}(V, v) = \frac{1}{V \cdot v} \int_{V(u)} d\mathbf{u} \int_{v(u')} \gamma(\mathbf{u} - \mathbf{u}') d\mathbf{u}' \quad (1.6)$$

If the volume is very small, tending to point scale, then gammabar will be equal to zero as the lag separation \mathbf{h} also tends to zero. If the volume is very large and points are separated by a large lag \mathbf{h} , then the gammabar will be equal to the variance of the field.

Dispersion Variance

The variance of grades of small blocks v within larger block V is known as the dispersion variance of v in V , denoted as $D^2(v, V)$. The dispersion within a fixed volume V decreases as the support block v increases. The dispersion variance is defined as [3, 10]:

$$D^2(v, V) = E\{[z_v - m_v]^2\} \quad (1.7)$$

The dispersion variance can be calculated using average variogram (gammabar) values. The dispersion variance can be expressed in terms of gammabar as follows:

$$D^2(v, V) = \bar{\gamma}(V, V) - \bar{\gamma}(v, v) \quad (1.8)$$

where, $\bar{\gamma}(v, v) = \frac{1}{|v|^2} \int_{v(u)} d\mathbf{u} \int_{v(u')} \gamma(\mathbf{u} - \mathbf{u}') d\mathbf{u}'$ and $\bar{\gamma}(V, V) = \frac{1}{|V|^2} \int_{V(u)} d\mathbf{u} \int_{V(u')} \gamma(\mathbf{u} - \mathbf{u}') d\mathbf{u}'$

The additive relationship of dispersion variance for increasing block size can be written as [10]:

$$D^2(v, A) = D^2(v, V) + D^2(V, A) \quad \forall v \subset V \subset A \quad (1.9)$$

where, v is for small blocks, V is for large blocks and A is the total domain of interest. So, dispersion variance of small blocks v in the domain is the summation of the dispersion variance of small blocks in large block and dispersion variance of large blocks in the whole domain.

Variance Correction Factor

The variance correction factor f is the ratio of the block dispersion variance $D^2(v, A)$ and the point dispersion variance $D^2(\cdot, A)$ within the deposit. The variance correction factor measures the amount of change in the variance of grade distribution for a block size.

$$f = \frac{D^2(v, A)}{D^2(., A)} = \frac{D^2(., A) - D^2(., v)}{D^2(., A)} = 1 - \frac{D^2(., v)}{D^2(., A)} \quad (1.10)$$

The variance of (.) within in the block size is given by the average variogram $\bar{\gamma}(v, v)$.

$$f = 1 - \frac{\bar{\gamma}(v, v)}{\sigma^2} \quad (1.11)$$

where, σ^2 is the variance and $\bar{\gamma}(v, v)$ can be calculated from the fitted variogram model. Variance correction factor will be used in case of post-processing of indicator kriging output. As the output of indicator kriging (section 1.2.2) is in the form of point scale probability so variance correction factor is used get the variance of block scale.

1.4 Estimation Methods

There are several geostatistical techniques available for estimation of reserves. All these techniques have their applicability, advantages and limitations. There are some techniques that give information of reserves at only global scale like discrete Gaussian method for reserves calculation. Most techniques provide local estimates of grade.

1.4.1 Discrete Gaussian Method

Discrete Gaussian method is a volume variance correction approach. In volume variance correction approach, probability distributions of unsampled point support grades are built from point support data. These point support distributions are then corrected for the volume support of block size. The discrete Gaussian model can be used as change of support model based on Gaussian probabilistic models. It is based on the concept that the general shape of distribution is honored during the change of support. This model follows different steps to get the recoverable reserves at global scale. The first step is to determine the average variogram of raw data within the SMU size of interest. The next step is to calculate dispersion variance of data at the block support. The sample data are transformed to a Gaussian distribution, known as Gaussian anamorphosis. The discrete Gaussian method now can deduce the histogram of raw block grades. The global recoverable reserves can be calculated by applying appropriate cutoff grade to the histogram [11].

1.4.2 Ordinary Kriging

Kriging is a widely used and well established estimation method, where the estimate is a weighted summation of sample data. The weights are calculated to minimize the error variance. In spite of being known as Best Linear Unbiased Estimator (BLUE) it has some drawbacks. The major consideration is that kriging creates a smoother representation of grades than the true one. Another consideration is that kriging does not provide a good measure of uncertainty. A kriged estimate can be defined as:

$$z^*(\mathbf{u}) = \sum_{i=1}^n \lambda_i \cdot z(\mathbf{u}_i) + \left[1 - \sum_{i=1}^n \lambda_i\right] \cdot m \quad (1.12)$$

where, $z^*(\mathbf{u})$ is the estimate at location \mathbf{u} , $z(\mathbf{u}_i)$ is sample data at location \mathbf{u}_i , n is the number of sample data, m is the global mean and λ_i is the weight assigned to i^{th} sample data. For simplification, trend is removed from the data and kriging is performed with residuals. So, the system of equations becomes:

$$y(\mathbf{u}) = z(\mathbf{u}) - m$$

$$y^*(\mathbf{u}) = \sum_{i=1}^n \lambda_i \cdot y(\mathbf{u}_i)$$

The kriging error variance is:

$$\begin{aligned} \sigma_E^2 &= E\left\{[Y^*(\mathbf{u}) - Y(\mathbf{u})]^2\right\} \\ &= E\left\{[Y^*(\mathbf{u})]^2\right\} - 2 \cdot E\left\{Y^*(\mathbf{u}) \cdot Y(\mathbf{u})\right\} + E\left\{[Y(\mathbf{u})]^2\right\} \\ &= \sum_{i=1}^n \sum_{j=1}^n \lambda_i \lambda_j E\left\{Y(\mathbf{u}_i) \cdot Y(\mathbf{u}_j)\right\} - 2 \cdot \sum_{i=1}^n \lambda_i E\left\{Y(\mathbf{u}_i) \cdot Y(\mathbf{u})\right\} + Cov(0) \\ &= \sum_{i=1}^n \sum_{j=1}^n \lambda_i \lambda_j Cov_{ij} - 2 \cdot \sum_{i=1}^n \lambda_i Cov_{i0} + \sigma^2 \end{aligned} \quad (1.13)$$

where, 0 refers to the unsampled location, Cov_{ij} is the covariance between data at i and j , Cov_{i0} is the covariance between the data at i and the location to be estimated, n is the number of sample data and σ^2 is the variance of data. The weights are calculated by minimizing the kriging error variance.

$$\begin{aligned} \frac{\partial[\sigma_E^2]}{\partial \lambda_i} &= 2 \cdot \sum_{j=1}^n \lambda_j Cov_{ij} - 2 \cdot Cov_{i0} \quad , \quad i = 1, \dots, n \\ \sum_{j=1}^n \lambda_j Cov_{ij} &= Cov_{i0} \quad , \quad i = 1, \dots, n \end{aligned} \quad (1.14)$$

In ordinary kriging, the calculated weights are constrained to sum to one. So, the mean m is filtered from the kriging estimator (Equation 1.12). The system of equation for ordinary kriging is:

$$\begin{cases} \sum_{j=1}^n \lambda_j Cov_{ij} + \mu = Cov_{i0} \quad , \quad i = 1, \dots, n \\ \sum_{j=1}^n \lambda_j = 1 \end{cases} \quad (1.15)$$

where, μ is the lagrange parameter.

1.4.3 Indicator Kriging

The idea of indicator kriging for continuous variables is to estimate the distribution of uncertainty $F_z(\mathbf{u})$ at unsampled location \mathbf{u} . The cumulative distribution function (cdf) is estimated at a series of threshold values: $z_k = 1, \dots, K$. The indicator formalism of the values can be written as follows:

$$i(\mathbf{u}_i; z_k) = Prob\{Z(\mathbf{u}_i) \leq z_k\} \quad (1.16)$$

$$= \begin{cases} 1, & \text{if } Z(\mathbf{u}_i) \leq z_k \\ 0, & \text{otherwise} \end{cases}$$

The indicator kriging derived cumulative distribution function at an unsampled location at threshold z_k is calculated as:

$$F_{IK}(\mathbf{u}; z_k) = \sum_{i=1}^n \lambda_i(z_k)[i(\mathbf{u}_i; z_k) - F(z_k)] + F(z_k) \quad (1.17)$$

This indicator kriging procedure requires a variogram measure corresponding to each threshold $z_k = 1, \dots, K$ so that the weights $\lambda_i(z_k), i = 1, \dots, n; k = 1, \dots, K$ can be determined. The thresholds are often chosen to be equally spaced quantiles, for example the nine deciles are often chosen [5, 8].

1.4.4 Simulation

Conditional simulation (SGS) is often done in Gaussian space. So, this requires transforming the data in to Gaussian/normal space, followed by simulation then back transformation to original units. Conditional simulation removes the smoothing effect generated by kriging. In other words, conditionally simulated maps are better representative of local variability patterns. Conditionally simulated maps are also used to assess uncertainty.

The smoothing effect of kriging makes the variance of kriged estimates too small. The variance of kriged estimate is:

$$Var\{y^*(\mathbf{u})\} = \sigma^2 - \sigma_E^2 \quad (1.18)$$

where, $y^*(\mathbf{u})$ is the kriged estimate at location \mathbf{u} , σ^2 is the variance of data and σ_E^2 is the kriging variance. In simulation the variance of the estimates is corrected by adding a random component in the simulated value, which removes the effect of missing variance.

$$y_s(\mathbf{u}) = y^*(\mathbf{u}) + R(\mathbf{u}) \quad (1.19)$$

where, $y_s(\mathbf{u})$ is the simulated value at location \mathbf{u} , and $R(\mathbf{u})$ is a random component with a mean of zero and a variance of σ_E^2 . There are different simulation algorithms available, e.g. matrix approach, turning bands, simulated annealing, sequential Gaussian simulation (SGS) etc. Sequential Gaussian simulation is used for the study. The advantage with Gaussian distribution is that the global mean and variance of distribution will be preserved if we always use Gaussian distributions. It is simple and easy to use. The steps are [3, 4]:

1. transform data to “normal space”,
2. establish grid network and coordinate system,
3. assign data to the nearest grid nodes,
4. determine a random path through all the grid nodes,
 - (a) find nearby data and previously simulated grid nodes,
 - (b) construct the conditional distribution by kriging,
 - (c) draw simulated value from the conditional distribution,
5. honor data and input variogram,
6. back transform the realization,
7. go to step 4 and generate another realization.

There are some drawbacks of SGS. It can cause maximum spatial disorder beyond variogram and maximum spatial entropy, i.e. low and high values are disconnected.

1.5 Goodness of Prediction

1.5.1 Cross Validation

Cross validation is done to check the goodness and reliability of parameters used in estimation. In cross validation, one sample or an entire drill hole is removed from the sample database. Estimation is done at that location with the remaining samples, using the decided spatial parameters for the estimation. This activity is performed for every known sample in the domain. In other words, it is “leave one out and estimate with the remaining” principal. The true and estimated values are plotted on scatter-plot and the error statistics is given by error histogram, where error is the difference between estimate and true values. The scatter-plot should show unbiasedness and high correlation between the true and the estimated values. The error histogram should be equally distributed on both sides of zero value with a mean closure to zero.

1.5.2 Accuracy Plot

The goodness of a probabilistic model can be checked by accuracy and precision. These accuracy and precision are based on the actual fraction of true values falling within symmetric probability intervals of varying width p [6]. A probability distribution is accurate if the fraction of true values falling in the p interval exceeds p for all p in $[0, 1]$. The precision of an accurate probability distribution is measured by closeness of the fraction of true values to p for all p in $[0, 1]$. It says that on accuracy plot (Figure 1.4), points above 45° line indicate an accurate model and points close to the 45° line represent the preciseness of the distribution. The points below the 45° line show inaccuracy. So, all points are desired to be close and above 45° line. A $\pm 7.5\%$ of tolerance from the 45° (ideal case) line can be considered.

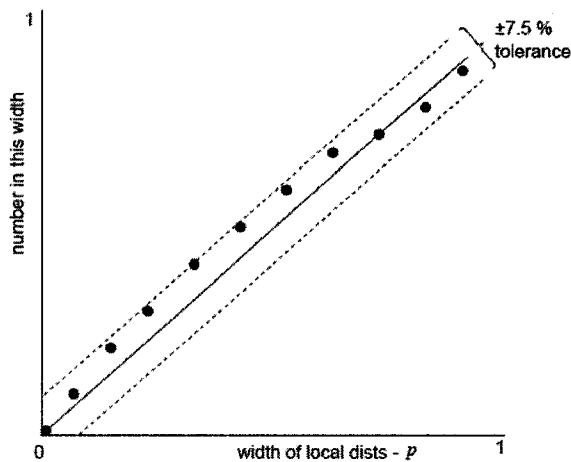


Figure 1.4: Schematic diagram of accuracy plot.

1.6 Thesis Outline

The thesis has been divided in five chapters. All the variogram models used in the study are shown in the appendices at the end of the thesis.

Chapter 2 discusses the problem and the methodology used for calculation of estimates of grade and quantity of ore for different cases used in the study. Then, the criteria and statistical tools used for the comparative study are discussed.

Chapter 3 illustrates the comparative study done on synthetic data. It also includes the sensitivity study of variogram model used in estimation.

Chapter 4 demonstrates the comparative study done with the real data of Misima gold/silver deposit in Papua New Guinea.

Finally, discussions on the results of the comparative study are concluded followed by proposed future work in Chapter 5.

Chapter 2

Methodology

The methodology and estimation methods used for evaluation of a particular deposit are subjective to the type of available information, individual knowledge, available time, available resources, type of deposit means whether the deposit has one mineral only or a poly-metallic deposit. In this chapter, the recoverable reserves calculation methodologies for both single variable and poly-metallic deposit having two minerals have been discussed. Setting up true/reference results on grid and the methodology for comparison of estimation results to the reference results have also been discussed in detail.

Each SMU is defined as ore or waste on the basis of its estimated grade and the applied cutoff grade. The estimation is done with the sampled exploration information, which is widely scattered in the area and the amount of sample taken from the field is relatively small in comparison to the whole deposit.

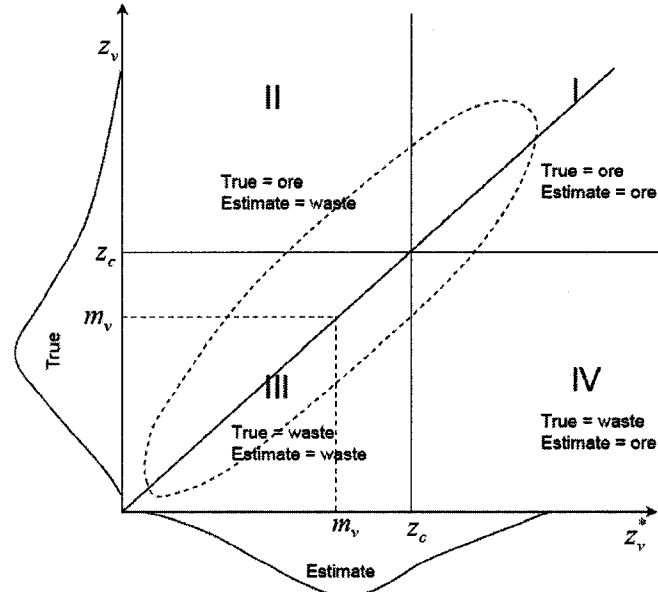


Figure 2.1: Schematic scatter-plot of the true versus estimates [1, 12].

While estimating with exploration data, the estimates are likely to be different than the truth (actual grades). The joint distribution of the true values and estimates is shown by a schematic diagram (Figure 2.1). The true distribution is shown on left side of the

true axis and the distribution of estimates is shown below the axis of estimates. The variance of estimates is shown as smaller than the variance of true distribution. The cutoff value z_c defines four quadrants on the scatter-plot. I quadrant correctly classifies ore, III quadrant correctly classifies the waste, II quadrant misclassifies as waste and IV quadrant misclassifies as ore [1, 12]. This phenomenon always increases the complexities between estimated reserve model and actual production. It is always better to have majority of the points in I and III quadrant. A high correlation coefficient and less number of points in the II and IV quadrant are also desirable.

To see this phenomenon, a comparative study of different reserve estimation techniques with reference (true) results is proposed. Ordinary kriging, indicator kriging and simulation are methods of estimation for comparison with established true values. Ordinary kriging is robust. Indicator kriging estimates the distribution of uncertainty directly. Simulation gives multiple realizations and variability.

2.1 Comparative Study

In the domain of interest, blasthole data and exploration data are known. The blasthole information is closely spaced and collected while mining in the area. The exploration data are widely spaced and collected before mining, generally in the phase of prospecting and detailed exploration to estimate the reserves for feasibility and economical study. The methodology adopted is to compare the reference results to the estimates from different methods at panel scale. The reference results are established from blasthole data and estimates for individual estimation methods are established using exploration data. The panel comparison is based on estimates and reference values on scatter-plots for both grade and ore quantity. The softwares used in this study are *GSLIB*, *Pangeos* for geostatistical analysis, estimation and plotting and *Petrel* for visualization.

2.2 Reference Results

The reference results are established on a grid using blasthole data with ordinary kriging. A short search radius will be used to avoid extending the estimates beyond close range to the blastholes. In a panel, the SMUs above cutoff grade are averaged to get the grade at that panel scale. The proportion of SMUs above cutoff grade in every panel is also calculated. The proportion represents the ore quantity in that panel. The spatial and estimation parameters for setting up reference results will be discussed in Chapters 3 and 4.

2.3 Calculation of Ore Grade and Quantity for Panels

Estimates are established at SMU scale. These estimated SMUs are used to calculate grade and tonnage of panels. Then, considering all the SMUs of a particular panel, apply a cutoff grade to those SMUs in that panel and calculate average grade and proportion of ore in that panel (Figure 2.2). Panels above cutoff grade only will be used in panel grade

calculation. In case of tonnage calculation, a panel will be assigned zero tonnage, if the panel grade is below cutoff grade.

To deal with the missing values due to unavailability of data and parameter constraints, while calculating panel grades and proportions, more than 80% estimated panel at SMU scale will be taken as the minimum amount to be representative for the whole panel for the comparison. The grade and quantity will be calculated from those estimated SMUs only.

In case of ordinary kriging, estimation is performed directly at SMU scale. The estimated SMUs are used to calculate panel grades and tonnages. In case of indicator kriging the kriged output is post-processed with volume-variance correction and E-type estimates are calculated at SMU scale. These E-type estimates are used to establish panel grade and quantity of ore. Simulation gives multiple realizations at small scale (smaller than SMU scale). These simulated realizations are block-averaged to get them at the SMU scale. The grade and tonnage for every realization is calculated separately at panel scale applying the cutoff grade (z_c). To get the estimate for a particular panel, all the values of that panel are averaged from all the realizations. Missing values (below cutoff grade) are not taken in to account in this averaging.

In this study, a synthetic example having one variable is shown then a real example with two variables is shown. The calculation of grade and quantity can be explained as follows:

Case 1

In this case, data with single variable information in the domain are available. Estimation is done at SMU scale followed by calculation of grade and quantity at panel scale for this variable. This is the case for synthetic example (Chapter 3).

Let $i_v^*(\mathbf{u}_j; z_c)$ denote the indicator associated with a SMU declared as profitable on the basis of the estimate $z_v^*(\mathbf{u}_j)$ and n is the total number of SMUs in a panel,

$$i_v^*(\mathbf{u}_j; z_c) = \begin{cases} 1 & \text{if } z_v^*(\mathbf{u}_j) \geq z_c \\ 0 & \text{otherwise} \end{cases}$$

where, z_c is the cutoff value, \mathbf{u}_j refers for location of SMU in the panel. Then, grade of a panel $G_V^*(z_c)$ and ore proportion $P_V^*(z_c)$ are calculated as:

$$G_V^*(z_c) = \frac{\sum_{j=1}^n i_v^*(\mathbf{u}_j; z_c) \cdot z_v^*(\mathbf{u}_j)}{\sum_{j=1}^n i_v^*(\mathbf{u}_j; z_c)} \quad (2.1)$$

$$P_V^*(z_c) = \frac{\sum_{j=1}^n i_v^*(\mathbf{u}_j; z_c)}{n} \quad (2.2)$$

Case 2

In this case, data have two variables information in the domain. Estimation for each variable is done at SMU scale. One variable is considered as primary and the other as secondary variable as per economical importance. The equivalent grade at SMU scale is calculated from the estimates of both the collocated variables. Calculation of quantity of ore, grade of equivalent variable is done at panel scale using the cutoff grade [13]. Recoverable grade and quantity of both the variables are calculated at panel scale separately. This case applies to real data example (Chapter 4).

Let $x_v^*(\mathbf{u}_j)$ denote the grade estimate for the first (primary) variable, $y_v^*(\mathbf{u}_j)$ for the second (secondary) variable estimate and $z_v^*(\mathbf{u}_j)$ for the equivalent variable calculated from the first and the second variables estimates at SMU scale (Equation 2.3). If P_y is selling price for secondary variable, P_x is selling price for primary variable, rf_y is recovery factor for secondary variable and rf_x is the recover factor for primary variable then, equivalent variable in terms of primary variable is calculated as:

$$z_v^*(\mathbf{u}_j) = x_v^*(\mathbf{u}_j) + y_v^*(\mathbf{u}_j) \cdot \frac{P_y}{P_x} \cdot \frac{rf_y}{rf_x} \quad (2.3)$$

Let $i_v^*(\mathbf{u}_j; z_c)$ denote the indicator associated with an SMU declared as profitable on the basis of the equivalent variable $z_v^*(\mathbf{u}_j)$ at SMU scale and n is the total number of SMUs in a panel,

$$i_v^*(\mathbf{u}_j; z_c) = \begin{cases} 1 & \text{if } z_v^*(\mathbf{u}_j) \geq z_c \\ 0 & \text{otherwise} \end{cases}$$

where, z_c is the equivalent variable cutoff value in units of primary variable, \mathbf{u}_j refers for location. Then, for the equivalent variable the grade $G_{Vz}^*(z_c)$, proportion of ore $P_{Vz}^*(z_c)$ and quantity of ore $T_V^*(z_c)$ at panel scale are calculated as:

$$G_{Vz}^*(z_c) = \frac{\sum_{j=1}^n i_v^*(\mathbf{u}_j; z_c) \cdot z_v^*(\mathbf{u}_j)}{\sum_{j=1}^n i_v^*(\mathbf{u}_j; z_c)} \quad (2.4)$$

$$P_{Vz}^*(z_c) = \frac{\sum_{j=1}^n i_v^*(\mathbf{u}_j; z_c)}{n} \quad (2.5)$$

$$T_V^*(z_c) = \sum_{j=1}^n i_v^*(\mathbf{u}_j; z_c) \cdot v_j \cdot s_j \cdot rf_j \quad (2.6)$$

where, v is the volume of an SMU, s is the specific gravity and rf is the ore recovery factor.

The specific gravity and volume of every SMU is taken as the same for all, so the simplified formulae for quantity of ore calculation in a panel of volume V can be written as:

$$T_V^*(z_c) = P_{Vz}^*(z_c) \cdot V \cdot s \cdot rf \quad (2.7)$$

Then, for primary variable the grade $G_{Vx}^*(z_c)$ and quantity $Q_{Vx}(z_c)$ at panel scale is calculated as:

$$G_{Vx}^*(z_c) = \frac{\sum_{j=1}^n i_v^*(\mathbf{u}_j; z_c) \cdot x_v^*(\mathbf{u}_j)}{\sum_{j=1}^n i_v^*(\mathbf{u}_j; z_c)} \quad (2.8)$$

$$Q_{Vx}(z_c) = G_{Vx}^*(z_c) \cdot T_V^*(z_c) \quad (2.9)$$

Then, for secondary variable the grade $G_{Vy}^*(z_c)$ and quantity $Q_{Vy}(z_c)$ at panel scale is calculated as:

$$G_{Vy}^*(z_c) = \frac{\sum_{j=1}^n i_v^*(\mathbf{u}_j; z_c) \cdot y_v^*(\mathbf{u}_j)}{\sum_{j=1}^n i_v^*(\mathbf{u}_j; z_c)} \quad (2.10)$$

$$Q_{Vy}(z_c) = G_{Vy}^*(z_c) \cdot T_V^*(z_c) \quad (2.11)$$

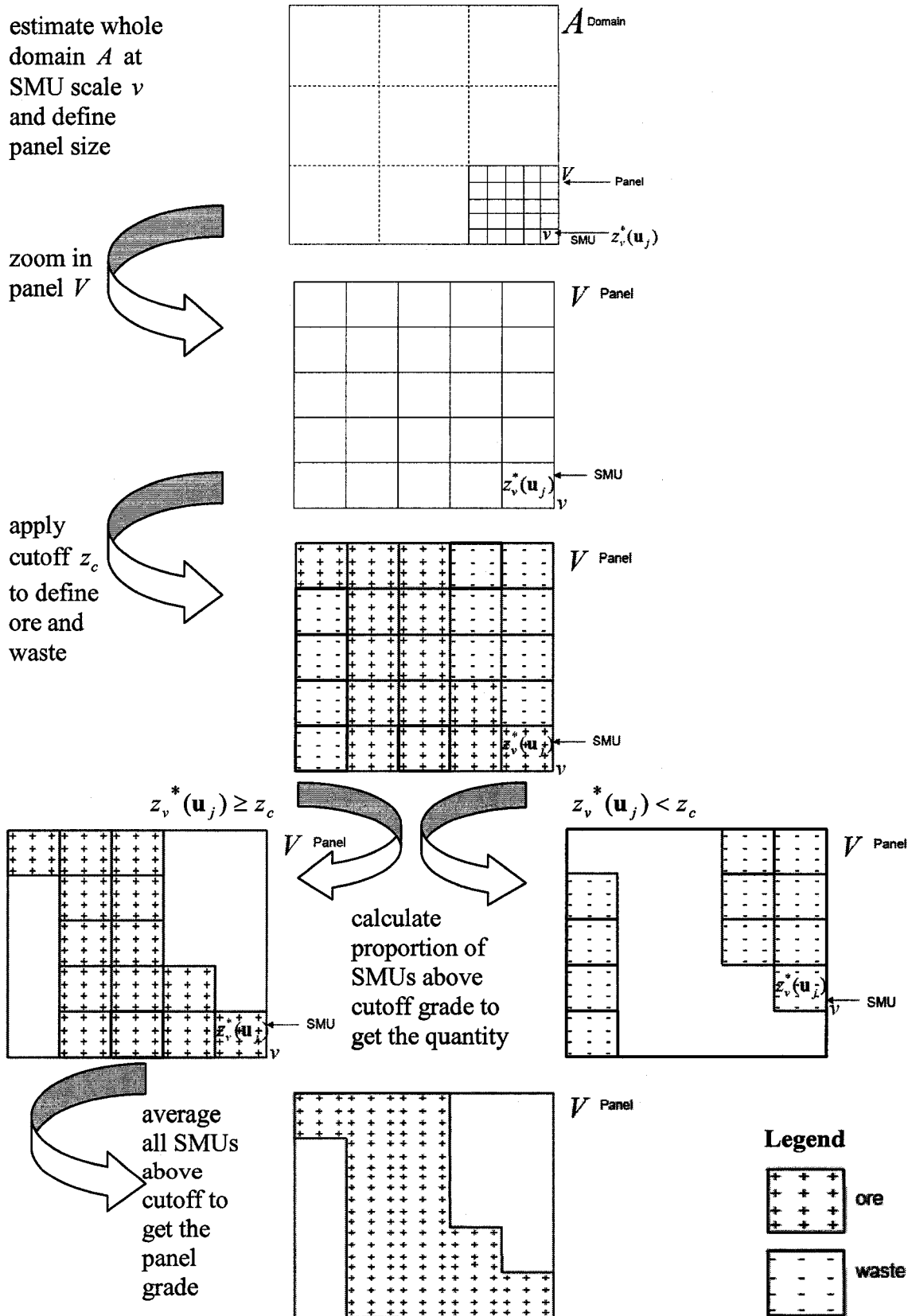


Figure 2.2: Schematic diagram for calculating grade and quantity of ore for a panel.

2.4 Comparison

Different estimation methods can be compared using the estimates and true values if we have true values from some source, e.g. reference blastholes. Panel wise comparison is done for both grade and quantity. For comparison, the panel estimates of a particular method are plotted against the reference panel results on scatter-plot (Figure 2.3).

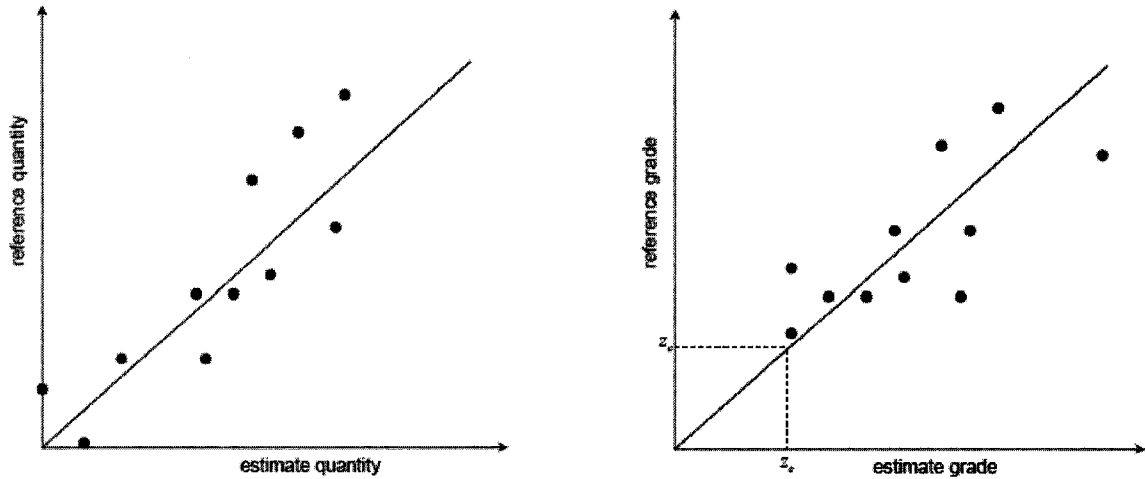


Figure 2.3: Schematic diagram of ore grade and quantity comparison at panel scale on scatter-plot.

In case of tonnage or quantity comparison, waste (below cutoff grade) panel is taken as zero quantity of ore. So, few points can be expected on zero line, i.e. on reference and estimate axis. In case of grade comparison only those panels are compared that are above cutoff grade. So, there are no points below cutoff grade on the scatter-plot of grade comparison. This comparative study will be done using various statistical measures such as:

- Mean Error (ME)

$$ME = \frac{\sum_{i=1}^n (z_i^* - z_i)}{n} \quad (2.12)$$

where, z_i^* is the estimated value, z_i is the true value and n is total number of pairs.

- Mean Squared Error (MSE)

$$MSE = \frac{\sum_{i=1}^n (z_i^* - z_i)^2}{n} \quad (2.13)$$

where, z_i^* is the estimated value, z_i is the true value and n is total number of pairs.

- Mean Absolute Error (MAE)

$$\text{MAE} = \frac{\sum_{i=1}^n |z_i^* - z_i|}{n} \quad (2.14)$$

where, z_i^* is the estimated value, z_i is the true value and n is total number of pairs.

- Correlation

$$\text{correlation} = \frac{\text{Cov}\{z, z^*\}}{\sqrt{\text{Var}\{z\}\text{Var}\{z^*\}}} \quad (2.15)$$

where, z^* is for estimated values and z is for true values.

The means of both estimate and reference true values should be close to each other to make it unbiased. The error ($z_i^* - z_i$) is used to calculate the error variograms for each method. The error variogram should show a pure nugget behavior. The pure nugget effect of variogram shows the unbiasedness of estimates.

Chapter 3

Comparative Case Study – A Synthetic Example

A comparative panel-wise study of different estimation techniques, i.e. ordinary kriging, indicator kriging and simulation is performed using synthetic data. These data are created at a very close spacing. Exploration data at wide spacing and blasthole data at an intermediate spacing are extracted from these data. The estimation is done using the exploration data. The estimated results of different methods are compared to the reference results, where the reference results are setup using the blasthole data.

3.1 Data

A $500\text{m} \times 500\text{m}$ area of interest is defined. An Unconditional simulation is performed in normal units at a $1\text{m} \times 1\text{m}$ grid interval. An isotropic spherical variogram with a range of 100m is used for the simulation. The simulated values are transformed to lognormal distribution with a mean of 0.75 and standard deviation of 1.39 (Figure 3.1). These data are used to generate blasthole and exploration data, required for the study. The important criterion, while extracting blasthole and exploration data is that these data distribution statistics should be unbiased and consistent with statistics of synthetic data distribution [9]. While creating these data sets, mean, standard deviation and type of distribution are chosen considering the consistency with available real data statistics (Chapter 4).

The blasthole data set is created by extracting data from the 2-D synthetic data in a 5m square grid pattern. The blasthole data distribution appears lognormal with a mean of 0.76 and standard deviation of 1.40. There are 9801 blasthole data in the area of $500\text{m} \times 500\text{m}$ (Figure 3.2).

The exploration data set is created by extracting data from 2-D synthetic data in a 30m square grid pattern. The exploration data distribution also appears lognormal with a mean of 0.75 and standard deviation of 1.29. There are 272 exploration data in the area of $500\text{m} \times 500\text{m}$ (Figure 3.3).

Cell declustering of exploration data with a cell size of 32m gives almost all the weights near to 1. The declustered statistics show almost the same mean as of exploration data, which is expected as the exploration data are not clustered; rather they are at regular interval in grid pattern (Figure 3.5). This step is included only for completeness because SGS is performed using declustered weights. The QQ-plot (Figure 3.4) between blasthole

and exploration data distribution is quite consistent and close to the 45° line, which implies that both the distributions are similar and close to each other.

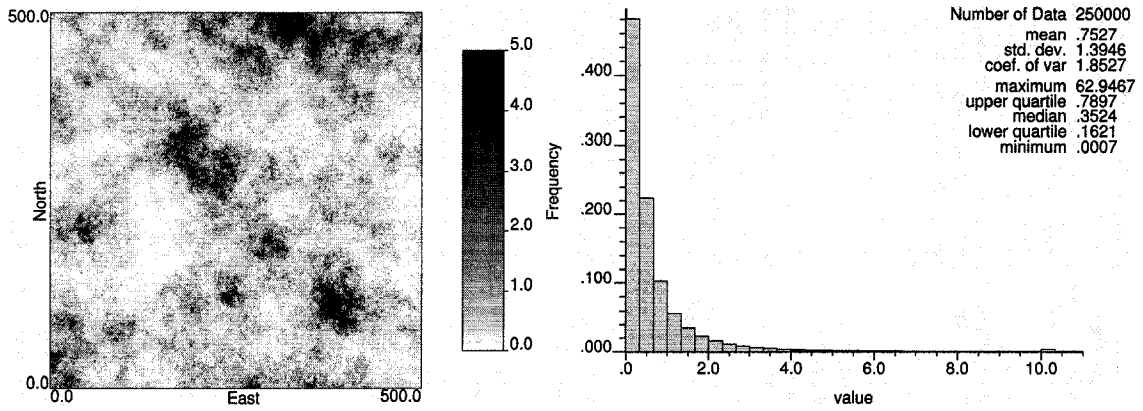


Figure 3.1: Synthetic data at 1m x 1m spacing.

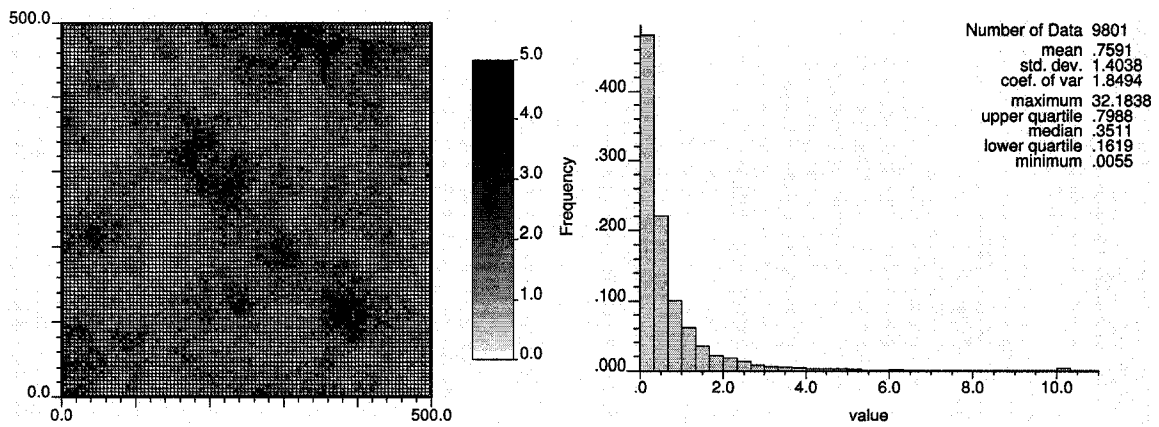


Figure 3.2: Sampled blasthole data from synthetic data.

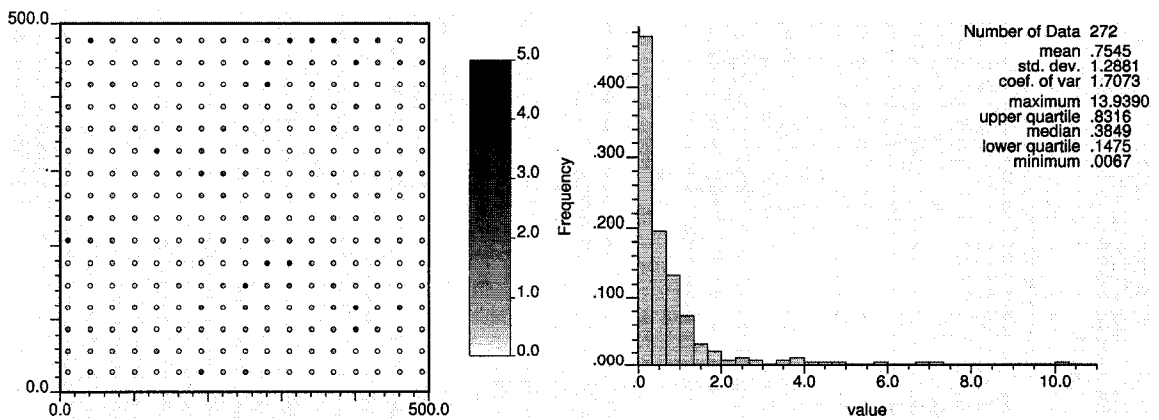


Figure 3.3: Sampled exploration data from synthetic data.

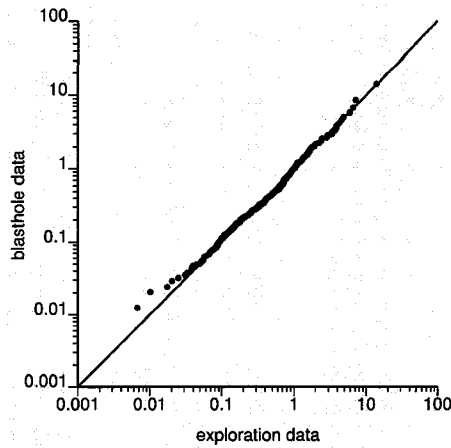


Figure 3.4: QQ-plot between blasthole data and exploration data distribution.

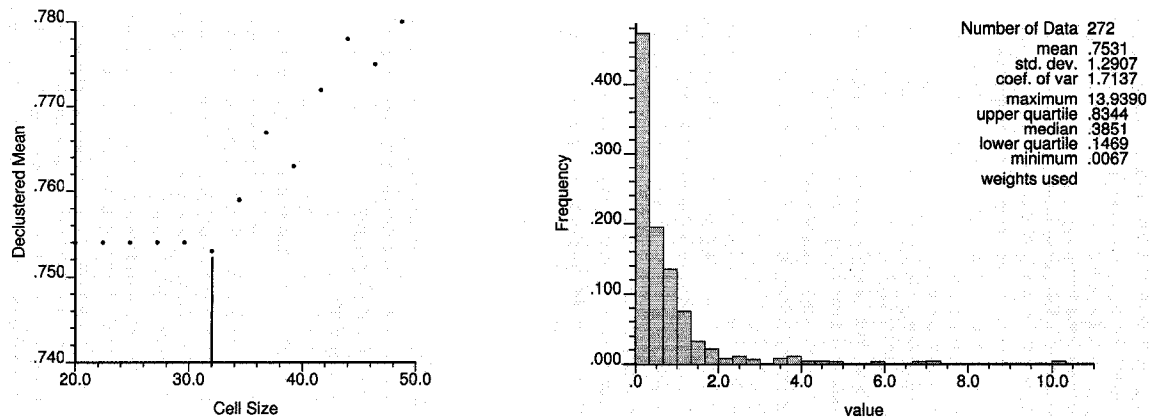


Figure 3.5: Cell declustering of exploration data.

3.2 Parameters and Criterion for Comparative Study:

The SMU size, panel size, and cutoff grade must be specified. The panel size is chosen as $100\text{m} \times 100\text{m}$, so that there are considerable numbers of panels for the study (25 panels). The SMU size is chosen as $5\text{m} \times 5\text{m}$, considering that every SMU should have at least one blasthole data. There are 400 SMUs in each panel. The cutoff grade should not be selected too low that it does not show the importance of applying cutoff and should not be too high that it reduces the number of panels for the comparative study. So, the cutoff grade is defined as 0.40 considering that all the panels should have ore for comparison.

Indicator kriging requires the number of thresholds to be chosen. Thresholds at each decile are taken for this purpose, so there are 9 thresholds: 0.0805, 0.1194, 0.1805, 0.2598, 0.3850, 0.5084, 0.7194, 0.9840 and 1.5951, respectively.

Taking the estimates of SMU scale, the grade and proportion of ore is calculated for every panel. The estimated panel grades and proportions of ore for different estimation techniques are compared to the reference ore grade and proportion values of those panels on the criterion of unbiasedness, mean error (ME), mean squared error (MSE), mean absolute error (MAE) and correlation between estimates and the truth.

3.3 Variography Analysis:

Variogram maps for both blasthole (Figure 3.6) and exploration data (Figure 3.7) are calculated. The variogram map and the ranges of calculated variograms in different directions are used for fitting.

In case of blasthole data variogram map (Figure 3.6), the data show continuity in 130° azimuth direction. 130° azimuth direction is selected as principal (major) direction and 40° azimuth direction as perpendicular (minor). The fitted variogram model for blasthole data (reference variogram) is (Figure i; APPENDIX I):

$$\gamma(\mathbf{h}) = 0.49 + 0.1sp_{h_{\max=40}, h_{\min=40}}(\mathbf{h}) + 0.41sp_{h_{\max=130}, h_{\min=90}}(\mathbf{h}) \quad (3.1)$$

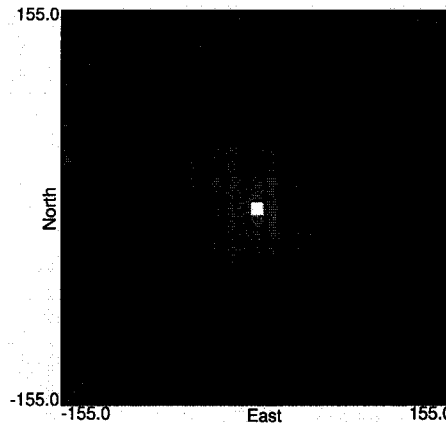


Figure 3.6: Variogram map for blasthole data.

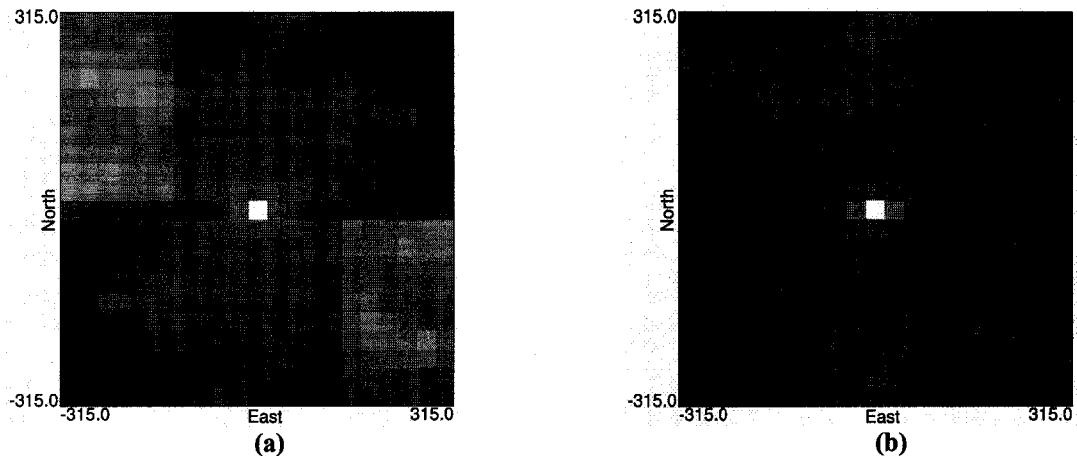


Figure 3.7: Variogram map for exploration data (a) original data (b) normal scored data.

In the case of the exploration data variogram map (Figure 3.7), the direction of continuity is not very clear. So, the variograms are calculated in different directions. The longest range, 130° azimuth is chosen as principal (major) direction and 40° azimuth as perpendicular (minor) direction.

To check the sensitivity of variogram, three cases of ordinary kriging estimation are run using exploration data and different variogram models. The fitted variogram model to the exploration data in the Case 1 is (Figure ii; APPENDIX I):

$$\gamma(\mathbf{h}) = 0.35 + 0.45sph_{h_{\max}=70, h_{\min}=33}(\mathbf{h}) + 0.2sph_{h_{\max}=500, h_{\min}=300}(\mathbf{h}) \quad (3.2)$$

The fitted variogram model to the exploration data in the Case 2 is:

$$\gamma(\mathbf{h}) = 0.3 + 0.37sph_{h_{\max}=80, h_{\min}=80}(\mathbf{h}) + 0.33exp_{h_{\max}=400, h_{\min}=270}(\mathbf{h}) \quad (3.3)$$

In the Case 3, the variogram model fitted to the blasthole data (Equation 3.1) is used.

For indicator kriging, each individual threshold variogram is calculated separately in the 130° azimuth direction as principal (major) and 40° azimuth as perpendicular (minor) direction. The fitted variogram models to the exploration data for 9 thresholds at each decile are (APPENDIX II):

$$\text{Threshold 1 (0.0805) at 0.1 decile} \quad \gamma(\mathbf{h}) = 0.2 + 0.5sph_{h_{\max}=10, h_{\min}=10}(\mathbf{h}) + 0.3sph_{h_{\max}=65, h_{\min}=45}(\mathbf{h}) \quad (3.4)$$

$$\text{Threshold 2 (0.1194) at 0.2 decile} \quad \gamma(\mathbf{h}) = 0.2 + 0.5sph_{h_{\max}=10, h_{\min}=10}(\mathbf{h}) + 0.3sph_{h_{\max}=75, h_{\min}=75}(\mathbf{h}) \quad (3.5)$$

$$\text{Threshold 3 (0.1805) at 0.3 decile} \quad \gamma(\mathbf{h}) = 0.2 + 0.5sph_{h_{\max}=10, h_{\min}=10}(\mathbf{h}) + 0.3sph_{h_{\max}=110, h_{\min}=85}(\mathbf{h}) \quad (3.6)$$

$$\text{Threshold 4 (0.2598) at 0.4 decile} \quad \gamma(\mathbf{h}) = 0.2 + 0.5sph_{h_{\max}=10, h_{\min}=10}(\mathbf{h}) + 0.3sph_{h_{\max}=110, h_{\min}=85}(\mathbf{h}) \quad (3.7)$$

$$\text{Threshold 5 (0.3850) at 0.5 decile} \quad \gamma(\mathbf{h}) = 0.2 + 0.35sph_{h_{\max}=10, h_{\min}=10}(\mathbf{h}) + 0.45sph_{h_{\max}=110, h_{\min}=90}(\mathbf{h}) \quad (3.8)$$

$$\text{Threshold 6 (0.5084) at 0.6 decile} \quad \gamma(\mathbf{h}) = 0.2 + 0.5sph_{h_{\max}=10, h_{\min}=60}(\mathbf{h}) + 0.3sph_{h_{\max}=150, h_{\min}=80}(\mathbf{h}) \quad (3.9)$$

$$\text{Threshold 7 (0.7194) at 0.7 decile} \quad \gamma(\mathbf{h}) = 0.2 + 0.65sph_{h_{\max}=10, h_{\min}=60}(\mathbf{h}) + 0.15sph_{h_{\max}=200, h_{\min}=80}(\mathbf{h}) \quad (3.10)$$

$$\text{Threshold 8 (0.9840) at 0.8 decile} \quad \gamma(\mathbf{h}) = 0.2 + 0.5sph_{h_{\max}=45, h_{\min}=45}(\mathbf{h}) + 0.3sph_{h_{\max}=170, h_{\min}=100}(\mathbf{h}) \quad (3.11)$$

$$\text{Threshold 9 (1.5951) at 0.9 decile} \quad \gamma(\mathbf{h}) = 0.2 + 0.5sph_{h_{\max}=65, h_{\min}=65}(\mathbf{h}) + 0.3sph_{h_{\max}=80, h_{\min}=80}(\mathbf{h}) \quad (3.12)$$

Simulation is performed in normal space, which requires the variogram model of the normal scored exploration data. Normal scored variograms are calculated in 130° azimuth direction as principal (major) and 40° azimuth as perpendicular (minor) direction. To check the sensitivity of variogram model used in simulation, two cases with different

variogram models are run. The fitted variogram model to the normal scored exploration data for the Case 1 is (Figure iv; APPENDIX I):

$$\gamma(\mathbf{h}) = 0.2 + 0.45 \exp_{\substack{h_{\max}=35 \\ h_{\min}=35}}(\mathbf{h}) + 0.35 \text{sp}h_{\substack{h_{\max}=120 \\ h_{\min}=90}}(\mathbf{h}) \quad (3.13)$$

The fitted variogram model to the normal scored exploration data for the Case 2 is (Figure v; APPENDIX I):

$$\gamma(\mathbf{h}) = 0.2 + 0.43 \text{sp}h_{\substack{h_{\max}=50 \\ h_{\min}=85}}(\mathbf{h}) + 0.37 \text{sp}h_{\substack{h_{\max}=125 \\ h_{\min}=85}}(\mathbf{h}) \quad (3.14)$$

3.4 Reference Results

The reference results at SMU scale (5m × 5m) are calculated by ordinary kriging of blasthole data. A short search radius of 40m and up to 11 data were used in kriging. The reference variogram model (Equation 3.1) was used in the kriging.

The reference result distribution at SMU scale has a mean of 0.76 and standard deviation of 0.98 (Figure 3.8). The statistics of estimates show unbiasedness and consistency with the original 2-D created data (synthetic data) and blasthole data distribution.

Cross validation of the ordinary kriging shows an error histogram of mean close to zero and an unbiased cross-plot between true and estimates (Figure 3.9).

Now, panel reference results for each panel are calculated by averaging the SMUs grade above cutoff and proportion of SMUs above cutoff within in that panel. The proportion represents the quantity of ore within the panel.

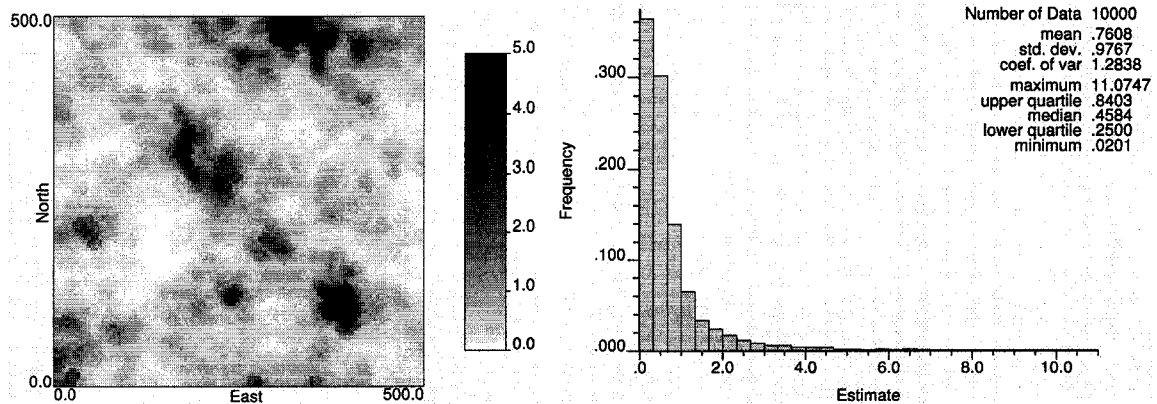


Figure 3.8: Reference model at 5m × 5m grid interval.

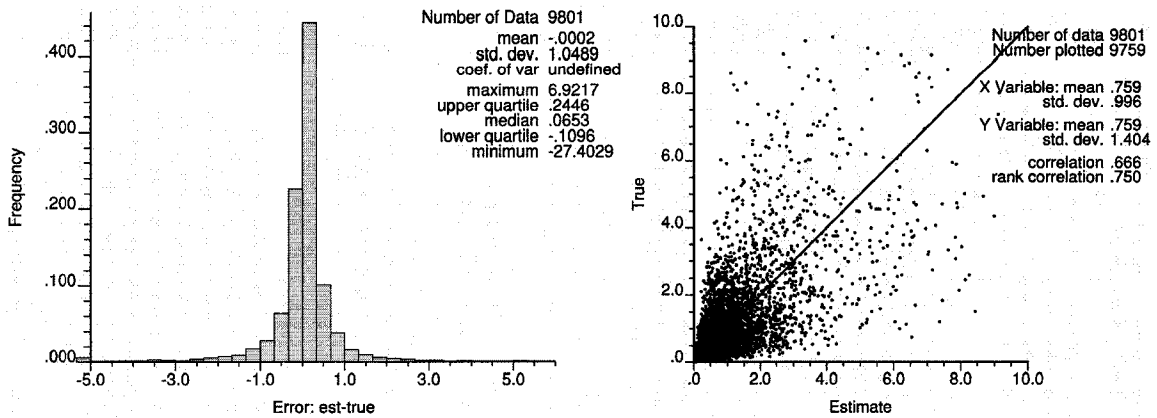


Figure 3.9: Cross validation results for ordinary kriging of blasthole data for reference 5m results.

3.5 Change of Support

Change of support or block size has an impact on the variance of the grade distribution in the field. As the support size increases the variance goes down. To understand and incorporate this phenomenon in the estimation one of the change of support models, i.e. discrete Gaussian method is discussed here.

Discrete Gaussian model results are compared to ordinary kriging estimated model at global scale. Different support sizes of 5m×5m, 10m×10m, 20m×20m are considered.

The ordinary kriging model shows almost the same results for all support sizes due to the smoothing effect of kriging, whereas the discrete Gaussian method shows an impact of change of support size on the grade and tonnage.

Ordinary kriging with 3 data has a good match with the discrete Gaussian model. As the number of data used in kriging increases to 9, the ordinary kriging results goes farther from the discrete Gaussian model, especially at higher cutoff grades (Figure 3.10). It looks that with less number of data in ordinary kriging, we get more variance as desired but mean squared error increases.

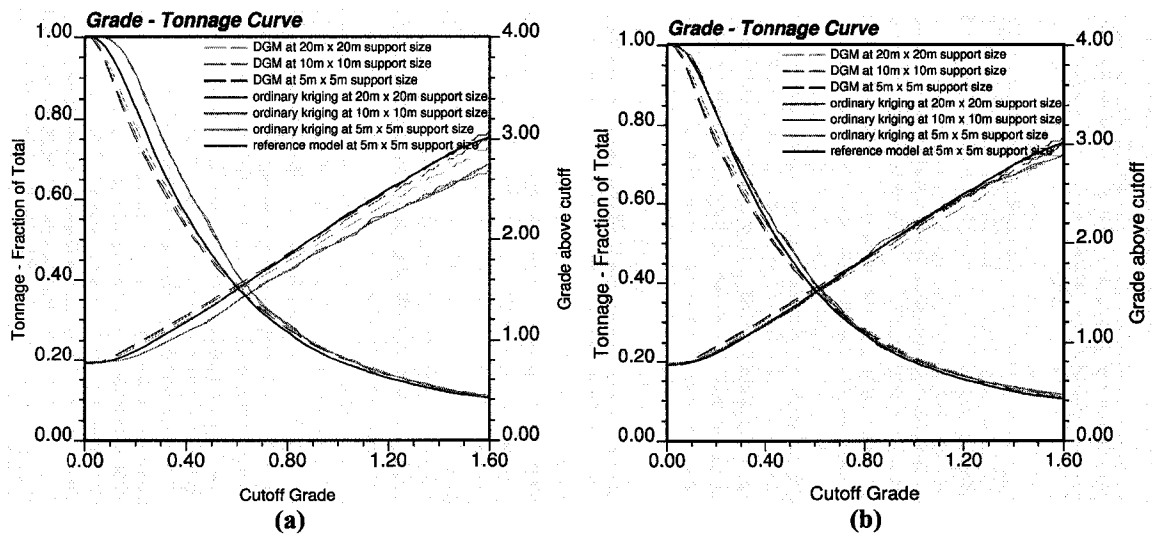


Figure 3.10: Grade-tonnage comparison for discrete Gaussian model and ordinary kriging models (a) Ordinary kriging with 9 data (b) Ordinary kriging with 3 data.

3.6 Ordinary Kriging

In case of ordinary kriging with exploration data, an anisotropic search of 500m by 350m and up to 9 data were used for kriging. The panel reference results are calculated by averaging the SMUs grade above cutoff and proportion of SMUs above cutoff within each panel. The proportion represents the quantity of ore within the panel. To check the sensitivity of fitted variogram model, three cases with different variogram models were run as follows:

Case 1

The fitted variogram model as discussed in the variography section (Equation 3.2) was used. The kriged distribution at SMU scale has a mean of 0.77 and standard deviation of 0.86 (Figure 3.11). It shows unbiasedness with the exploration data distribution. Cross validation of the ordinary kriging, with the set parameters shows an error histogram of mean close to zero and an unbiased cross-plot between true and estimates (Figure 3.12).

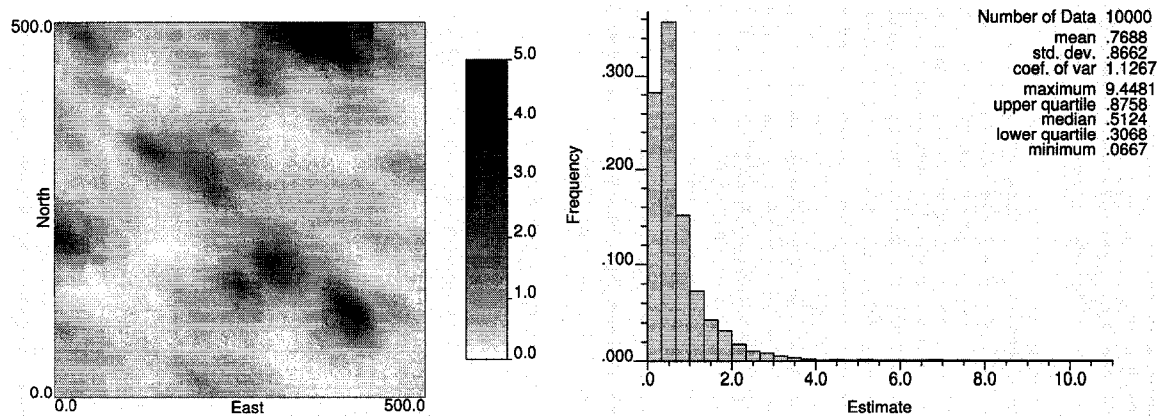


Figure 3.11: Ordinary kriging estimates at 5m x 5m grid interval.

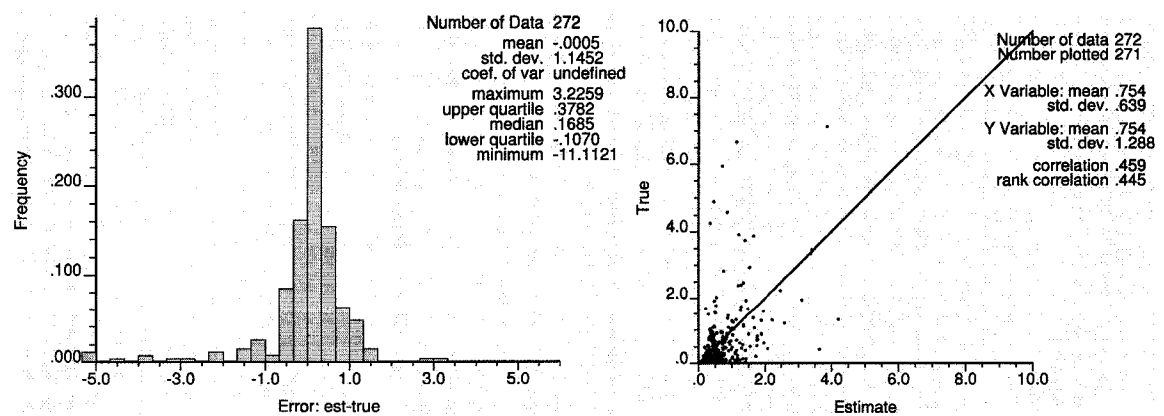


Figure 3.12: Cross validation results for ordinary kriging of exploration data.

Case 2

In this case, the fitted variogram model as discussed in the variography section (Equation 3.2) was used. The kriged distribution at SMU scale has a mean of 0.78 and standard deviation of 0.88 (Figure 3.13). It shows unbiasedness with the exploration data distribution. Cross validation of the ordinary kriging with the set parameters shows an error histogram of mean close to zero and almost unbiased cross-plot between true and estimates (Figure 3.14).

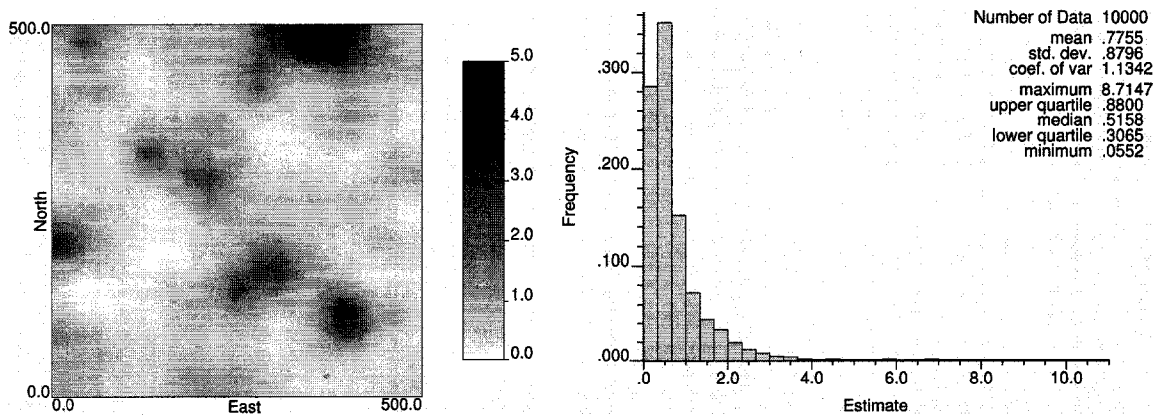


Figure 3.13: Ordinary kriging estimates at 5m x 5m grid interval.

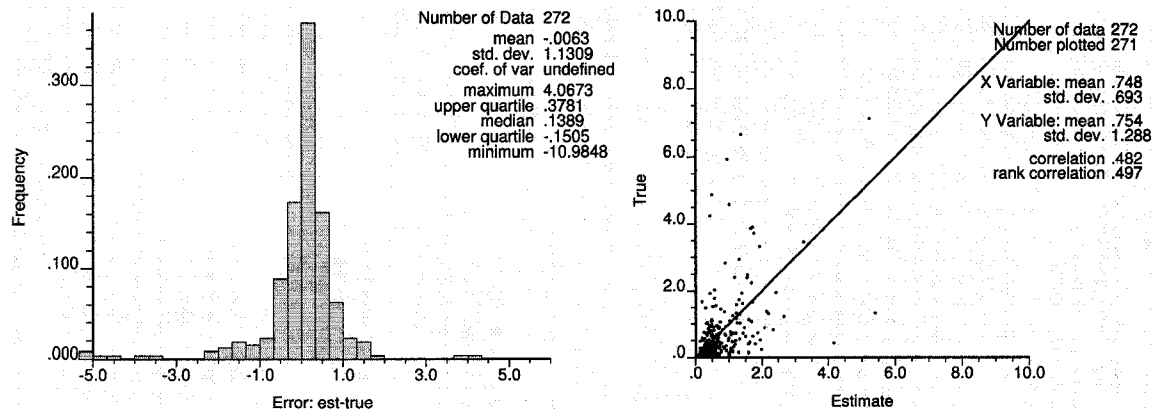


Figure 3.14: Cross validation results for ordinary kriging of exploration data.

Case 3

In this case, the reference variogram model fitted to the blasthole data (Equation 3.1) was used. The kriged distribution at SMU scale has a mean of 0.77 and standard deviation of 0.80 (Figure 3.15). It shows unbiasedness with the exploration data distribution. Cross validation of the ordinary kriging with the set parameters shows an error histogram of mean close to zero and almost unbiased cross-plot between true and estimates (Figure 3.16).

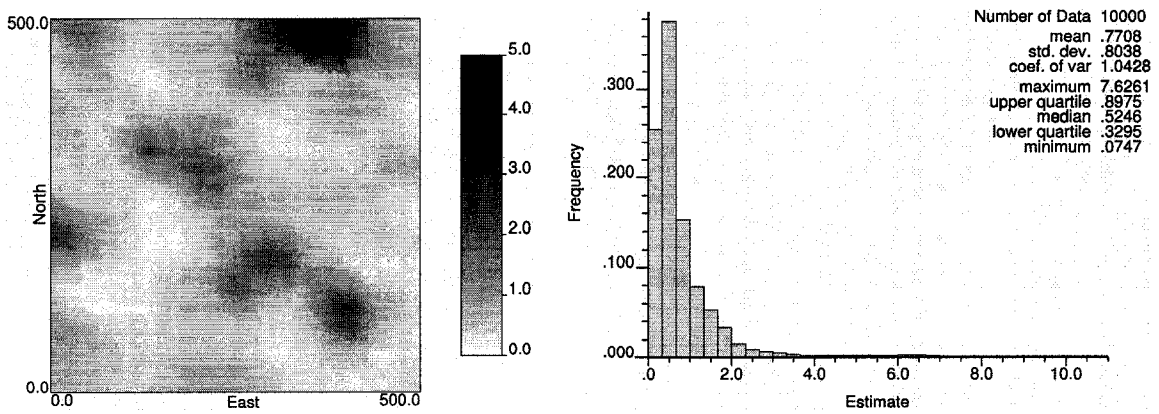


Figure 3.15: Ordinary kriging estimates at 5m × 5m grid interval.

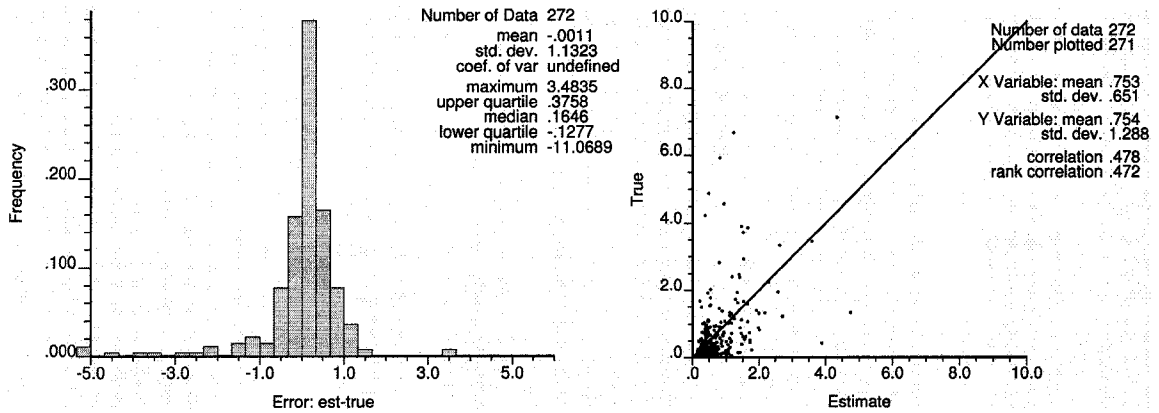


Figure 3.16: Cross validation results for ordinary kriging of exploration data.

3.7 Indicator Kriging

The indicator kriging of exploration data at SMU scale was done considering 9 thresholds at each decile as discussed (Section 3.2). Up to 16 data for kriging and an isotropic search radius of 500m were used. The output was point scale probabilities to be within selected thresholds. This output was post-processed using lognormal volume-support correction with a variance correction factor (f) of 0.76. While post-processing, the upper tail parameter was interpolated with power model (power 0.24) to build the cdf. The power model was chosen after trying different interpolation models, considering good histogram reproduction. The variance correction factor f is calculated by using gammabar value of 0.39, where the gammabar value was calculated with the fitted variogram model to the exploration data and variance of exploration data, i.e. 1.66.

$$f = 1 - \frac{\bar{\gamma}}{\sigma^2} = 1 - \frac{0.39}{1.66} = 0.76$$

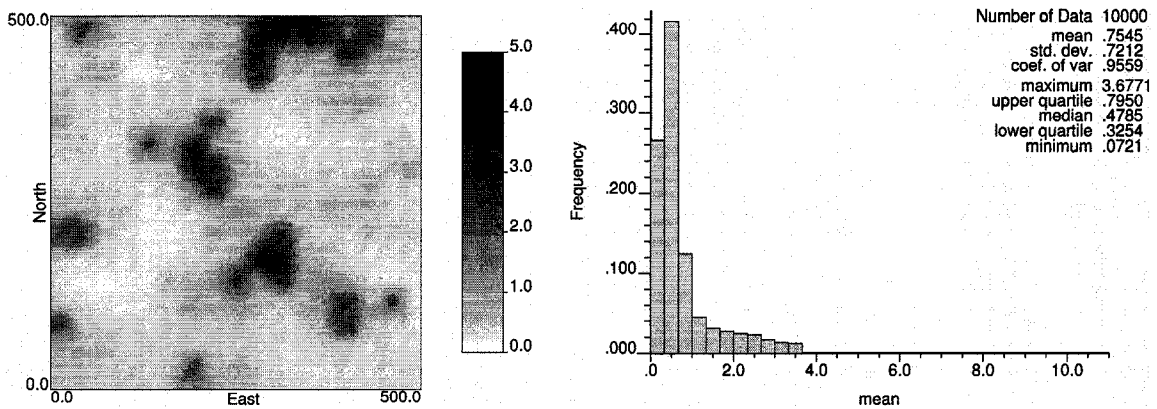


Figure 3.17: Indicator kriging estimates at 5m × 5m grid interval.

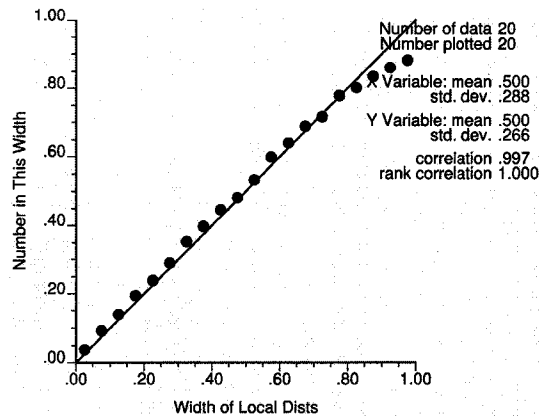


Figure 3.18: Accuracy plot from cross validation results of indicator kriging using exploration data.

The indicator kriged distribution at SMU scale has a mean of 0.75 and standard deviation of 0.72 (Figure 3.17). Cross validation results are plotted on the accuracy plot (Figure 3.18), where all the points are very close and above 45° line, except few at the end intervals. The anisotropy of indicator kriging map does not look as good as of the ordinary kriging cases.

3.8 Simulation

Simulation (SGS) was performed at small scale of 1m × 1m interval. Then, it was block-averaged to the SMU scale. 50 realizations were generated. Histogram and variogram reproduction were checked. The average SMU grade above cutoff and proportion above cutoff within in each panel for every realization was calculated separately. The proportion represents the quantity of ore within the panel. The panel grade and quantity was averaged from all the realizations. To check the sensitivity of variogram, two cases were tried with different variogram models.

Case 1

The fitted variogram model to the normal scored exploration data as discussed in the variography section (Equation 3.13) was used. The variogram reproduction (Figure 3.20) is consistent with the fitted variogram model used in simulation and histogram reproduction (Figure 3.21) also consistent with the declustered exploration data distribution. The block-averaged statistics show unbiasedness of the results with the exploration data (Figure 3.19).

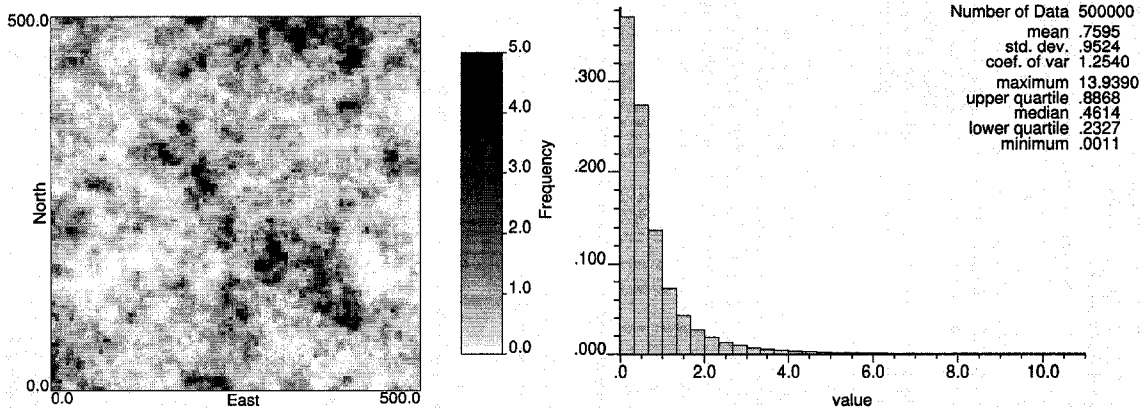


Figure 3.19: Block-averaged 50 realizations statistics and plotted one of the realizations.

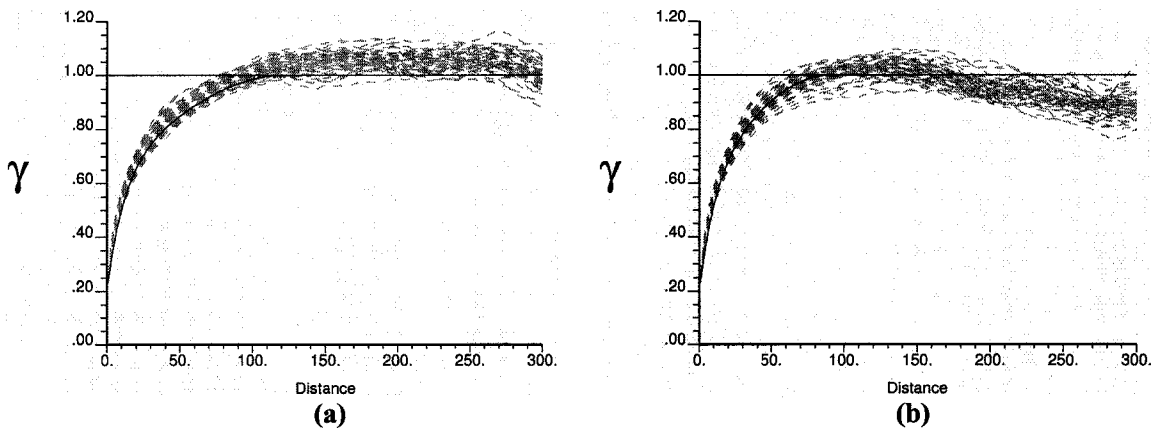


Figure 3.20: Reproduction of variograms from 50 realizations generated by SGS at $1\text{m} \times 1\text{m}$ grid interval. (a) principal direction (b) perpendicular direction.

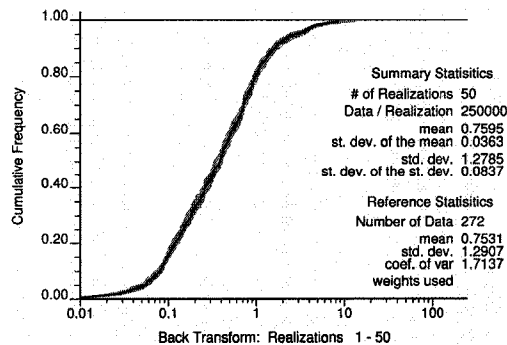


Figure 3.21: Reproduction of histograms from 50 realizations generated by SGS at $1\text{m} \times 1\text{m}$ grid interval.

Case 2

In this case, the fitted variogram to normal scored exploration data (Equation 3.14) was used. The histogram reproduction (Figure 3.24) looks good, but variogram reproduction (Figure 3.23) is better in the previous case. The block-averaged statistics show unbiasedness of the results with the exploration data (Figure 3.22).

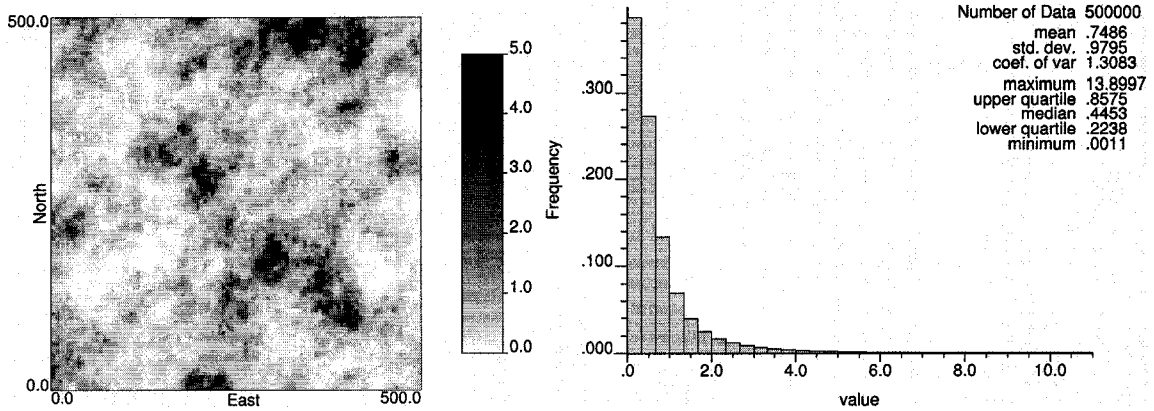


Figure 3.22: Block-averaged 50 realizations statistics and plotted one of the realizations.

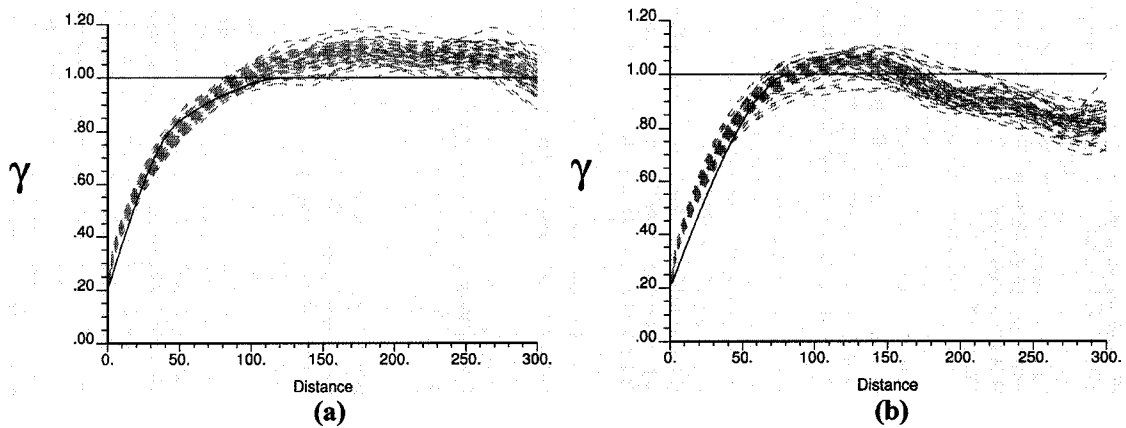


Figure 3.23: Reproduction of variograms from 50 realizations generated by SGS at 1m x 1m grid interval. (a) principal direction (b) perpendicular direction.

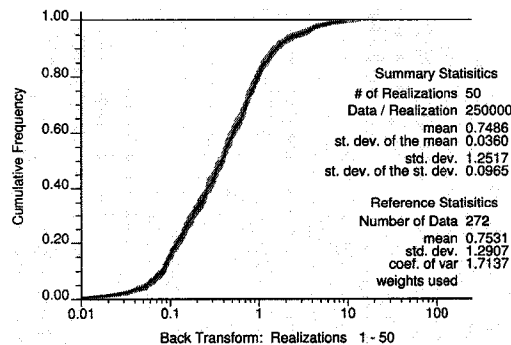


Figure 3.24: Reproduction of histograms from 50 realizations generated by SGS at 1m x 1m grid interval.

3.9 Comparison

The comparison of ordinary kriging results with reference results on scatter-plot at panel scale shows a correlation of around 0.85 for proportion and around 0.89 for grade comparison, in three different cases of ordinary kriging (Figures 3.25, 3.26 and 3.27). Cases 1 and 2 are better than Case 3 in both grade and proportion comparison because of less bias. Between Case 1 and 2, the first case is better than the second one, in both proportion and grade comparison, in terms of correlation, mean squared error (MSE) and mean absolute error (MAE). See also Tables 3.1 and 3.2. The error variograms for ordinary kriging estimation errors show a pure nugget behavior as per expectation (Figure 3.31).

The comparison of indicator kriging with the reference results on scatter-plot shows a correlation of 0.86 in proportion comparison and 0.84 in grade comparison for all the panels (Figure 3.28). Indicator kriging gives less bias than ordinary kriging for proportion/quantity comparison, whereas in grade comparison, ordinary kriging results show less bias. While comparing different types of errors (Table 3.1 and Table 3.2); in proportion comparison, indicator kriging shows less error but in grade comparison and correlation comparison, ordinary kriging looks better than indicator kriging. Error variograms for indicator kriging also show nugget behavior (Figure 3.32).

The comparison of SGS results with the reference results on scatter-plot (Figures 29 and 30) show a correlation of 0.93 in proportion and around 0.90 in grade comparison in both the cases with different variograms (Cases 1 and 2). SGS gives maximum correlation in both proportion and grade comparisons, among all the methods dealt in this study. Case 1 shows better results for proportion comparison than Case 2, whereas in grade comparison, Case 2 shows better results than Case 1. Overall, simulation results show less bias than ordinary kriging and indicator kriging results. In the errors comparison (Tables 3.1 and 3.2), simulation shows better results for both proportion and grade estimation. The error variograms for simulation show tendency of pure nugget effect (Figure 3.33).

Table 3.1: Proportion/quantity comparison.

Comparison Criterion	Ordinary Kriging			Indicator Kriging	Simulation (SGS)	
	Case 1	Case 2	Case 3		Case 1	Case 2
mean error	0.071	0.0699	0.1013	0.0519	-0.0034	-0.0173
mean squared error	0.0212	0.0235	0.0291	0.022	0.003	0.0073
mean absolute error	0.115	0.1237	0.1329	0.1157	0.0746	0.0641
correlation	0.864	0.85	0.845	0.862	0.933	0.933
rank correlation	0.837	0.845	0.838	0.872	0.93	0.917

Table 3.2: Grade comparison.

Comparison Criterion	Ordinary Kriging			Indicator Kriging	Simulation (SGS)	
	Case 1	Case 2	Case 3		Case 1	Case 2
mean error	-0.0836	-0.0705	-0.1149	-0.087	0.0517	0.0278
mean squared error	0.0568	0.0645	0.0622	0.0791	0.0623	0.0449
mean absolute error	0.1974	0.2042	0.2	0.1925	0.2019	0.1703
correlation	0.898	0.885	0.897	0.839	0.901	0.902
rank correlation	0.774	0.768	0.794	0.825	0.768	0.745

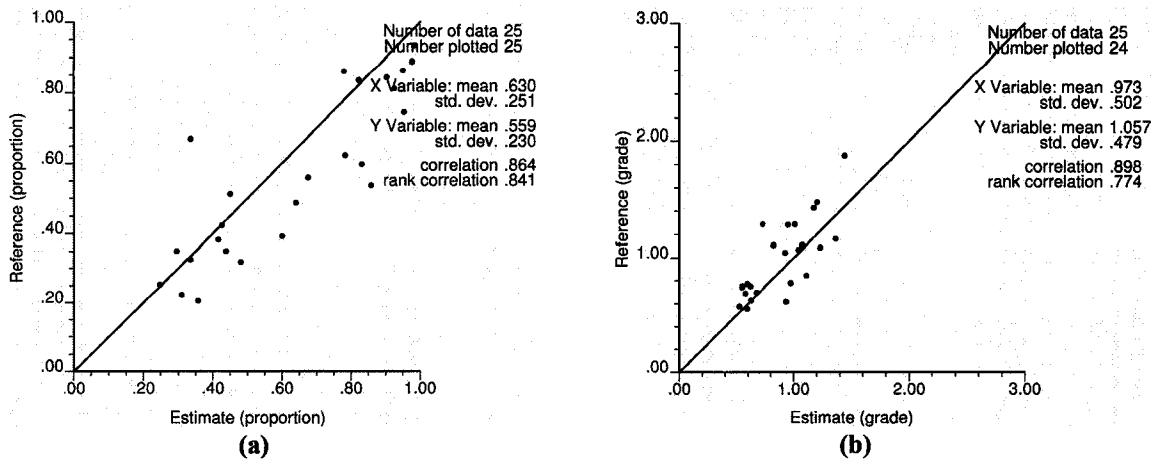


Figure 3.25: Comparison of ordinary kriging (Case 1) with reference results (a) proportion (b) grade.

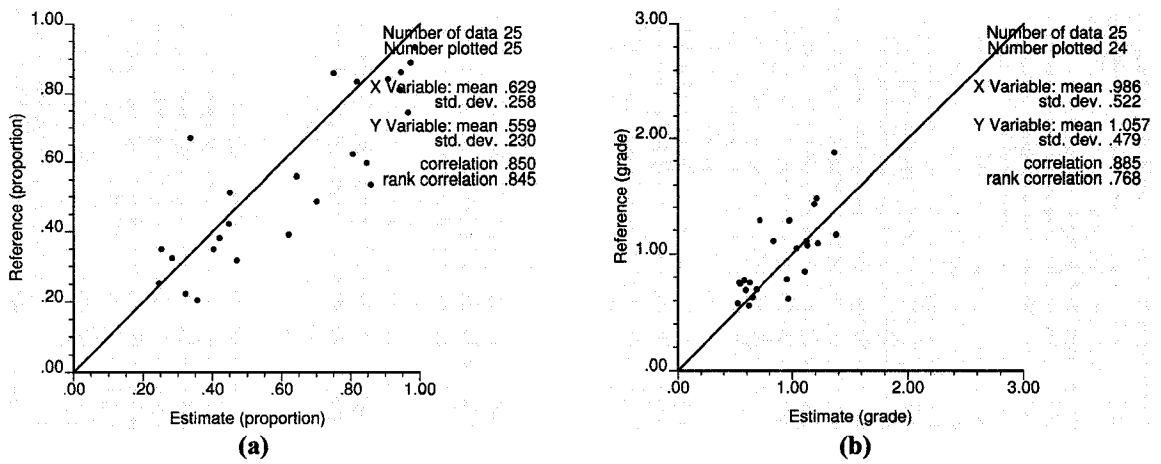


Figure 3.26: Comparison of ordinary kriging (Case 2) with reference results (a) proportion (b) grade.

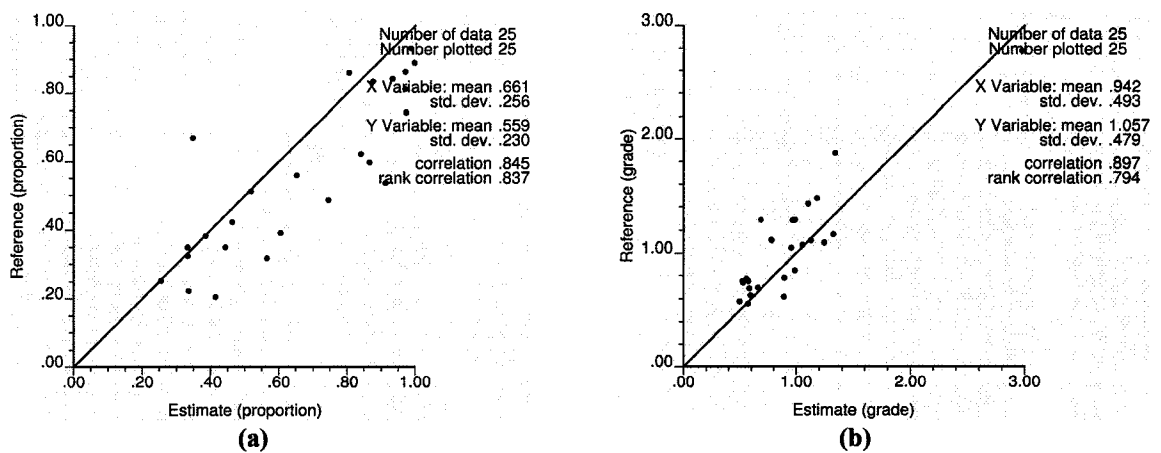


Figure 3.27: Comparison of ordinary kriging (Case 3) with reference results (a) proportion (b) grade.

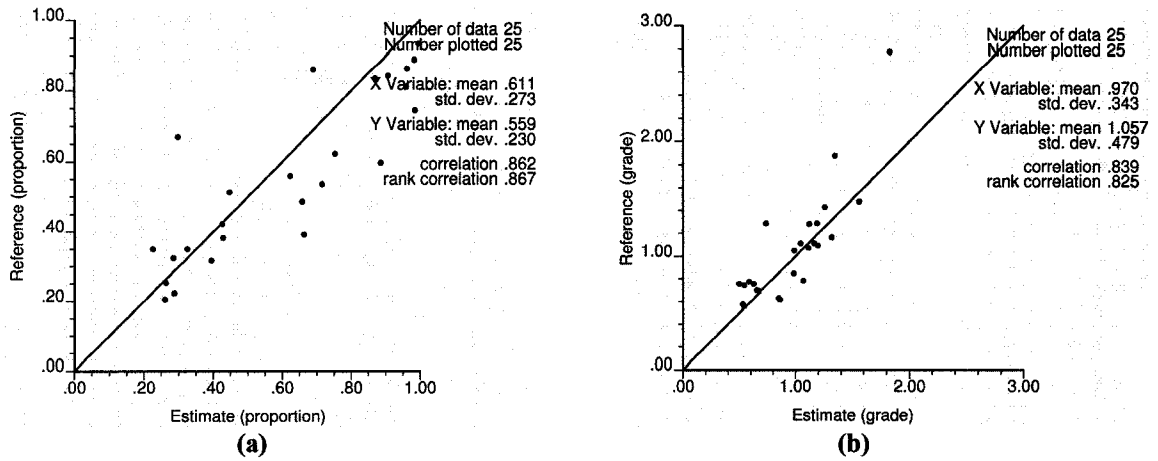


Figure 3.28: Comparison of indicator kriging with reference results (a) proportion (b) grade.

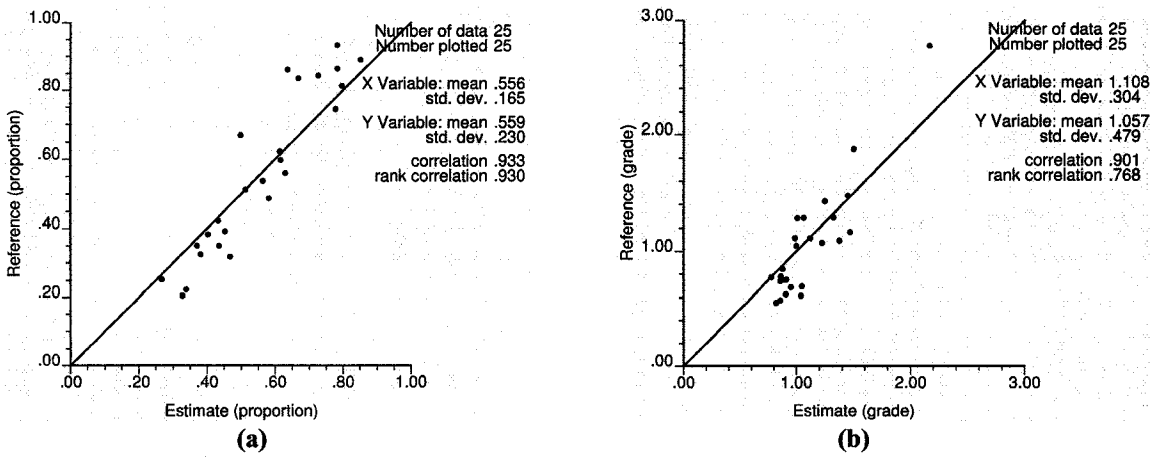


Figure 3.29: Comparison of SGS (Case 1) with reference results (a) proportion (b) grade.

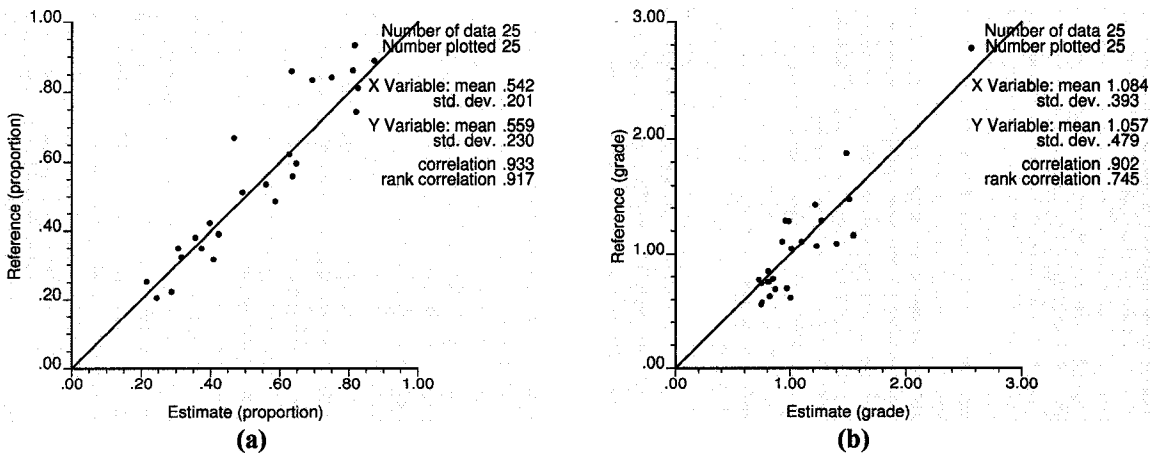


Figure 3.30: Comparison of SGS (Case 2) with reference results (a) proportion (b) grade.

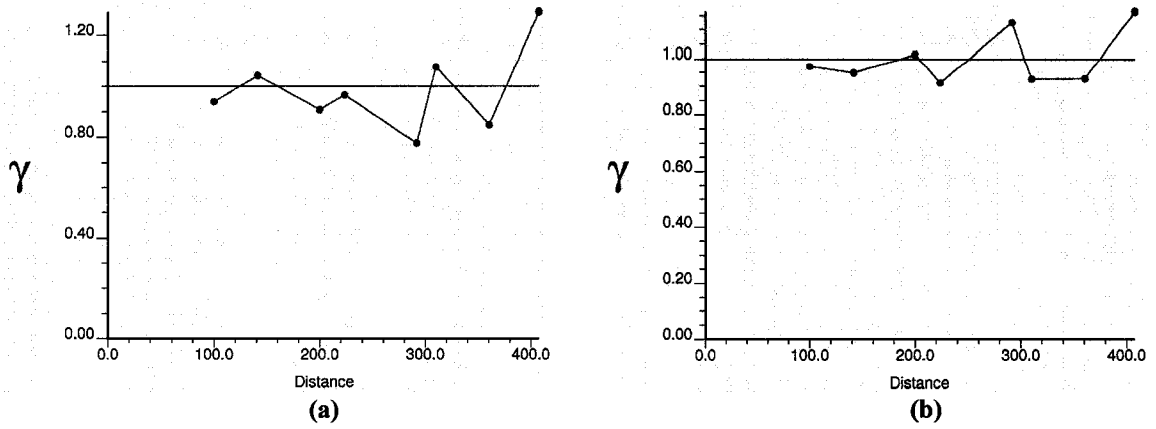


Figure 3.31: Error variograms for ordinary kriging comparison with reference results (a) proportion (b) grade.

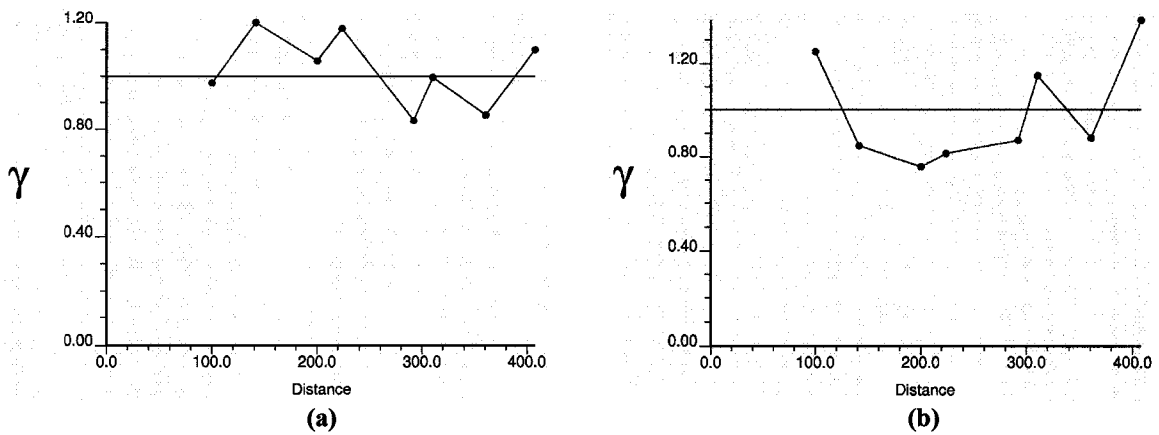


Figure 3.32: Error variograms for indicatory kriging comparison with reference results (a) proportion (b) grade.

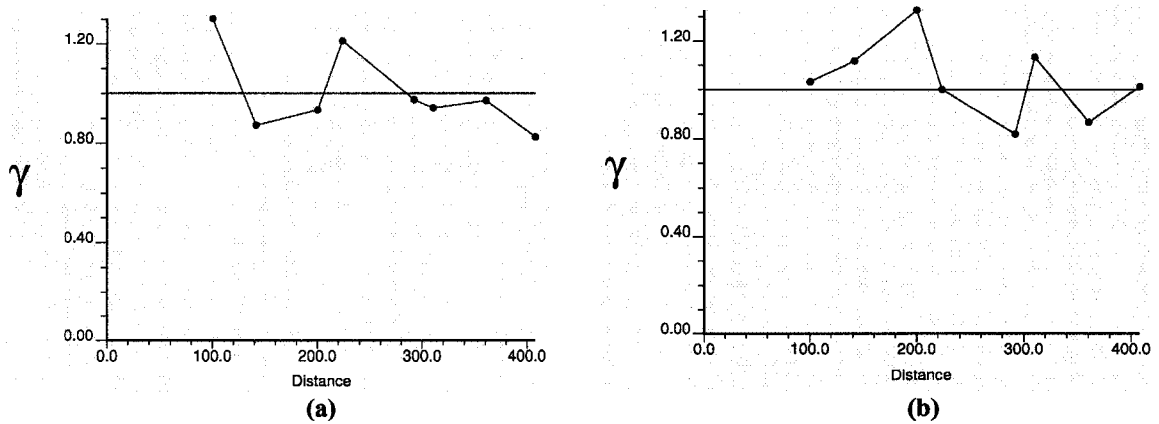


Figure 3.33: Error variograms for SGS comparison with reference results (a) proportion (b) grade.

Chapter 4

Comparative Case Study – A Real Data Example

The case is from Misima open pit gold/silver mine, lies in the east of Misima Island, 200km east of mainland Papua New Guinea (PNG). Mining ended at Misima in 2001. In the deposit both gold and silver mineralization occurs in quartz and breccia zones. The mineralization is disseminated throughout highly fractured host rocks including microgranite intrusions, low grade metamorphic schists and green schists.

A panel-wise comparative study of different estimation techniques, i.e. ordinary kriging, indicator kriging and simulation using the real field data information is performed. The available information is from exploration data and blasthole data. All the methods are compared with the reference results. The reference results are setup using blasthole data.

4.1 Data

The data for the case study are of two types. One is exploratory data, which has sampled information from 943 drill holes in the domain. Another one is blastholes sample information which is exhaustive and closely spaced in nature. All the sample data are defined by easting, northing and elevation for their spatial locations (Figure 4.1). The data consist of gold and silver grade at those locations.

The blasthole data histograms have skewed distribution; appear lognormal for both gold and silver grades (Figure 4.2). The gold grade distribution has a mean of 0.72 and standard deviation of 1.48. The silver grade distribution shows a mean of 10.80 and standard deviation of 24.63. There are 165867 data in the domain. The data are closely spaced in particular zones.

Cell declustering (Figure 4.3) of blasthole data with an arbitrary cell size of 25m gives the declustered distribution of a mean 0.65 and standard deviation of 1.34 for gold grade. The declustered silver grade distribution has a mean of 8.96 and standard deviation of 21.18.

The exploration data histograms also have skewed distribution; appear lognormal for both gold and silver grades (Figure 4.4). The gold grade distribution shows a mean of 0.45 and standard deviation of 1.29. The silver grade distribution shows a mean of 5.43

and standard deviation of 14.37. There are 31996 data in the domain, which are relatively widely spaced and scattered.

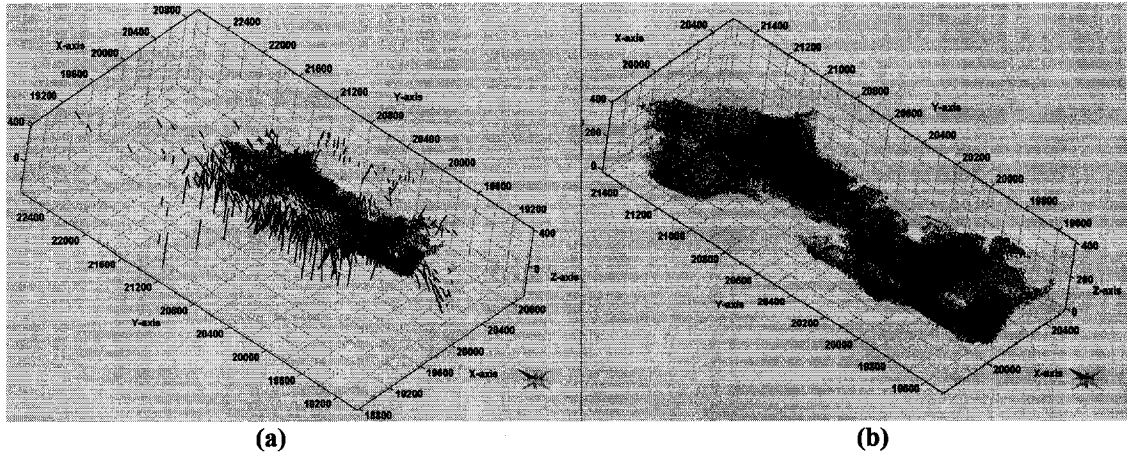


Figure 4.1: Location of blasthole (light dots) and exploration data (dark dots) (a) all the data (b) exploration data with a constrained search of 7m from blast hole data.

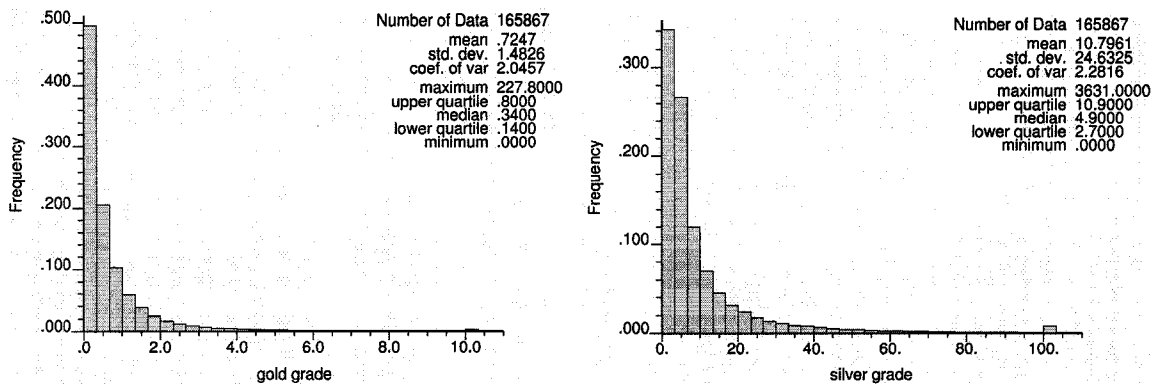


Figure 4.2: Histogram plots of gold and silver grades of blasthole data.

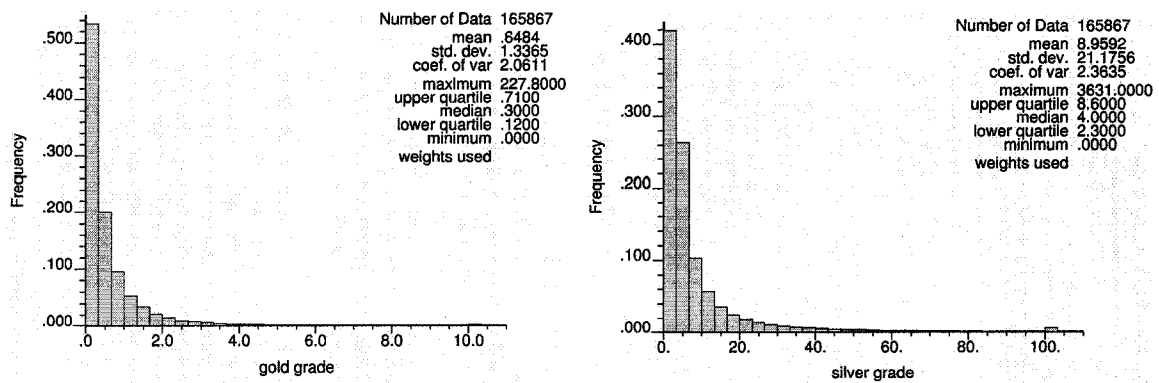


Figure 4.3: Cell declustering of gold and silver grades of blasthole data with a cell size of 25m.

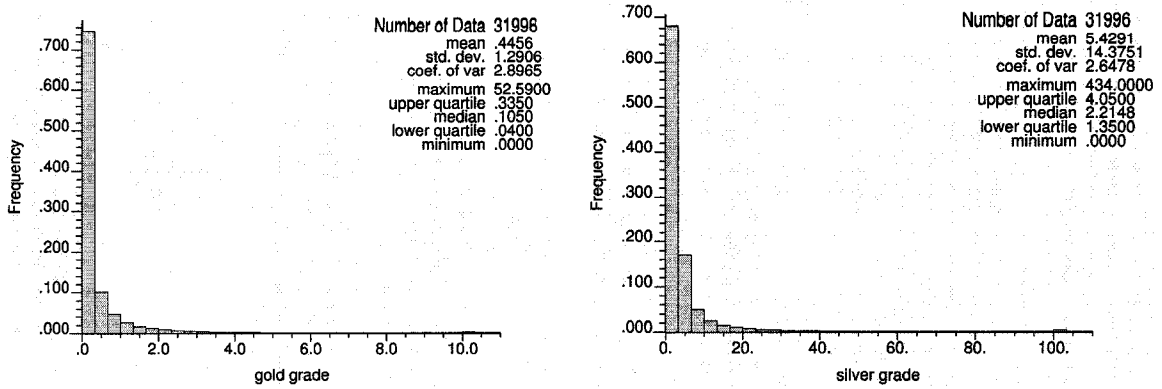


Figure 4.4: Histogram plots of gold and silver grades of exploration data.

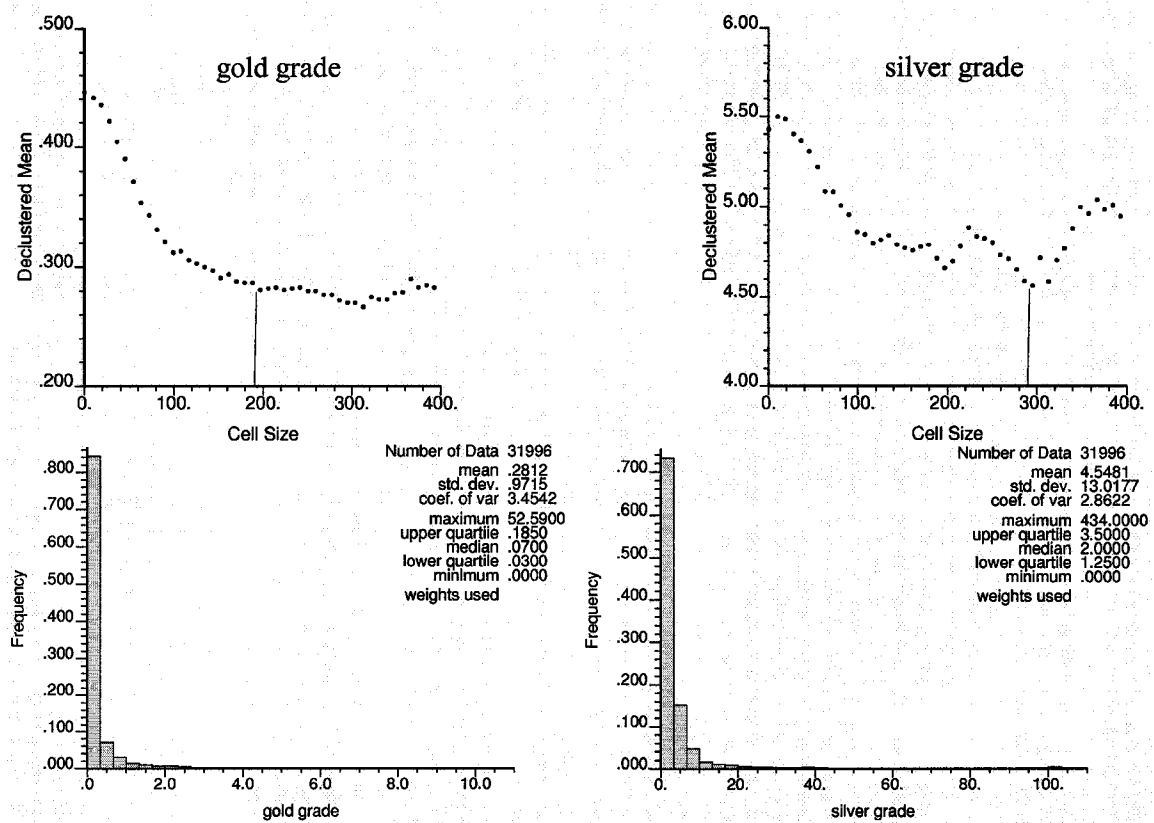


Figure 4.5: Cell declustering of gold (cell size 195m) and silver grades (cell size 295m) of exploration data.

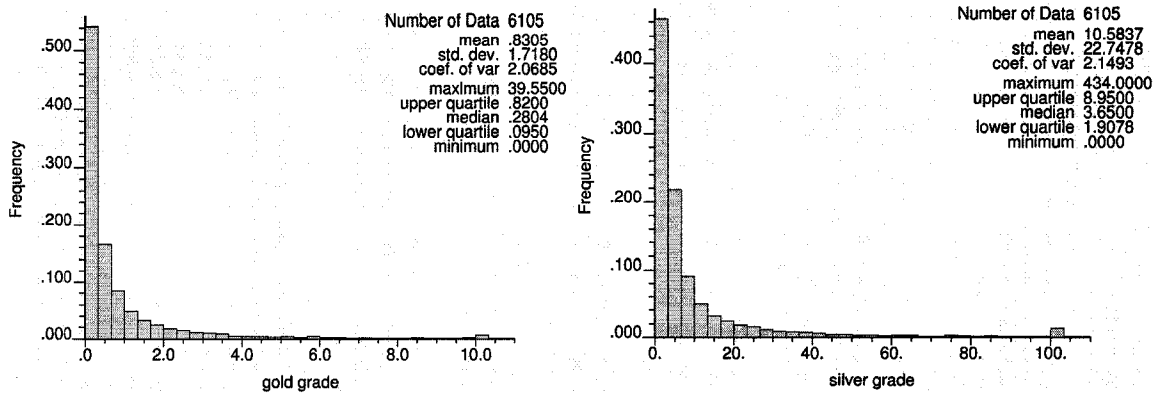


Figure 4.6: Histogram plots of exploration data that are in close proximity (7m radius) of blasthole data for both gold and silver grades.

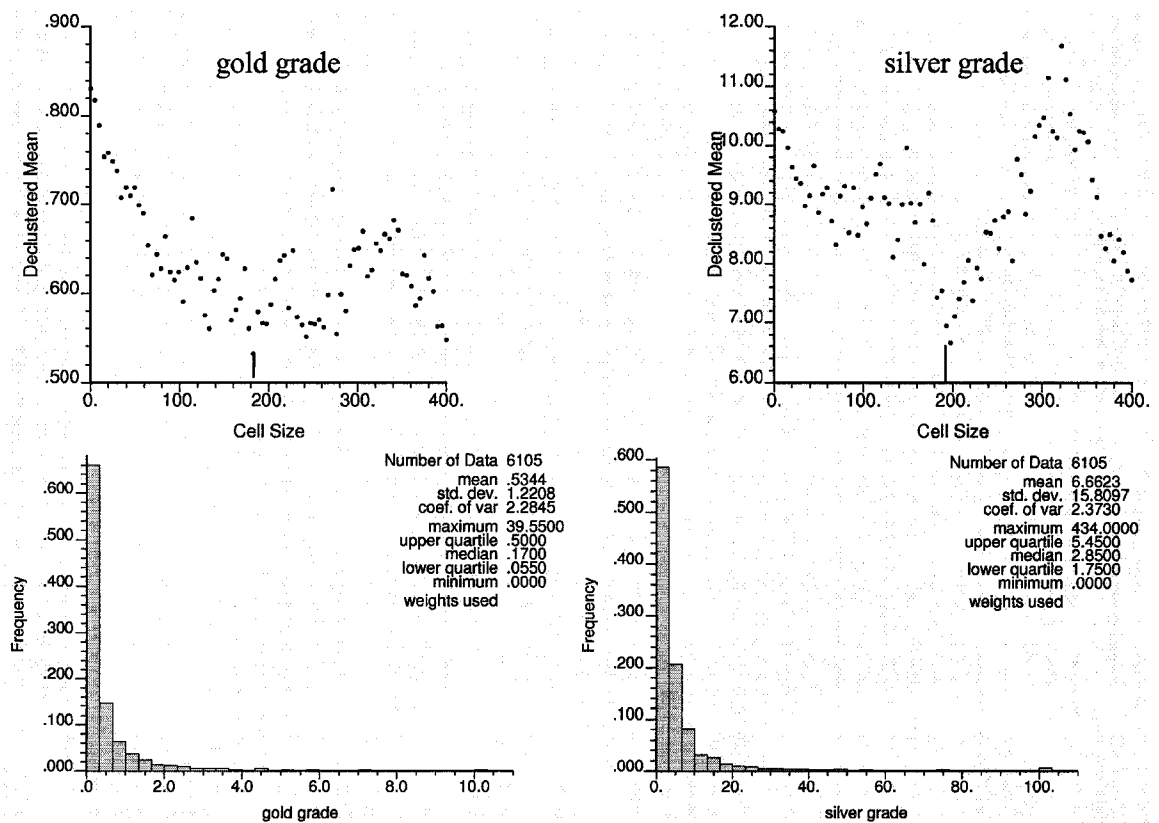


Figure 4.7: Cell declustering of gold (cell size 182m) and silver grades (cell size 197.5m) of exploration data that are in close proximity (7m radius) of blasthole data.

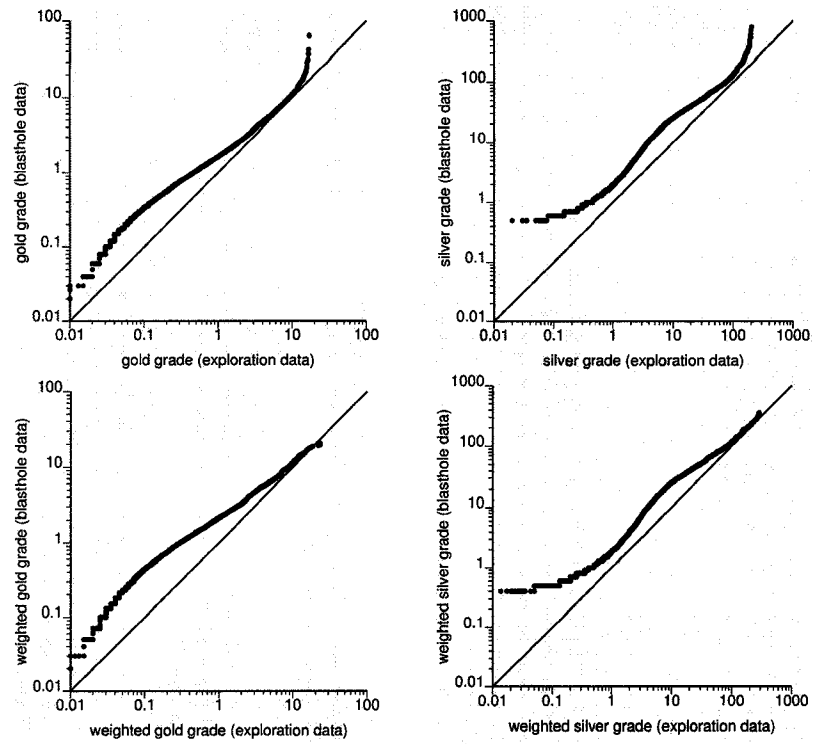


Figure 4.8 (a): QQ-plot of all blasthole and exploration data.

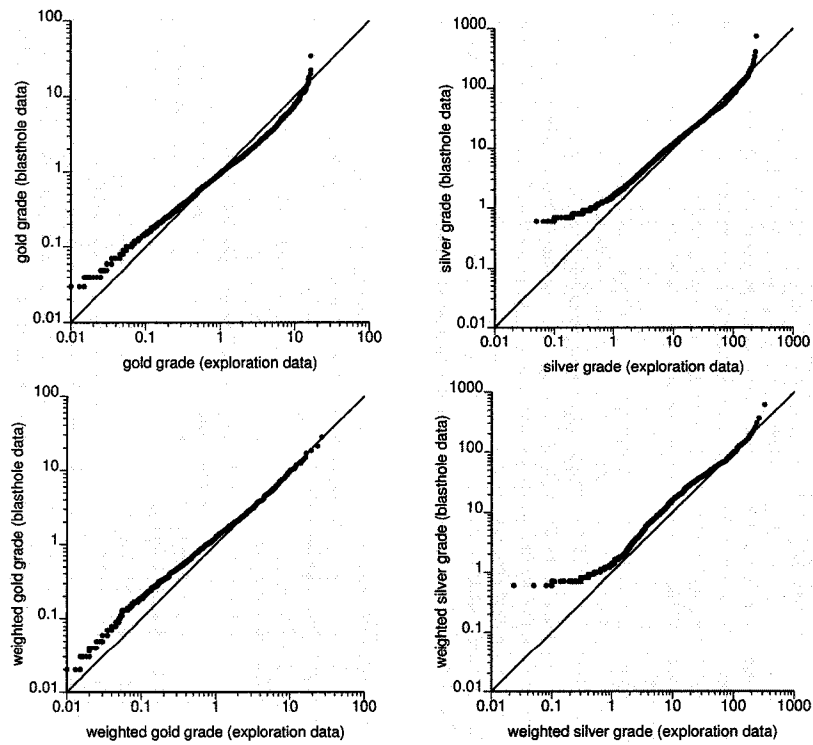


Figure 4.8 (b): QQ-plot of all blasthole data and exploration data that are in close proximity (7m radius) of blast-hole data.

Different cell sizes were tried for both gold and silver exploration grades declustering to reduce the bias between simulated and reference results. Cell declustering (Figure 4.5) of exploration data with a cell size of 195m for gold and 295m for silver variable give a mean of 0.28, standard deviation of 0.97 for gold grade distribution and a mean of 4.55, standard deviation of 13.02 for silver grade distribution.

The spatial distribution of exploration and blasthole data (Figure 1(a)) shows that a big part of the domain has both blasthole and exploration data information, a considerable part has exploration data but no blasthole data are available; areas that were not mined. Exploration data in these zones are distributed in a scattered manner. These far and scattered exploration data cause inconsistency while comparing with the blasthole data distribution. The QQ-plots (Figure 4.8 (a)); both using declustered weights and without using weights show a difference between exploration and blasthole data for both gold and silver grades. To reduce this difference, exploration data within a 7m search radius to blasthole data (Figure 4.1(b)) are taken. These close exploration data histograms also have skewed lognormal like distributions for both gold and silver grades (Figure 4.6). The gold grade distribution shows a mean of 0.83 and standard deviation of 1.72. The silver grade distribution shows a mean of 10.58 and standard deviation of 22.75. There are 6105 close exploration data in the domain.

Different cell sizes were tried for both close gold and silver exploration grades declustering to reduce the bias between simulated and reference results. Cell declustering (Figure 4.7) of these close exploration data with a cell size of 182m for gold and 197.5m for silver variable give the mean of 0.53, standard deviation of 1.22 for gold grade distribution and a mean of 6.66, standard deviation of 15.81 for silver grade distribution. QQ-plot of these exploration data and the blasthole data distribution (Figure 4.8 (b)) shows that the bias is reduced to a considerable extent.

4.2 Parameters and Criterion for Comparative Study

The SMU size, panel size, and cutoff grade must be chosen. The domain is defined where both blasthole and exploration data are available (Figure 4.1 (b)). In the domain of 2200m × 1100m × 500m, each panel size is defined as 100m × 100m × 20m considering the excavation of around 200000m³/month; a panel gives excavation of around one month. The SMU size depends on available equipments, type of mining, shape & size of the deposit. In mining the SMU size generally vary between 5m × 5m × 5m and 25m × 25m × 25m. The available blasthole data spacing ranges from around 3m to 20m. The SMU size is defined as 20m × 20m × 20m in this case study so that there are more chances that each SMU has at least one blasthole datum [1]. The cutoff grade is taken as 1g/t of gold equivalent grade, a figure representative of the practical cutoff grades (0.7 g/t for soft ore and 1.3 g/t for hard ore). The formula for gold equivalent grade calculation is:

$$z_v^*(\mathbf{u}_j) = x_v^*(\mathbf{u}_j) + y_v^*(\mathbf{u}_j) \frac{P_y r f_y}{P_x r f_x} \quad (4.1)$$

where, $x_v^*(\mathbf{u}_j)$ for the first (gold) variable grade, $y_v^*(\mathbf{u}_j)$ for the second (silver) variable grade and $z_v^*(\mathbf{u}_j)$ for the gold equivalent variable grade calculated from the first and the second variables at SMU scale, P_y is price for silver, P_x is price for gold, $r f_y$ is recovery

factor for silver and rf_x is the recover factor for gold. The price of gold is assumed as \$592.80/ounce and the price of silver is assumed as \$11.29/ounce. The recovery factor for both gold and silver is assumed equal (100%), that gives a ratio of gold and silver recovery factors as 1. The ratio of gold and silver price is 52.51. These two ratio factors are used to calculate the gold equivalent grade.

In the calculation of ore tonnage, gold equivalent cutoff grade is considered, which has combined information of both gold and silver grades in terms of gold grade. Even if gold is of low grade but there might be high silver grade, and together it makes an economic mining unit. The proportion of ore for individual panels is calculated. Specific gravity of 2.7 t/m³ (a feasible specific gravity for deposits having quartz and breccia as host rocks) and an assumed recovery factor of 0.85 (considering spillage and dilution in mining) are applied for converting it in to recoverable ore tonnage.

Indicator kriging requires the number of thresholds to be chosen. Thresholds at each decile are taken for this purpose, so there are 9 thresholds: 0.025, 0.035, 0.05, 0.07, 0.105, 0.16, 0.255, 0.46 and 1.015, respectively for gold data. Similarly, 9 threshold values for silver data are 0.8, 1.2, 1.5, 1.85, 2.2175, 2.7, 3.485, 5.0 and 9.5, respectively.

In a panel, gold grade, silver grade and gold equivalent grade are calculated as grade average of all SMUs above gold equivalent cutoff grade (1 g/t) within that panel. In the same panel, proportion is the ratio of SMUs considered as ore and total number of SMUs within that panel. All the panel estimates from different estimation techniques are compared to the reference values of those panels on the criterion of unbiasedness, correlation between true and estimates, mean error (ME), mean squared error (MSE) and mean absolute error (MAE). The comparative study is done for ore quantity, gold equivalent grade, gold quantity, gold grade, silver quantity and silver grade.

4.3 Variography Analysis

The major direction of continuity for gold and silver was taken as -10° azimuth, minor direction is at 80° azimuth and vertical direction has 90° of dip for both blasthole and exploration data [3]. Variogram maps are shown in Figure 9.

The variogram model for gold grade and silver grade of blasthole data (Figure i; APPENDIX III) are (reference variograms):

$$\gamma(\mathbf{h})_{gold} = 0.47 + 0.53 \exp_{\substack{h \max=57 \\ h \min=20 \\ h \text{vert}=20}}(\mathbf{h}) \quad (4.2)$$

$$\gamma(\mathbf{h})_{silver} = 0.3 + 0.7 \exp_{\substack{h \max=40 \\ h \min=20 \\ h \text{vert}=32}}(\mathbf{h}) \quad (4.3)$$

The variogram model for gold grade and silver grade of exploration data (Figure ii; APPENDIX III) were fitted considering better cross validation results for ordinary kriging. These variograms models are as follows [3]:

$$\gamma(\mathbf{h})_{gold} = 0.25 + 1.12 \exp_{\substack{h \max=85 \\ h \min=60 \\ h \text{vert}=17}}(\mathbf{h}) + 0.3sph_{\substack{h \max=440 \\ h \min=120 \\ h \text{vert}=250}}(\mathbf{h}) \quad (4.4)$$

$$\gamma(\mathbf{h})_{silver} = 20 + 152 \exp_{\substack{h_{max}=63 \\ h_{min}=75 \\ h_{vert}=50}}(\mathbf{h}) + 34 sph_{\substack{h_{max}=1120 \\ h_{min}=90 \\ h_{vert}=200}}(\mathbf{h}) \quad (4.5)$$

For indicator kriging, individual threshold variograms were calculated in -10° azimuth direction as principal (major) direction, 80° azimuth direction as perpendicular (minor) and 90° dip as vertical direction. The variogram models for each threshold of gold exploration data are (APPENDIX IV):

$$\text{Threshold 1 (0.025) at 0.1 decile } \gamma(\mathbf{h})_{gold} = 0.19 + 0.43 \exp_{\substack{h_{max}=48 \\ h_{min}=8 \\ h_{vert}=8}}(\mathbf{h}) + 0.38 sph_{\substack{h_{max}=1050 \\ h_{min}=350 \\ h_{vert}=80}}(\mathbf{h}) \quad (4.6)$$

$$\text{Threshold 2 (0.035) at 0.2 decile } \gamma(\mathbf{h})_{gold} = 0.2 + 0.4 \exp_{\substack{h_{max}=48 \\ h_{min}=8 \\ h_{vert}=8}}(\mathbf{h}) + 0.4 sph_{\substack{h_{max}=1050 \\ h_{min}=350 \\ h_{vert}=150}}(\mathbf{h}) \quad (4.7)$$

$$\text{Threshold 3 (0.05) at 0.3 decile } \gamma(\mathbf{h})_{gold} = 0.45 + 0.2 \exp_{\substack{h_{max}=170 \\ h_{min}=150 \\ h_{vert}=35}}(\mathbf{h}) + 0.35 sph_{\substack{h_{max}=1050 \\ h_{min}=300 \\ h_{vert}=200}}(\mathbf{h}) \quad (4.8)$$

$$\text{Threshold 4 (0.07) at 0.4 decile } \gamma(\mathbf{h})_{gold} = 0.2 + 0.38 \exp_{\substack{h_{max}=25 \\ h_{min}=15 \\ h_{vert}=15}}(\mathbf{h}) + 0.42 sph_{\substack{h_{max}=900 \\ h_{min}=270 \\ h_{vert}=180}}(\mathbf{h}) \quad (4.9)$$

$$\text{Threshold 5 (0.105) at 0.5 decile } \gamma(\mathbf{h})_{gold} = 0.2 + 0.4 \exp_{\substack{h_{max}=25 \\ h_{min}=15 \\ h_{vert}=15}}(\mathbf{h}) + 0.4 sph_{\substack{h_{max}=650 \\ h_{min}=245 \\ h_{vert}=180}}(\mathbf{h}) \quad (4.10)$$

$$\text{Threshold 6 (0.16) at 0.6 decile } \gamma(\mathbf{h})_{gold} = 0.25 + 0.42 \exp_{\substack{h_{max}=45 \\ h_{min}=20 \\ h_{vert}=25}}(\mathbf{h}) + 0.33 sph_{\substack{h_{max}=550 \\ h_{min}=200 \\ h_{vert}=280}}(\mathbf{h}) \quad (4.11)$$

$$\text{Threshold 7 (0.255) at 0.7 decile } \gamma(\mathbf{h})_{gold} = 0.28 + 0.42 \exp_{\substack{h_{max}=35 \\ h_{min}=35 \\ h_{vert}=35}}(\mathbf{h}) + 0.3 sph_{\substack{h_{max}=325 \\ h_{min}=90 \\ h_{vert}=325}}(\mathbf{h}) \quad (4.12)$$

$$\text{Threshold 8 (0.46) at 0.8 decile } \gamma(\mathbf{h})_{gold} = 0.45 + 0.35 \exp_{\substack{h_{max}=20 \\ h_{min}=35 \\ h_{vert}=140}}(\mathbf{h}) + 0.2 sph_{\substack{h_{max}=150 \\ h_{min}=55 \\ h_{vert}=300}}(\mathbf{h}) \quad (4.13)$$

$$\text{Threshold 9 (1.015) at 0.9 decile } \gamma(\mathbf{h})_{gold} = 0.45 + 0.42 \exp_{\substack{h_{max}=25 \\ h_{min}=20 \\ h_{vert}=150}}(\mathbf{h}) + 0.13 sph_{\substack{h_{max}=200 \\ h_{min}=45 \\ h_{vert}=300}}(\mathbf{h}) \quad (4.14)$$

The variogram models for each threshold of silver exploration data are (APPENDIX IV):

$$\text{Threshold 1 (0.8) at 0.1 decile } \gamma(\mathbf{h})_{silver} = 0.5 + 0.35 \exp_{\substack{h_{max}=80 \\ h_{min}=25 \\ h_{vert}=120}}(\mathbf{h}) + 0.15 sph_{\substack{h_{max}=180 \\ h_{min}=160 \\ h_{vert}=150}}(\mathbf{h}) \quad (4.15)$$

$$\text{Threshold 2 (1.2) at 0.2 decile } \gamma(\mathbf{h})_{silver} = 0.47 + 0.39 \exp_{\substack{h_{max}=90 \\ h_{min}=45 \\ h_{vert}=90}}(\mathbf{h}) + 0.14 sph_{\substack{h_{max}=280 \\ h_{min}=150 \\ h_{vert}=150}}(\mathbf{h}) \quad (4.16)$$

$$\text{Threshold 3 (1.5) at 0.3 decile } \gamma(\mathbf{h})_{silver} = 0.44 + 0.38 \exp_{\substack{h \max=70 \\ h \min=5 \\ hvert=80}}(\mathbf{h}) + 0.18 sph_{\substack{h \max=800 \\ h \min=300 \\ hvert=190}}(\mathbf{h}) \quad (4.17)$$

$$\text{Threshold 4 (1.85) at 0.4 decile } \gamma(\mathbf{h})_{silver} = 0.3 + 0.45 \exp_{\substack{h \max=40 \\ h \min=15 \\ hvert=50}}(\mathbf{h}) + 0.25 sph_{\substack{h \max=700 \\ h \min=300 \\ hvert=200}}(\mathbf{h}) \quad (4.18)$$

$$\text{Threshold 5 (2.2175) at 0.5 decile } \gamma(\mathbf{h})_{silver} = 0.21 + 0.49 \exp_{\substack{h \max=25 \\ h \min=15 \\ hvert=30}}(\mathbf{h}) + 0.3 sph_{\substack{h \max=700 \\ h \min=300 \\ hvert=200}}(\mathbf{h}) \quad (4.19)$$

$$\text{Threshold 6 (2.7) at 0.6 decile } \gamma(\mathbf{h})_{silver} = 0.16 + 0.52 \exp_{\substack{h \max=20 \\ h \min=20 \\ hvert=30}}(\mathbf{h}) + 0.32 sph_{\substack{h \max=700 \\ h \min=300 \\ hvert=220}}(\mathbf{h}) \quad (4.20)$$

$$\text{Threshold 7 (3.485) at 0.7 decile } \gamma(\mathbf{h})_{silver} = 0.12 + 0.51 \exp_{\substack{h \max=20 \\ h \min=20 \\ hvert=25}}(\mathbf{h}) + 0.37 sph_{\substack{h \max=650 \\ h \min=230 \\ hvert=250}}(\mathbf{h}) \quad (4.21)$$

$$\text{Threshold 8 (5.0) at 0.8 decile } \gamma(\mathbf{h})_{silver} = 0.17 + 0.47 \exp_{\substack{h \max=30 \\ h \min=30 \\ hvert=45}}(\mathbf{h}) + 0.36 sph_{\substack{h \max=750 \\ h \min=230 \\ hvert=310}}(\mathbf{h}) \quad (4.22)$$

$$\text{Threshold 9 (9.5) at 0.9 decile } \gamma(\mathbf{h})_{silver} = 0.28 + 0.44 \exp_{\substack{h \max=30 \\ h \min=30 \\ hvert=250}}(\mathbf{h}) + 0.28 sph_{\substack{h \max=500 \\ h \min=90 \\ hvert=400}}(\mathbf{h}) \quad (4.23)$$

The variogram model for normal scored gold and silver exploration data in the -10° azimuth direction as principal (major) direction, 80° azimuth direction as perpendicular (minor) and 90° dip as vertical direction are (Figure iii; APPENDIX III):

$$\gamma(\mathbf{h})_{gold} = 0.22 + 0.4 \exp_{\substack{h \max=40 \\ h \min=40 \\ hvert=70}}(\mathbf{h}) + 0.38 sph_{\substack{h \max=1100 \\ h \min=260 \\ hvert=220}}(\mathbf{h}) \quad (4.24)$$

$$\gamma(\mathbf{h})_{silver} = 0.2 + 0.51 \exp_{\substack{h \max=75 \\ h \min=40 \\ hvert=120}}(\mathbf{h}) + 0.29 sph_{\substack{h \max=1200 \\ h \min=350 \\ hvert=240}}(\mathbf{h}) \quad (4.25)$$

The variogram model for normal scored gold and silver close exploration data (within 7m search radius of blasthole data) in the -10° azimuth direction as principal (major) direction, 80° azimuth direction as perpendicular (minor) and 90° dip as vertical direction are (Figure iv; APPENDIX III):

$$\gamma(\mathbf{h})_{gold} = 0.15 + 0.25 sph_{\substack{h \max=10 \\ h \min=10 \\ hvert=10}}(\mathbf{h}) + 0.6 \exp_{\substack{h \max=180 \\ h \min=80 \\ hvert=100}}(\mathbf{h}) \quad (4.26)$$

$$\gamma(\mathbf{h})_{silver} = 0.12 + 0.2 \exp_{\substack{h \max=5 \\ h \min=50 \\ hvert=50}}(\mathbf{h}) + 0.68 \exp_{\substack{h \max=200 \\ h \min=80 \\ hvert=100}}(\mathbf{h}) \quad (4.27)$$

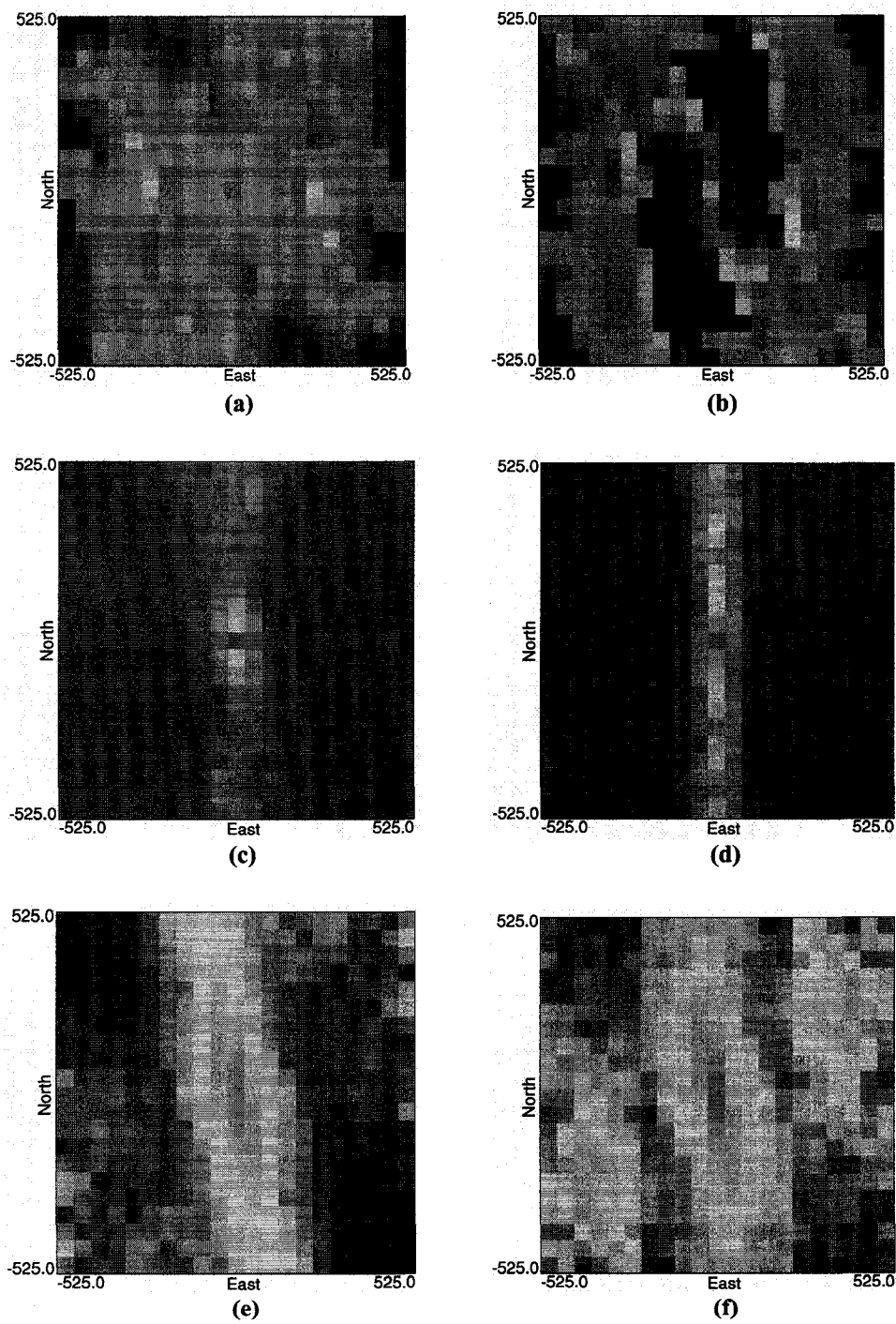


Figure 4.9: Variogram maps for real data. (a) gold blasthole data (b) silver blasthole data (c) gold exploration data (d) silver exploration data (e) normal scored gold exploration data (f) normal scored silver exploration data [3].

4.4 Reference results

The reference results were setup using ordinary kriging of blasthole data with a short search radius of 15m, up to 24 data for kriging and using fitted variogram models (Equations 4.2 and 4.3) to the blasthole data. The kriging was performed at SMU scale (20m × 20m × 20m) for both gold and silver grades separately using 2 × 2 × 2 block discretization. The reference model distribution for gold at SMU scale (Figure 4.10) has a mean of 0.67 and standard deviation of 0.69. The silver reference model distribution at SMU scale has a mean of 9.02 and standard deviation of 12.57.

The cross validation results were calculated by removing every sample then estimate the location with the remaining data. The results (Figure 4.11) show an error histogram of mean zero and an unbiased scatter-plot between true and the estimates with a correlation of 0.44 in gold case and 0.58 in silver case.

Gold equivalent grade at SMU scale was calculated with the gold and silver reference values at that scale (Equation 4.1). The panel reference results calculation was done by averaging the SMUs grade above gold equivalent cutoff grade (1 g/t) and the proportion of SMUs above cutoff within in that panel for gold equivalent, gold and silver. The proportion was converted in to ore volume by multiplying it with the panel volume, followed by multiplying with the specific gravity of 2.7 t/m³ and recovery factor of 0.85 to convert it in to recoverable ore tonnage.

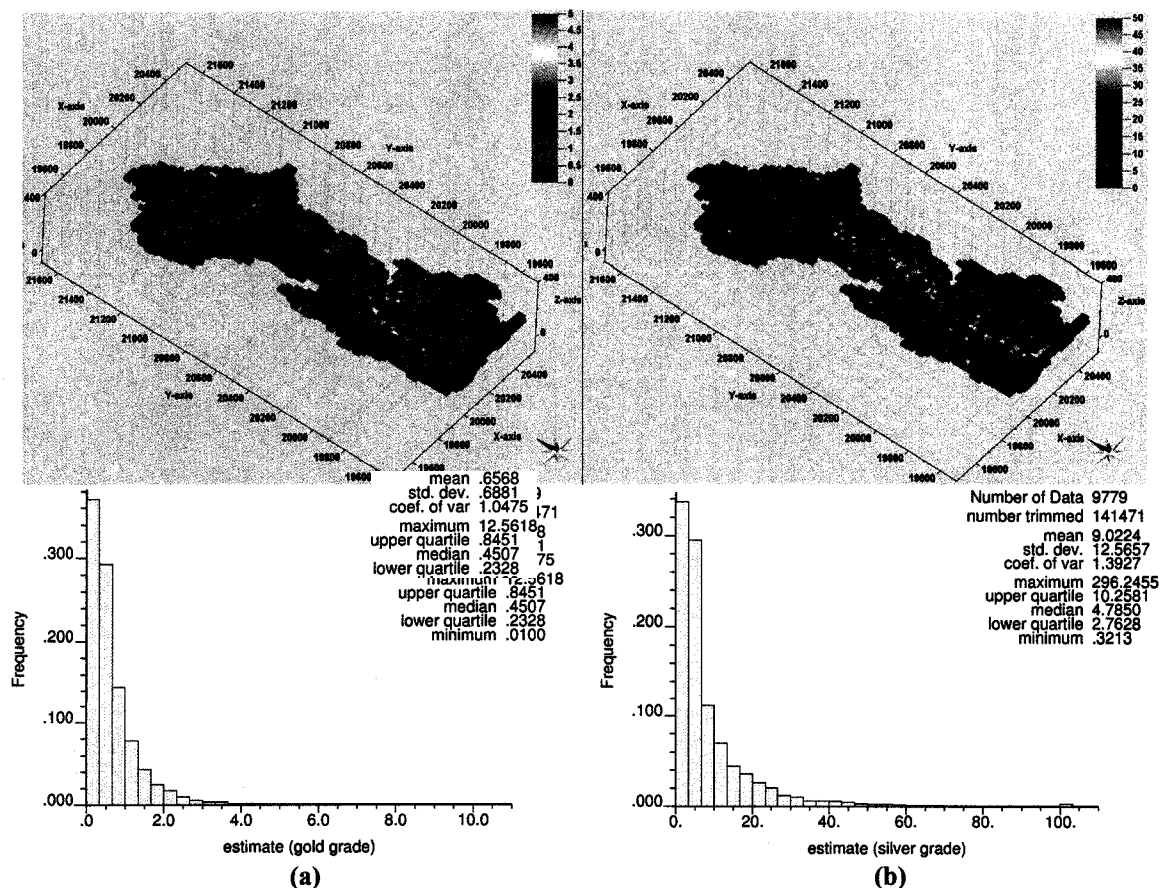


Figure 4.10: Reference model at SMU scale for (a) gold and (b) silver.

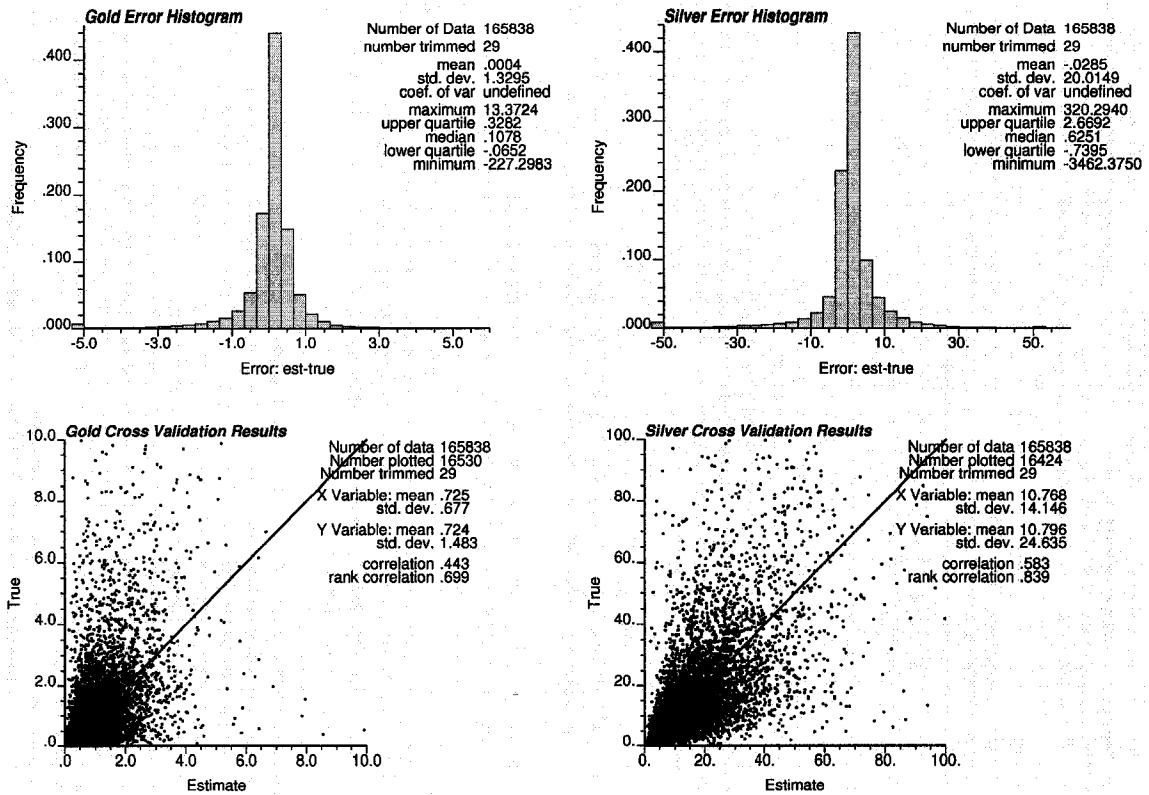


Figure 4.11: Cross validation results of ordinary kriging used to setup the reference models.

4.5 Ordinary Kriging

The variance of ordinary kriging estimates is sensitive to the number of data used for kriging. The desirable variance of estimated model should be as close as possible to the reference model variance. The graph between variance and number of data used in kriging (Figure 4.12) shows 8-10 data are good to use for estimation.

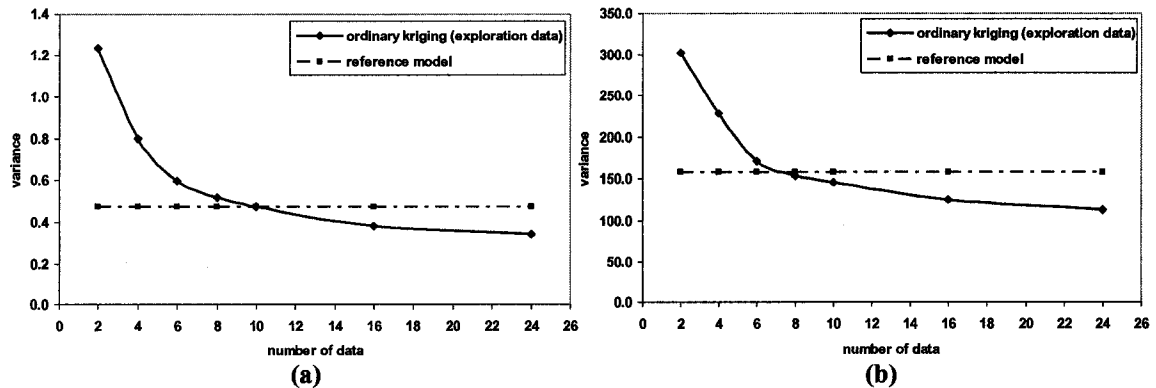


Figure 4.12: Relation between variance and number of data for ordinary kriging estimation. (a) gold and (b) silver grade estimation.

Up to 10 data and the fitted variogram models (Equations 4.4 and 4.5) were used for both gold and silver estimation at SMU scale. $2 \times 2 \times 2$ block discretization was used to perform kriging. These kriged models (Figure 4.13) were used to calculate gold equivalent grade model at SMU scale, followed by panel grade and quantity calculations.

The cross validation results were calculated by removing every sample then estimate the location with the remaining data. The results (Figure 4.14) show error histograms of mean close to zero and unbiased scatter-plots between true and estimates for both gold and silver cases. The scatter-plot correlation is 0.50 in gold case and 0.69 in silver case.

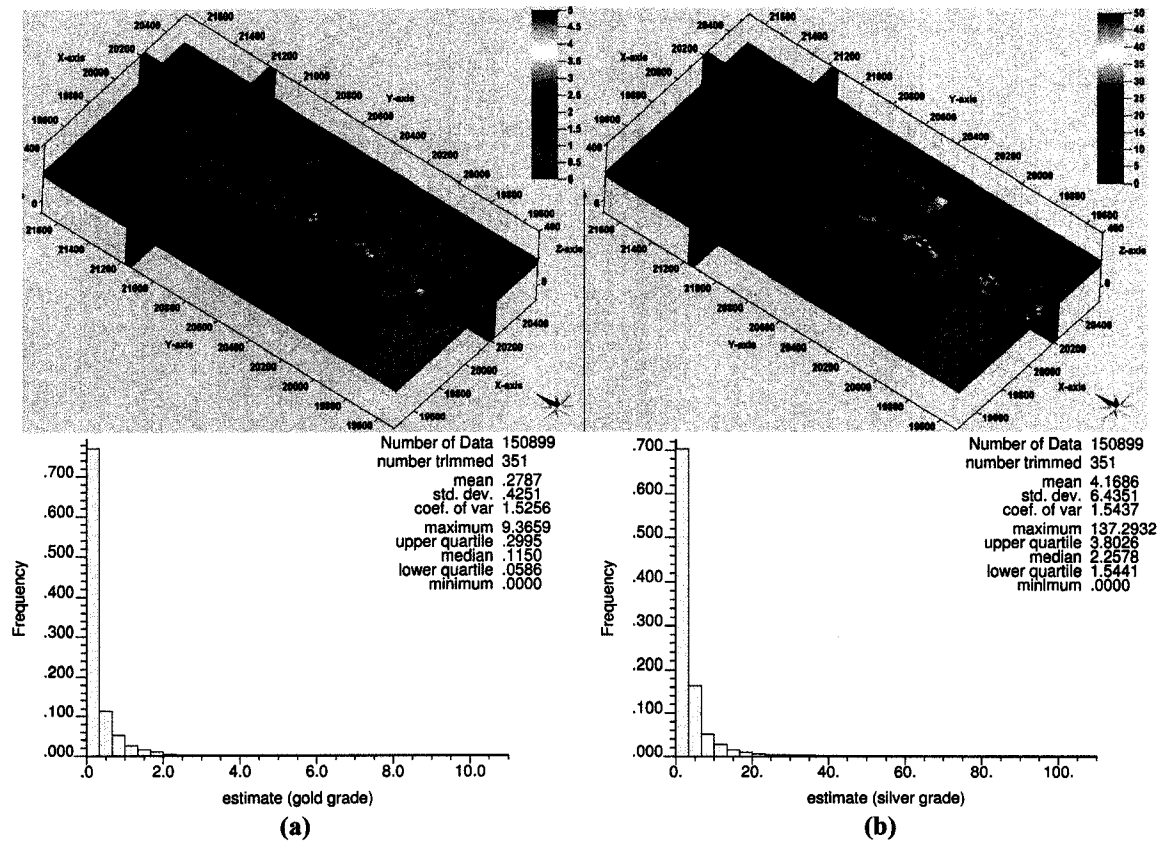


Figure 4.13: Ordinary kriging at SMU scale using exploration data for (a) gold and (b) silver grade estimation.

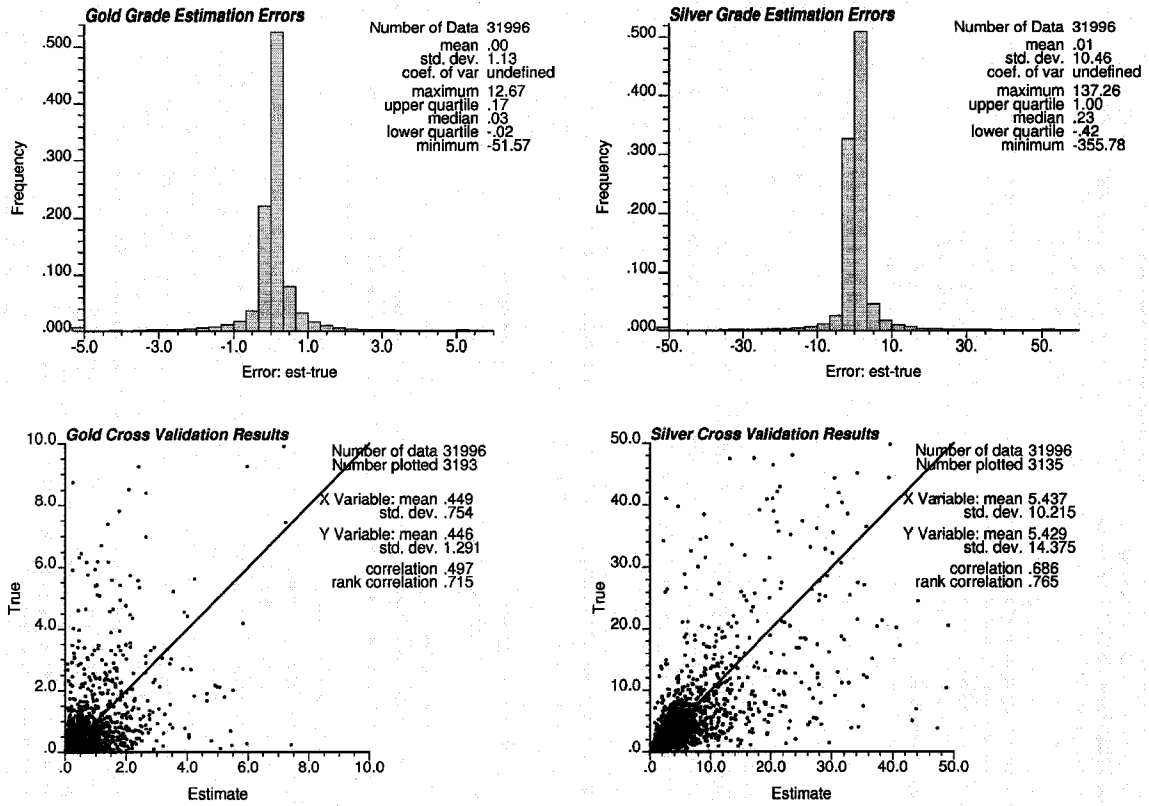


Figure 4.14: Cross validation results of ordinary kriging estimation using exploration data.

4.6 Indicator Kriging

The indicator kriging of exploration data at SMU scale was done using 9 thresholds for both gold and silver cases (Figure 4.15). The fitted variograms (Equations 4.6 – 4.23) of each threshold and up to 24 data were used for kriging. The output was point scale probability. Post-processing using a lognormal volume support correction with variance reduction factor (f) of 0.6 in gold case and 0.74 in silver case was done to convert the indicator output to the estimates. A power model with a power of 0.1 was used to build the cdf for both gold and silver cases. The power model was chosen after trying different interpolation models, considering good histogram reproduction. Gold equivalent grade at SMU scale was calculated using the post-processed (E-type) output for both gold and silver grades, followed by calculation of grade and quantity at panel scale.

$$f_{gold} = 1 - \frac{\bar{\gamma}}{\sigma^2} = 1 - \frac{0.71}{1.67} = 0.6$$

$$f_{silver} = 1 - \frac{\bar{\gamma}}{\sigma^2} = 1 - \frac{52.37}{206.64} = 0.74$$

Cross validation results were plotted on the accuracy plot for both gold and silver separately (Figure 4.16). All the points on accuracy plot are closure to the 45° line and within a reasonable limit of $\pm 7.5\%$ interval.

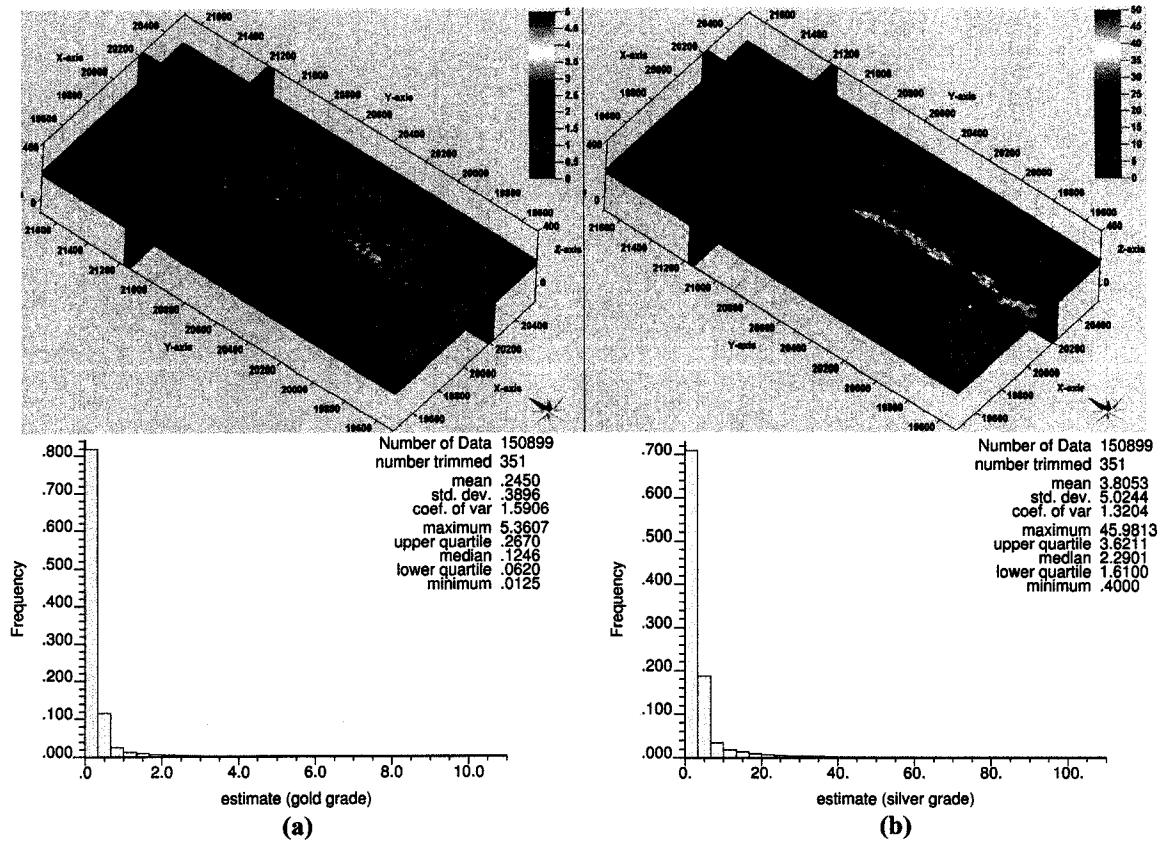


Figure 4.15: Indicator kriging at SMU scale using exploration data for (a) gold and (b) silver grade estimation.

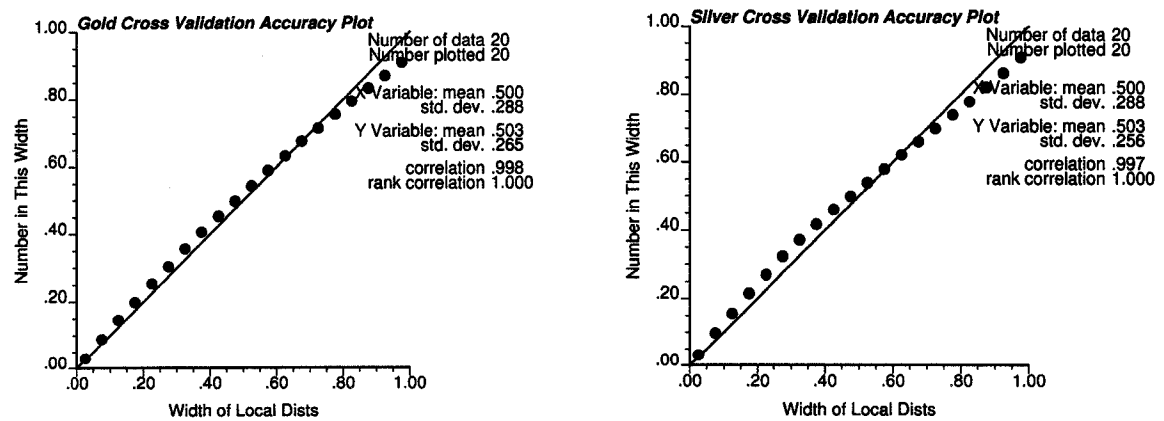


Figure 4.16: Accuracy plot from cross validation results of indicator kriging.

4.7 Simulation

Two different cases were run in simulation (SGS). In Case 1, SGS was performed using all exploration data and the corresponding fitted normal scored variogram (Equations 24 and 25). In Case 2, exploration data that are in close proximity (within 7m search radius) of the blasthole data and the corresponding fitted normal scored variograms (Equations 26 and 27) were used for SGS.

Simulation was performed at a small scale of $5\text{m} \times 5\text{m} \times 5\text{m}$ interval for gold. Silver grades were cosimulated at the same scale using the gold simulated output. The small scale output for both gold and silver were block-averaged to get SMU scale gold and silver values for both the Cases 1 and 2. 25 realizations were generated for both gold and silver simulations. Gold equivalent grade for every realization was calculated separately at SMU scale, using gold and silver simulated realizations at that scale. By applying the gold equivalent cutoff grade, panel-wise grade and quantity for every realization was calculated separately. All the panel-wise realizations were averaged to calculate the estimates for those panels.

Variogram and histogram reproduction was checked for gold and silver simulations in both Case 1 (Figure 4.17) and Case 2 (Figure 4.18). In both Cases 1 and 2, the variogram and histogram reproduction is spread around the used variogram model and original delclustered histogram, respectively for both gold and silver.

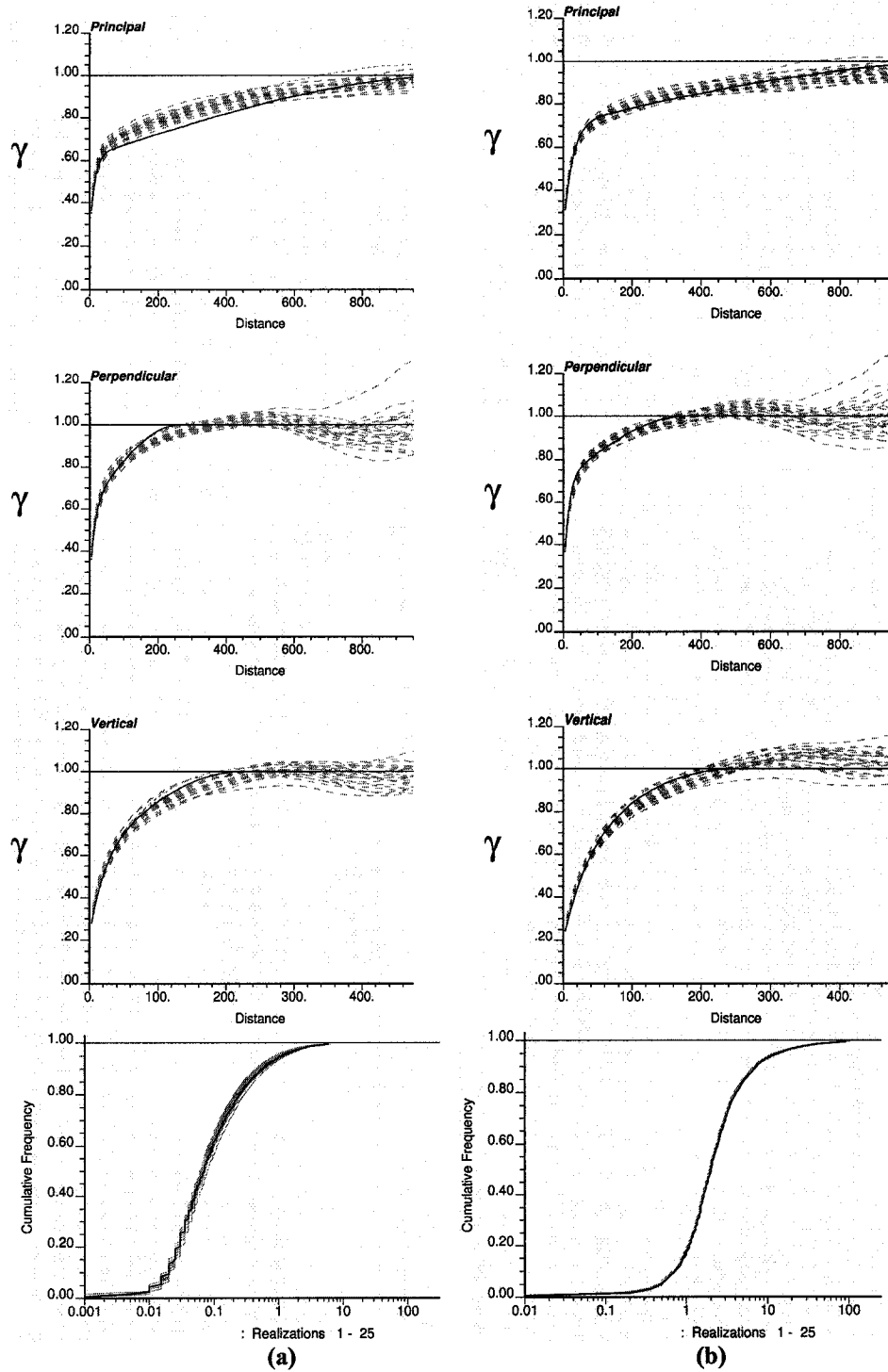


Figure 4.17: Variogram and histogram reproduction of 25 simulated realizations (Case 1). (a) gold
(b) silver

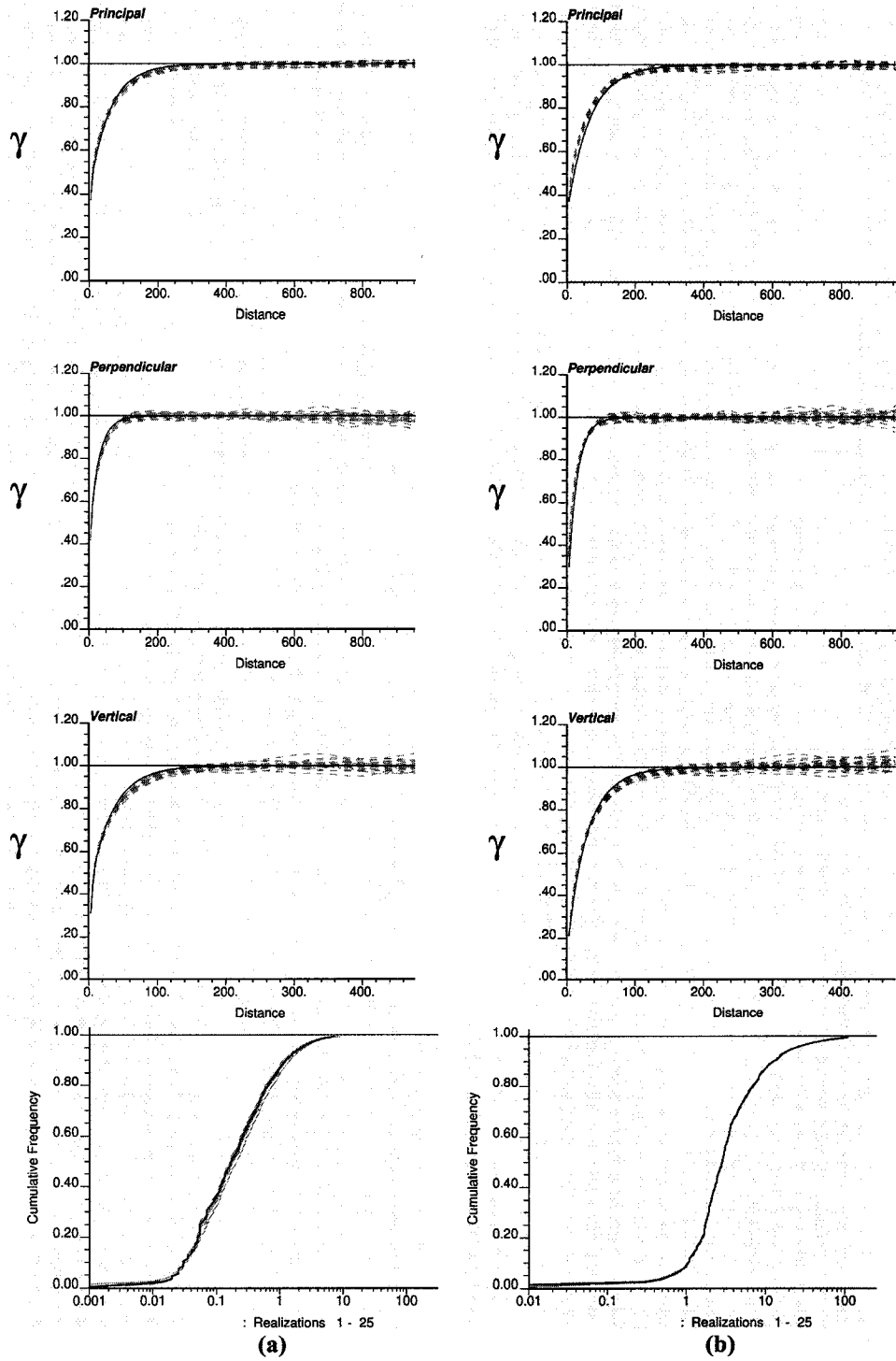


Figure 4.18: Variogram and histogram reproduction of 25 simulated realizations (Case 2). (a) gold
(b) silver

4.8 Comparison

The panel comparison of ordinary kriging with reference results on scatter-plot (Figure 4.19) shows a correlation of 0.72 for ore tonnage, 0.42 for gold equivalent grade, 0.70 for gold quantity, 0.44 for gold grade, 0.78 for silver quantity, 0.85 for silver grade. The mean of reference and estimates are also closure to each other, shows almost unbiasedness. The error variograms (Figure 4.20) for ore tonnage, gold equivalent grade, gold quantity, gold grade, silver quantity and silver grade show almost pure nugget behavior. Although the grade comparisons shows less correlation than quantity comparisons on scatter plot but the error variograms are better in case of grade comparisons.

The panel comparisons of indicator kriging with reference results (Figure 4.21) show a correlation of 0.77 for ore tonnage, 0.33 for gold equivalent grade, 0.76 for gold quantity, 0.31 for gold grade, 0.77 for silver quantity, 0.78 for silver grade. The error variograms (Figure 4.22) also show a high or pure nugget behavior in all grade and quantity comparisons. The closeness of mean of reference and estimates shows the unbiasedness of results. In quantity comparison the correlation for indicator kriging is more in ore tonnage and gold quantity comparisons but in grade comparisons and silver quantity comparison, ordinary kriging has better correlation. The error variograms of ordinary kriging are better than of indicator kriging in terms of nugget effect. It shows that the ordinary kriging is working better in more aspects than the indicator kriging.

In simulation (SGS), there are two different cases for comparison. Case 1, where all the scattered exploration data are taken for simulation (Figure 4.23), gives a correlation between 0.70 to 0.80 in case of quantity comparison, 0.30 in case of gold equivalent grade comparison, 0.32 for gold grade comparison and 0.76 for silver grade comparison but the mean shows bias, especially in silver grade and quantity comparison.

The bias of exploration and blasthole data distribution on QQ-plot (Figure 4.8 (a)) was discussed in Section 4.1. The spatially scattered and clustered exploration data far from blasthole data zones give an indication of bias of the results if all the exploration data are taken in to account for SGS because global statistics is honored and reproduced in case of SGS. The statistics of blasthole and exploration do not match. In Case 2, exploration data close (within 7m search radius) to the blasthole data are taken for SGS. These close exploration data shows better match of statistics and distribution with blasthole data than all exploration data. In this case, panel grade and quantity comparison on scatter-plots (Figure 4.25) show reduction in bias, especially in case of silver it is much improved. All the quantity comparison correlations are between 0.70 and 0.80. The gold equivalent, gold grade comparisons have correlations close to 0.30 and silver grade comparison correlation is 0.77. The error variograms in Case 2 also shift towards higher nugget effect than of Case 1. Although the silver grade comparison on scatter-plot improves a lot in Case 2 than in Case 1, but bias still exist because on QQ-plot (Figure 4.8 (b)) the bias is not removed completely.

Different error comparisons, i.e. mean error (ME), mean squared error (MSE) and mean absolute error (MAE) for ore tonnage (Table 4.1), gold equivalent grade (Table 4.2), gold quantity (Table 4.3), gold grade (Table 4.4), silver quantity (Table 4.5) and silver grade (Table 4.6) are shown. In all, simulation shows better results than other methods in error comparisons followed by ordinary kriging.

In the number of ore panel comparison, indicator kriging has 170 panels above cutoff grade, whereas ordinary kriging has 175 panels estimated above cutoff grade. In case of simulation, 205 panels are above cutoff grade, which is more than of indicator and ordinary kriging numbers (panels). Although not thoroughly investigated in this study, simulation also has one big advantage of having multiple realizations, which can be used to assess uncertainty at the locations of interest.

Table 4.1: Ore-tonnage comparison.

Comparison Criterion	Ordinary Kriging	Indicator Kriging	SGS (Case 1)	SGS (Case 2)
mean error	3164	-6285	422	-2437
mean squared error	8.87×10^9	7.88×10^9	6.88×10^9	6.72×10^9
mean absolute error	68.8×10^3	64.5×10^3	67.7×10^3	67.4×10^3
correlation	0.720	0.771	0.736	0.739
rank correlation	0.705	0.739	0.689	0.687

Table 4.2: Gold equivalent grade comparison.

Comparison Criterion	Ordinary Kriging	Indicator Kriging	SGS (Case 1)	SGS (Case 2)
mean error	0.0220	0.1427	0.2098	0.0493
mean squared error	0.3130	0.4054	0.3933	0.2862
mean absolute error	0.3917	0.4490	0.4789	0.3716
correlation	0.417	0.329	0.304	0.291
rank correlation	0.522	0.459	0.353	0.342

Table 4.3: Gold quantity (Kg) comparison.

Comparison Criterion	Ordinary Kriging	Indicator Kriging	SGS (Case 1)	SGS (Case 2)
mean error	8	23	29	8
mean squared error	26.9×10^3	32.7×10^3	25.7×10^3	19.6×10^3
mean absolute error	116	124	125	112
correlation	0.695	0.758	0.720	0.726
rank correlation	0.711	0.736	0.670	0.768

Table 4.4: Gold grade comparison.

Comparison Criterion	Ordinary Kriging	Indicator Kriging	SGS (Case 1)	SGS (Case 2)
mean error	0.0276	0.1267	0.0949	0.0303
mean squared error	0.2738	0.3722	0.2915	0.2447
mean absolute error	0.3710	0.4377	0.3969	0.3464
correlation	0.443	0.308	0.319	0.314
rank correlation	0.473	0.403	0.316	0.332

Table 4.5: Silver quantity (Kg) comparison.

Comparison Criterion	Ordinary Kriging	Indicator Kriging	SGS (Case 1)	SGS (Case 2)
mean error	248	189	1029	38
mean squared error	6.9×10^6	6.7×10^6	7.0×10^6	5.1×10^6
mean absolute error	1417	1449	1839	1506
correlation	0.783	0.769	0.786	0.773
rank correlation	0.769	0.724	0.695	0.678

Table 4.6: Silver grade comparison.

Comparison Criterion	Ordinary Kriging	Indicator Kriging	SGS (Case 1)	SGS (Case 2)
mean error	-0.2952	0.8394	6.0329	0.9984
mean squared error	77	75	143	119
mean absolute error	5	5	9	7
correlation	0.852	0.778	0.755	0.773
rank correlation	0.885	0.880	0.866	0.863

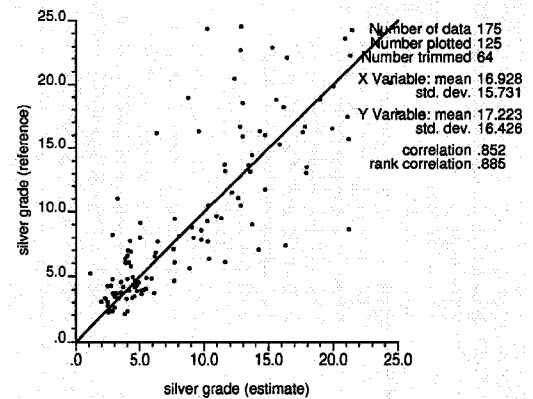
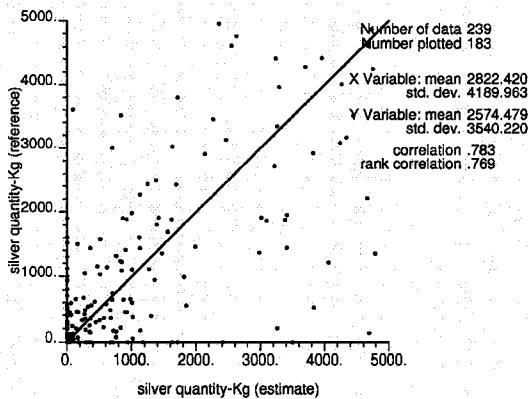
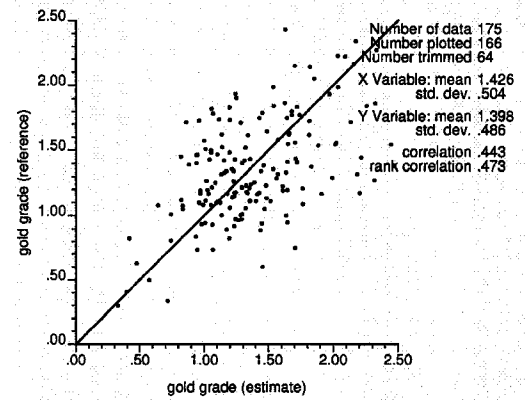
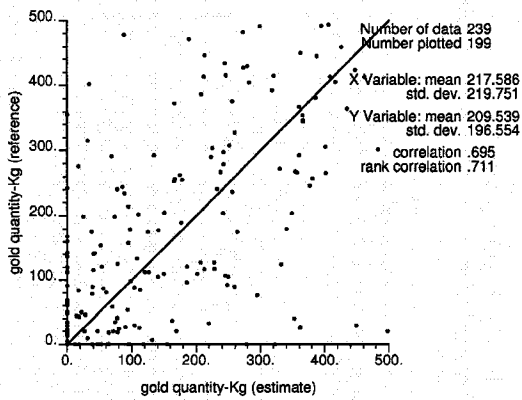
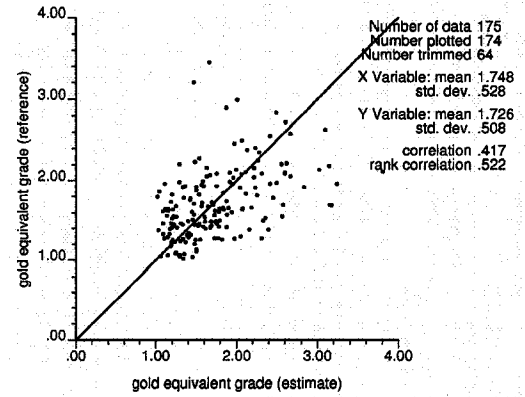
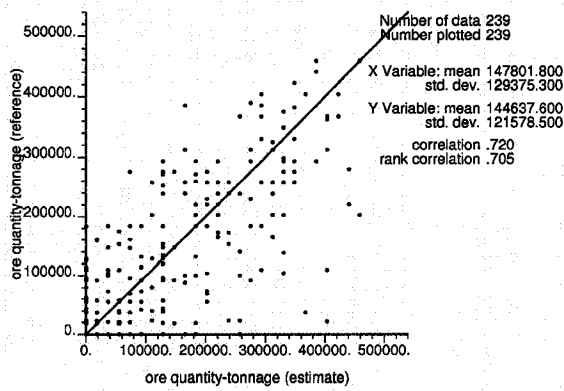


Figure 4.19: Scatter-plot comparison of ordinary kriging and reference results at panel scale (ore quantity, gold equivalent grade, gold and silver quantities, gold and silver grades).

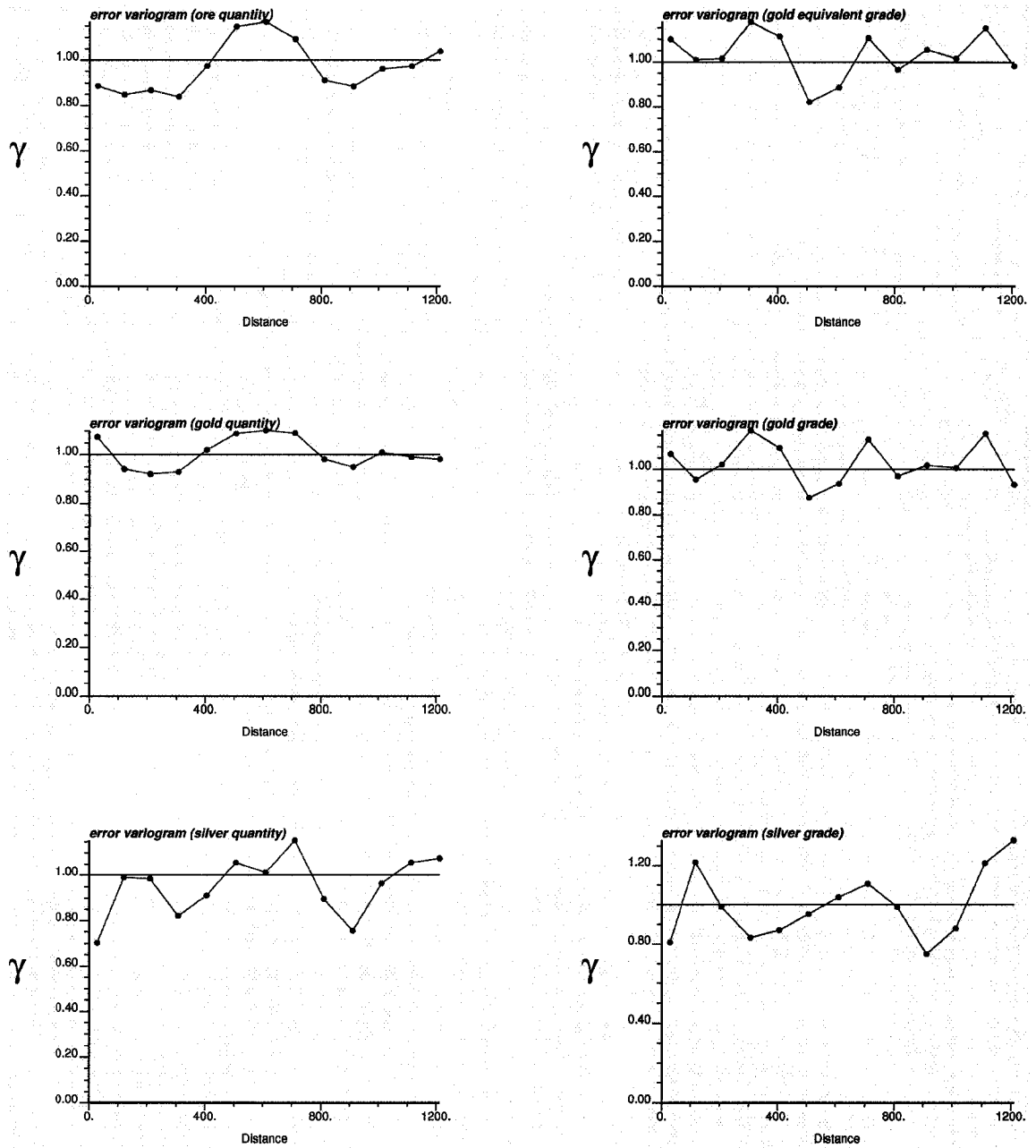


Figure 4.20: Error variograms for ordinary kriging.

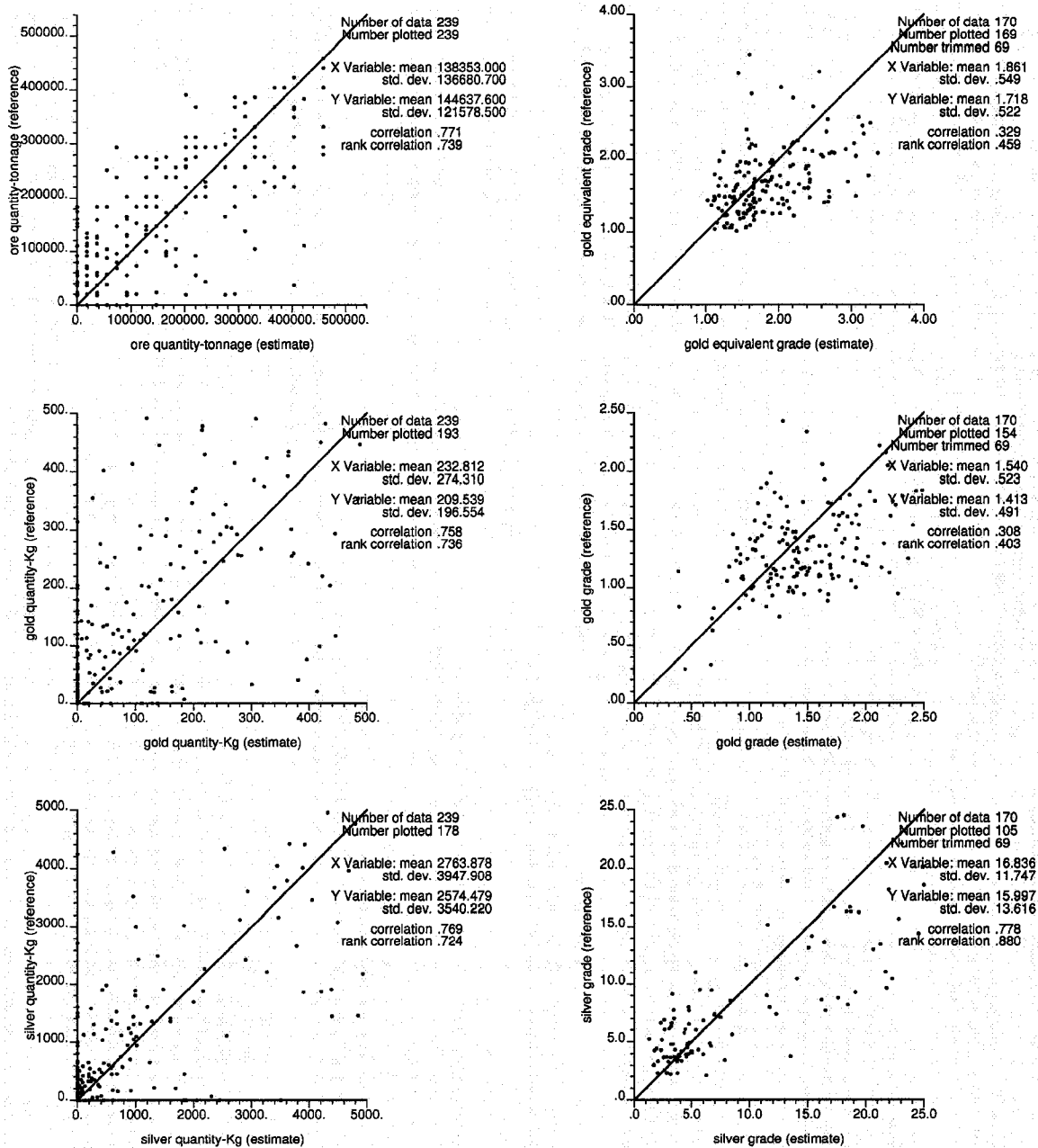


Figure 4.21: Scatter-plot comparison of indicator kriging and reference results at panel scale (ore quantity, gold equivalent grade, gold and silver quantities, gold and silver grades).

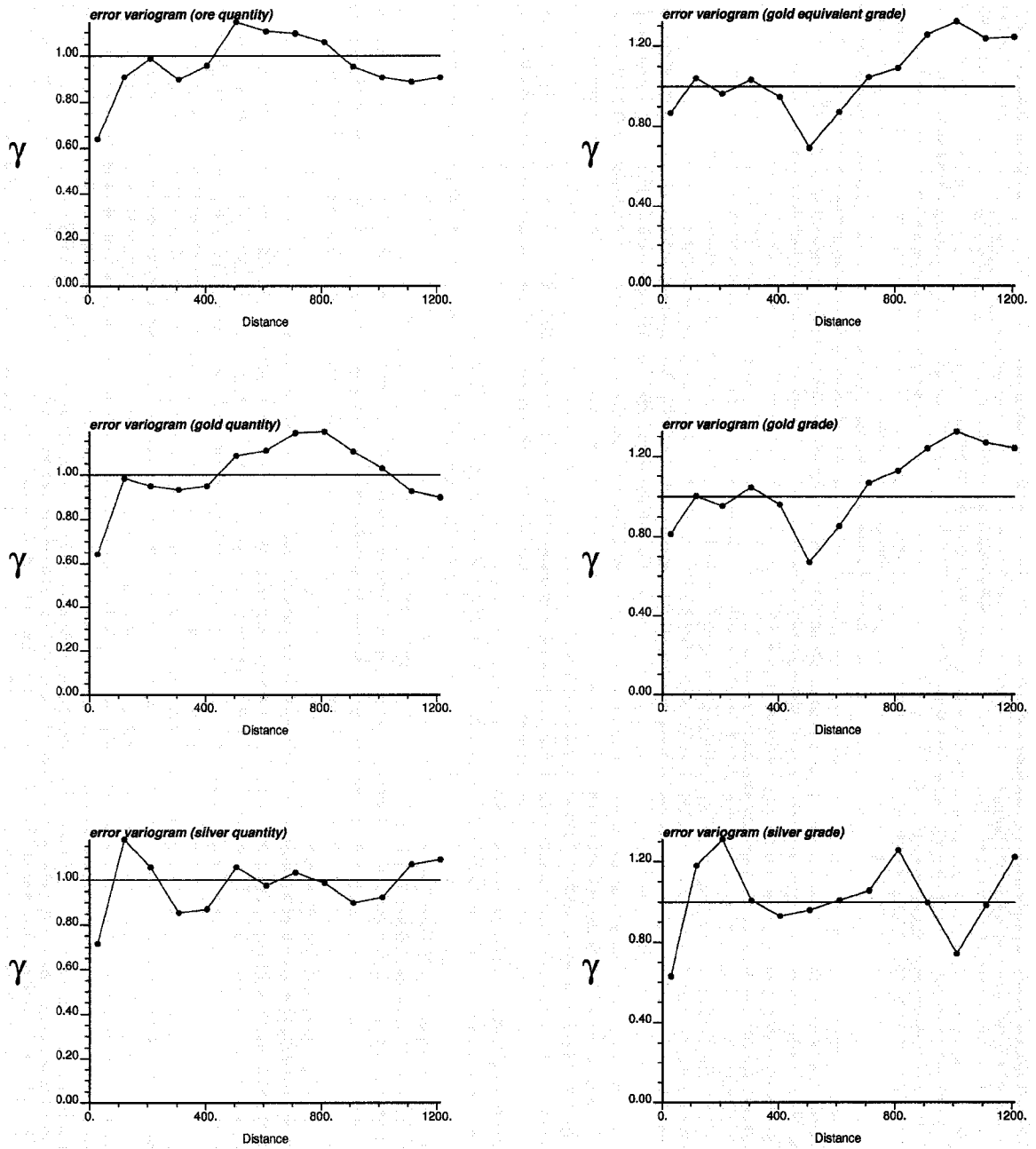


Figure 4.22: Error variograms for indicator kriging.

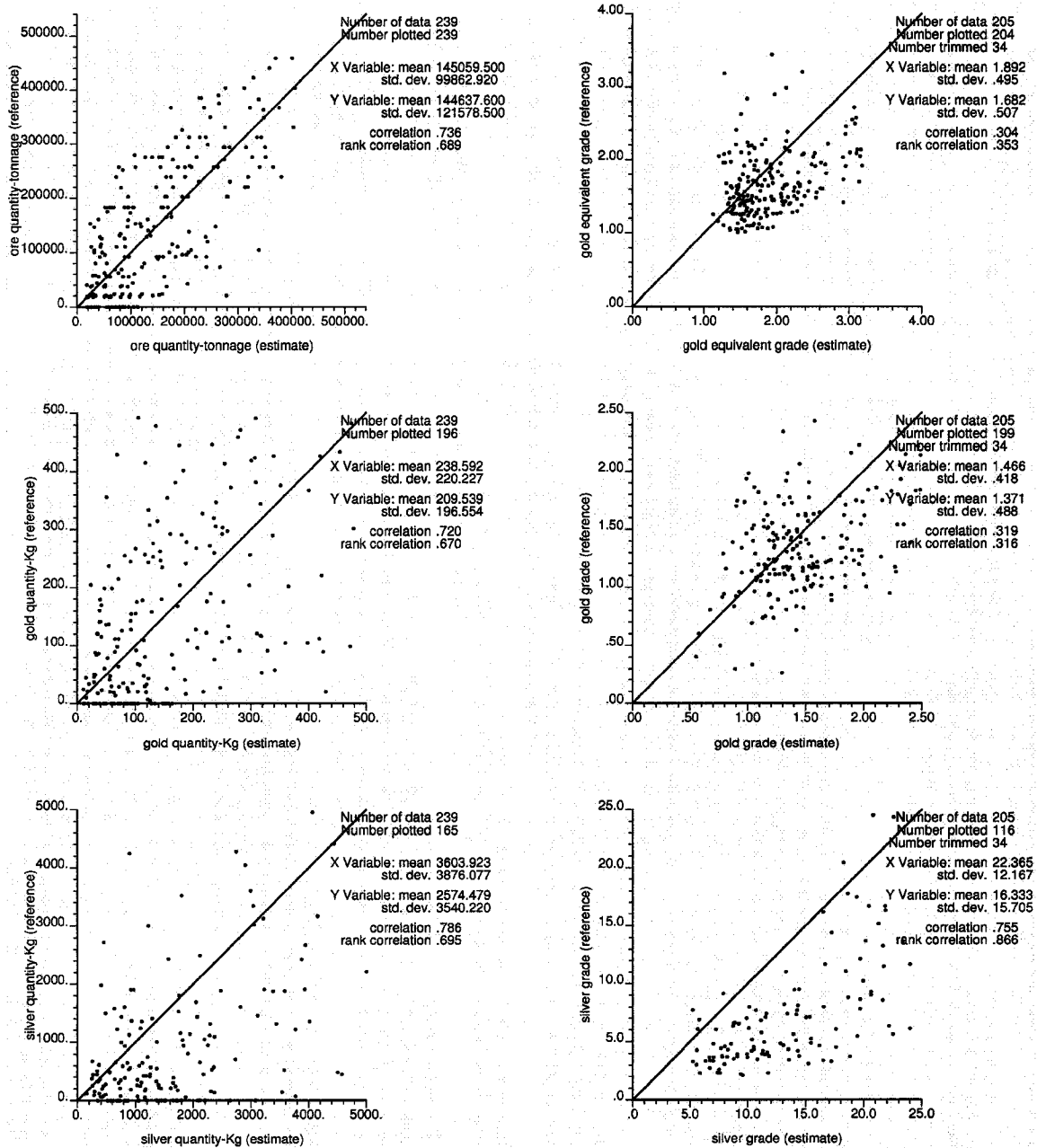


Figure 4.23: Scatter-plot comparison of SGS (Case 1) and reference results at panel scale (ore quantity, gold equivalent grade, gold and silver quantities, gold and silver grades).

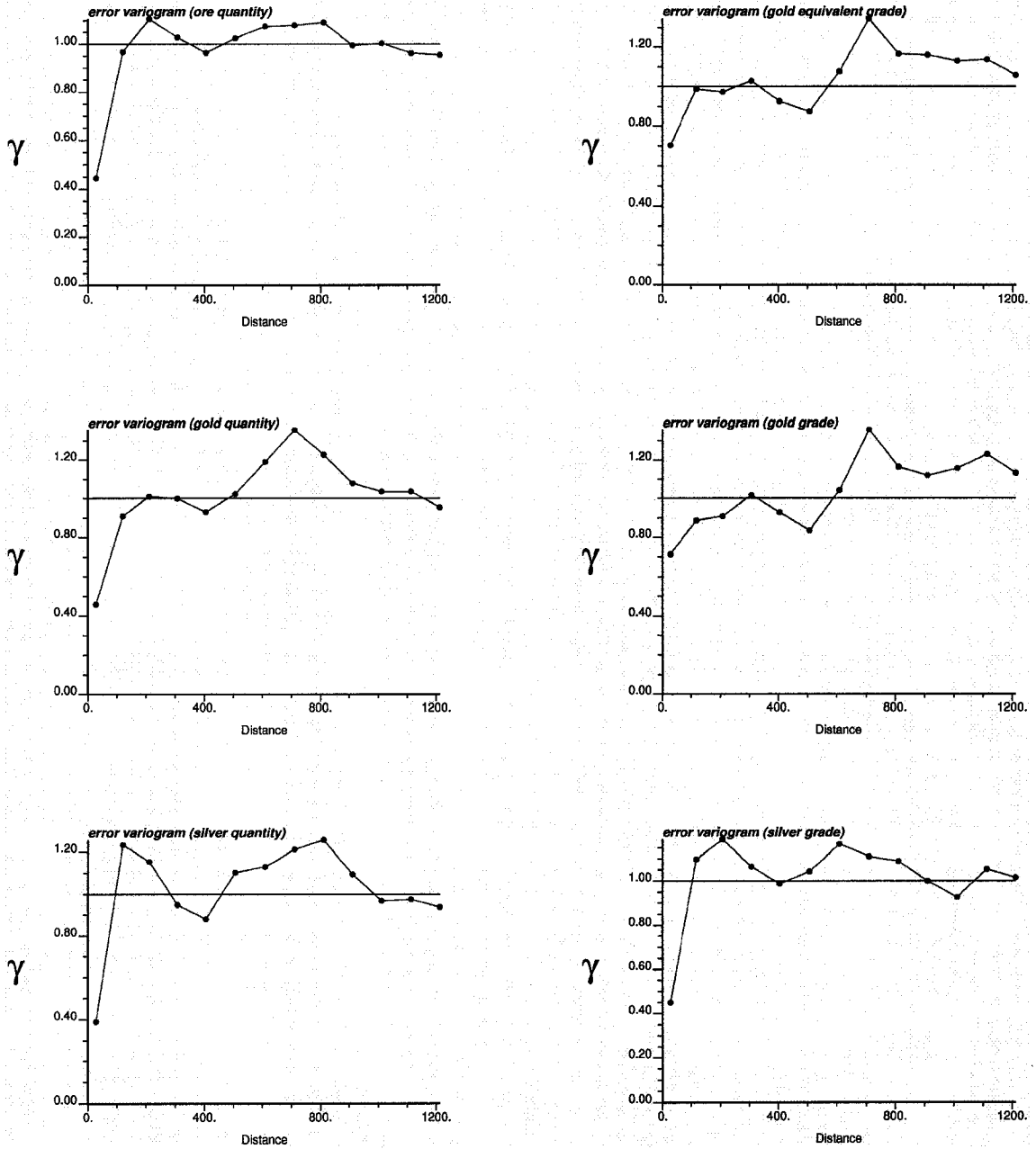


Figure 4.24: Error variograms for SGS (Case 1).

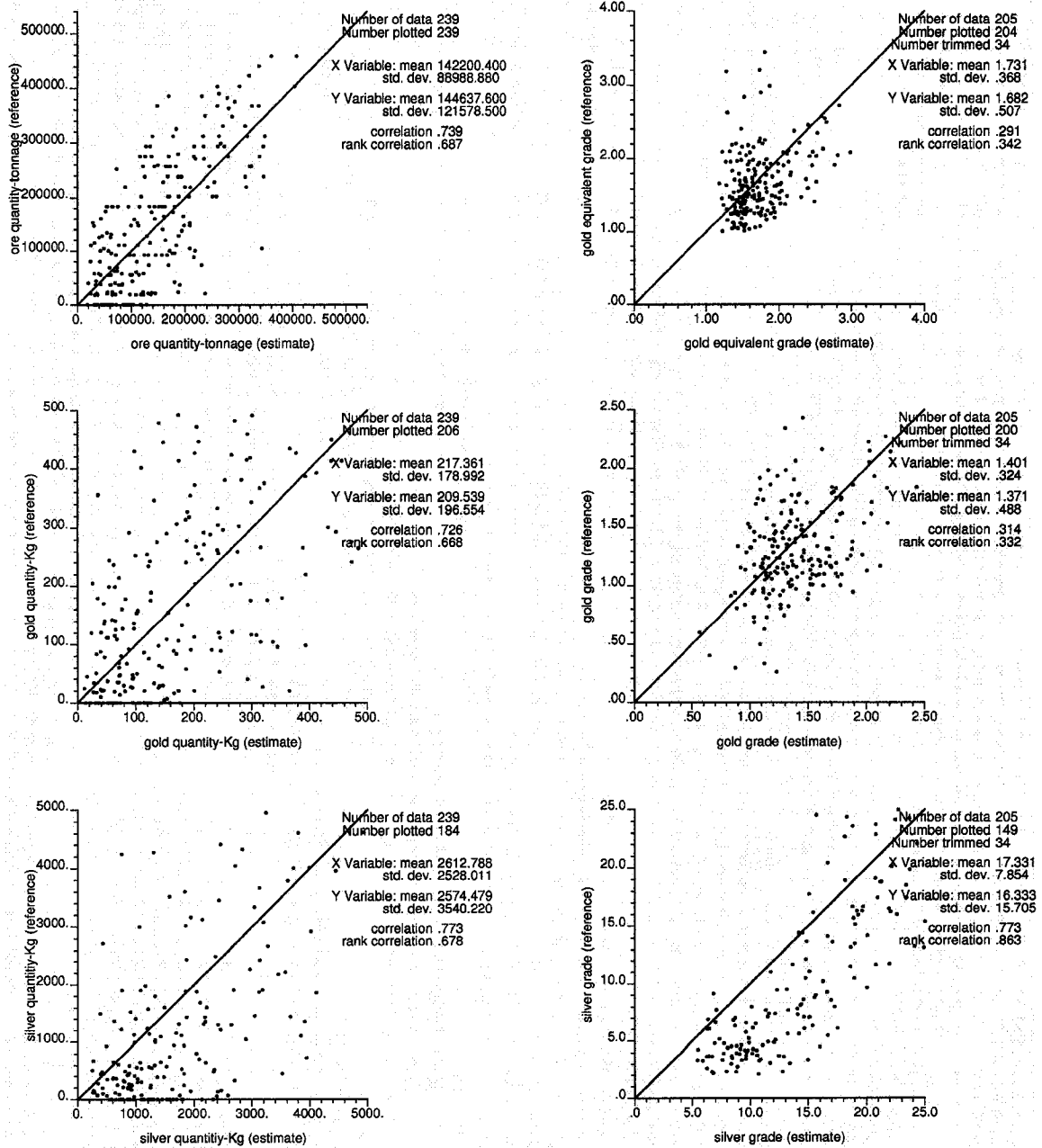


Figure 4.25: Scatter-plot comparison of SGS (Case 2) and reference results at panel scale (ore quantity, gold equivalent grade, gold and silver quantity, gold and silver grade).

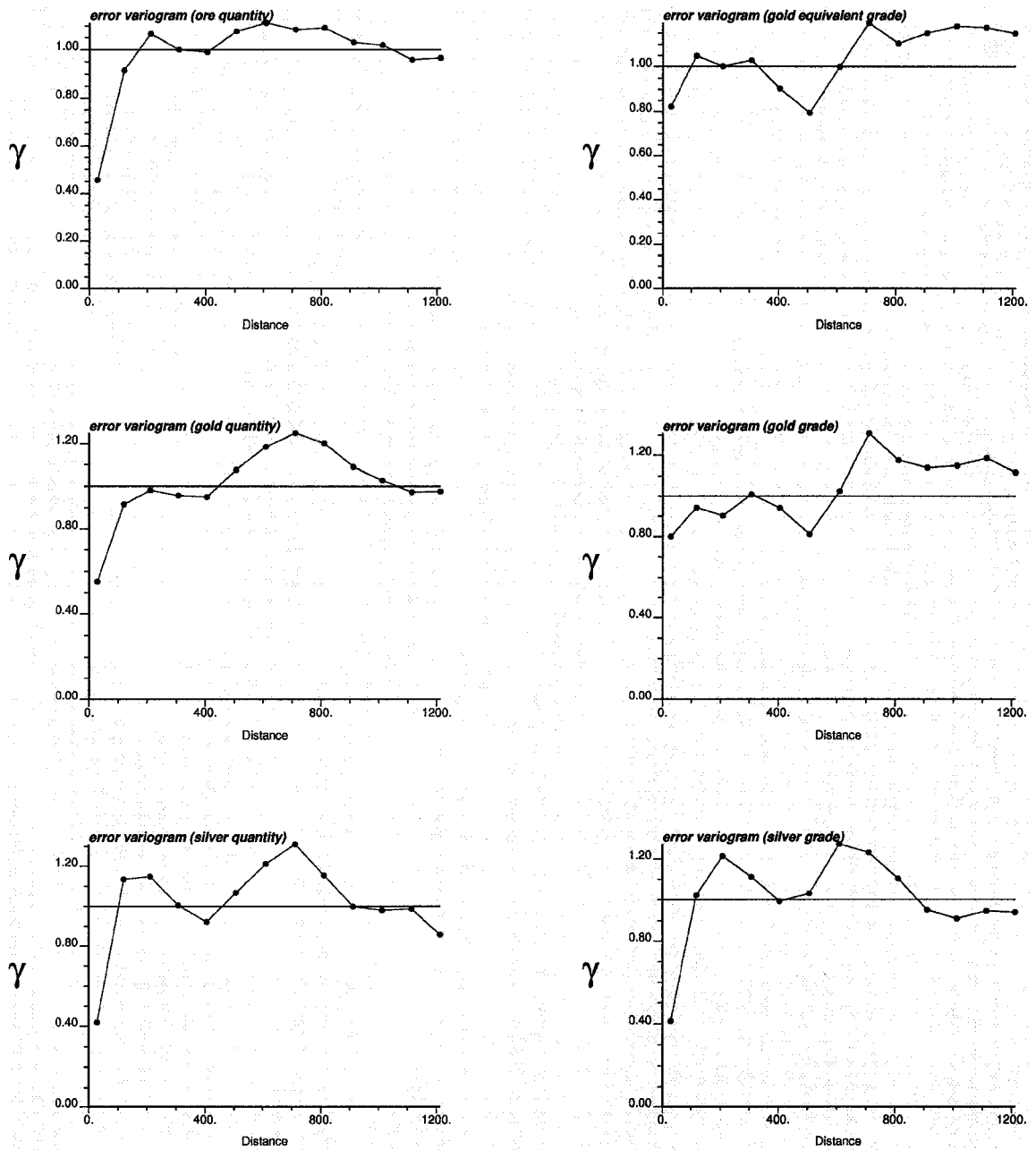


Figure 4.26: Error variograms for SGS (Case 2).

Chapter 5

Conclusion and Future Work

5.1 Conclusion

In this study, panel-wise comparison of estimated values to reference values for ordinary kriging, indicator kriging and simulation (SGS) was undertaken. The estimation considered widely spaced/exploration data and the reference results were assembled with closely spaced/blasthole data. These estimation methods have been compared under different error criterions (mean error, mean squared error and mean absolute error), bias and correlation between true and estimates. The data used in this study appear approximately lognormal distributed. A single variable case was shown in the synthetic example (Chapter 3) and a multivariable case was shown in the real data example (Chapter 4).

Reference results were computed with ordinary kriging of close spaced/blasthole data with short search radius. Ordinary kriging is considered more robust than alternative estimators and takes local mean in to account.

The panel-wise study for ordinary kriging, indicator kriging and simulation (SGS) shows ordinary kriging close to indicator kriging in both synthetic example and real data examples. Considering the small differences of ordinary kriging and indicator kriging results, the ordinary kriging looks better than the indicator kriging in both synthetic and real data examples especially in grade comparisons. In quantity of metal comparisons, indicator kriging is better in terms of bias. Simulation shows overall better results than ordinary kriging and indicator kriging estimation methods in both synthetic and real data examples.

Although simulation is better than ordinary kriging and indicator kriging methods in bias and error comparisons, there are some concerns with it. Simulation (SGS) reproduces the global declustered data histogram. If the data distribution is different from the reference distribution, then simulation results show significant bias compared to the reference results. In simulation, multiple realizations make it more complicated to perform mine design and production planning. In spite of these issues, simulation gives good comparable results with the reference results. It also has the big advantage of uncertainty assessment. Uncertainty can help in decision making. Indicator kriging also has the advantage of local uncertainty assessment.

In spite of being known as good linear unbiased estimator, kriging has an inherent tendency of smoothing the estimates (grade) over the domain. Simulation removes this

smoothing effect and has the capability of producing very high and very low values. So, in multivariable/poly-metallic deposits, simulation provides a strong decision making platform.

Ordinary kriging worked well with 8-10 data in the search, the more the data we use the lesser the variance of the estimates, causing poor estimation of recoverable reserves. The cross validation is improved. Indicator kriging works well with more data (16-24), but using more data requires more time for estimation.

In discrete Gaussian model for global estimation, the support size has an impact on the estimated global reserves (synthetic example). At zero cutoff grade, the average grade is the same. As the cutoff grade is increased, the average estimated grade goes down with the increase in support size and tonnage increases. In global comparison the grade-tonnage curve generated by discrete Gaussian method shows a good match with the grade-tonnage curve generated by ordinary kriging using few data. As we increase the number of data used in ordinary kriging, the global grade-tonnage curve does not match the discrete Gaussian model. Although discrete Gaussian model is not able to give local information at panel or SMU scale, it is good for tuning other methods at global scale.

5.2 Future Work

The SMU and panel size have an impact on the final estimates and calculated recoverable reserves. So, a sensitivity study of SMU size and panel size on recoverable reserves estimation would be informative and helpful in decision making, equipment selection and mine planning.

Uncertainty assessment is an important advantage of simulation. Local uncertainty comparison at panel scale can give a decision making base for investment and working in the field. So, the SMU and panel size impact on uncertainty assessment is important to assess in the future work.

Calibration of reference model with production data and using that model for comparative study can give more insight of the role and goodness of individual estimation method from the feasibility to the production stage.

Bibliography

- [1] A. G. Journel and Phaedon C. Kyriakidis. *Evaluation of Mineral Reserves A Simulation Approach*, pages 3-7. Oxford University Press, New York , 2004.
- [2] Alan C. Nobel. *Ore Reserve/Resource Estimation. Chapter 5.6, SME Mining Engineering Handbook, 2nd Edition, Volume 1, Howard L. Hartman, Senior Editor*, pages 344-359. Society for Mining, Metallurgy and Exploration, Inc. Littleton, Colorado, 1992.
- [3] C. Neufeld. *Probabilistic Estimation of Recoverable Reserves, MSc. Thesis*, pages 26-28. University of Alberta, Edmonton, 2006.
- [4] C. V. Deutsch and A. G. Journel. *GSLIB: Geostatistical Software Library: and User's Guide, Second Edition*. Oxford University Press, New York , 1998.
- [5] C. V. Deutsch. *Geostatistical Reservoir Modeling*, pages 168-171. Oxford University Press, New York, 2002.
- [6] C. V. Deutsch. *Direct Assessment of Local Accuracy and Precision, Geostatistics Wollongong 96*, pages 115-125. Baafi and Schofield, editors, Kluwer Academic Publishers, September 1996.
- [7] C. V. Deutsch. *The place of Geostatistical Simulation in Resource/Reserve Estimation*. in MININ Mining Innovation Conference, Santiago, Chile, April 2004.
- [8] E. H. Isaaks and R. M. Srivastava. *An Introduction to Applied Geostatistics*, pages 435-443. Oxford University Press, New York, 1989.
- [9] J. A. McLennan and C. V. Deutsch. *Conditional Non-Bias of Geostatistical Simulation for Estimation of Recoverable Reserves*. CIM Bulliten, Volume 97, No. 1080, May 2004.
- [10] J.-M Rendu. *An Introduction to Geostatistical Methods of Mineral Evaluation, Geostatistics Vol.2*, pages 45-49. South Africa Institute of Mining and Metallurgy, Johannesburg, 1981.
- [11] J. Vann and H. Sans. *Global Resource Estimation and Change of Support at the Enterprise Gold Mine, Pine Creek, Northern Territory- Application of the*

Geostatistical Discrete Gaussian Model, pages 171-179. APCOM XXV 1995 Conference, Brisbane 1995.

- [12] M. David. *Geostatistical Ore Reserve Estimation*, pages 58-60. Elsevier Scientific Publishing Company, 1977.
- [13] M. David. *Handbook of Applied Advanced Geostatistical Ore Reserve Estimation*, pages 16-24. Elsevier Science Publishers B.V., 1988.
- [14] Pierre Goovaerts. *Geostatistics for Natural Resources Estimation*, pages 59-63. Oxford University Press, New York, 1997.
- [15] S. Al-Hassan and A. E. Annels. *Geostatistical estimation of manganese oxide resources at the Nsuta Mine*, pages 157-169. Mineral Resources Evaluation II: Methods and Case Histories, Geological Society Special Publication No. 79, edited by M.K.G. Whateley and P.K. Harvey, The Geological Society, UK, 1994.
- [16] T. Coléou. *Cutoff Grade Optimization : A Panacea or A Fool's Paradise?*. pages 889-890. M. Armstrong, Editor. *Geostatistics*, Volume 2. Kluwer Academic Publishers, Dordrecht, 1989.

APPENDIX I

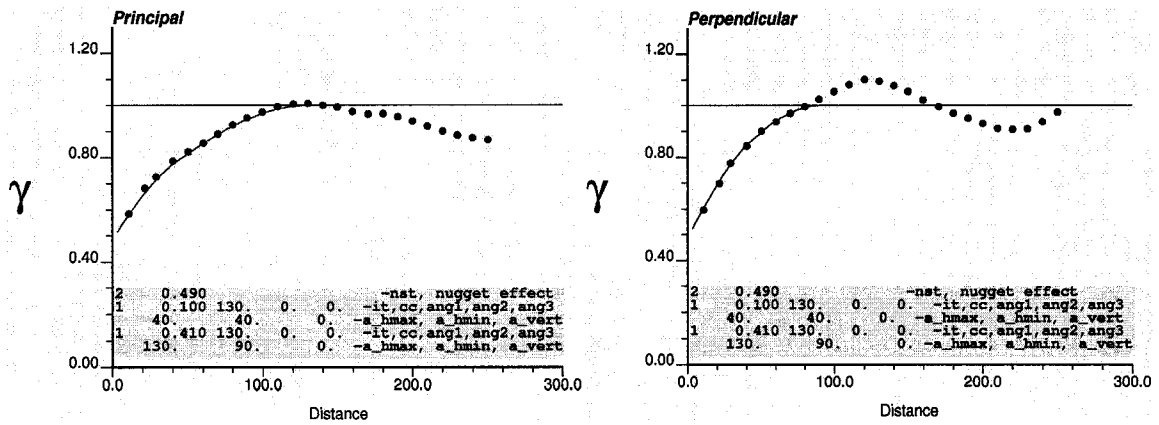


Figure i: Variogram with fitted model for blasthole data (principal direction is 130° azimuth)

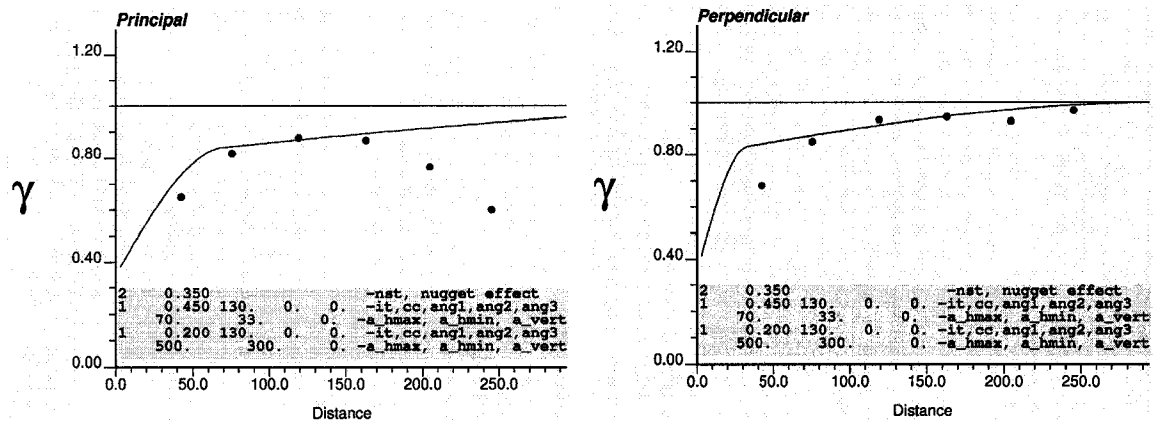


Figure ii: Variogram with fitted model for exploration data (principal direction is 130° azimuth): Case 1 of ordinary kriging.

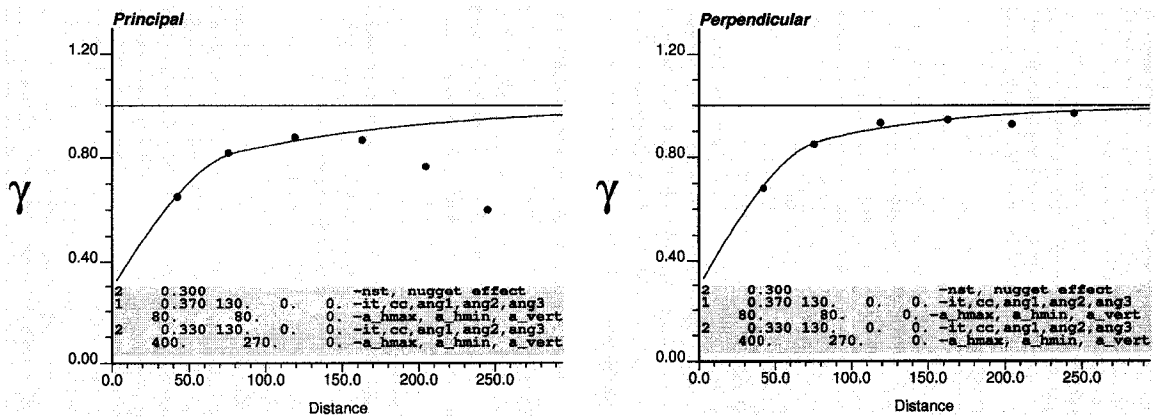


Figure iii: Variogram with fitted model for exploration data (principal direction is 130° azimuth): Case 2 of ordinary kriging.

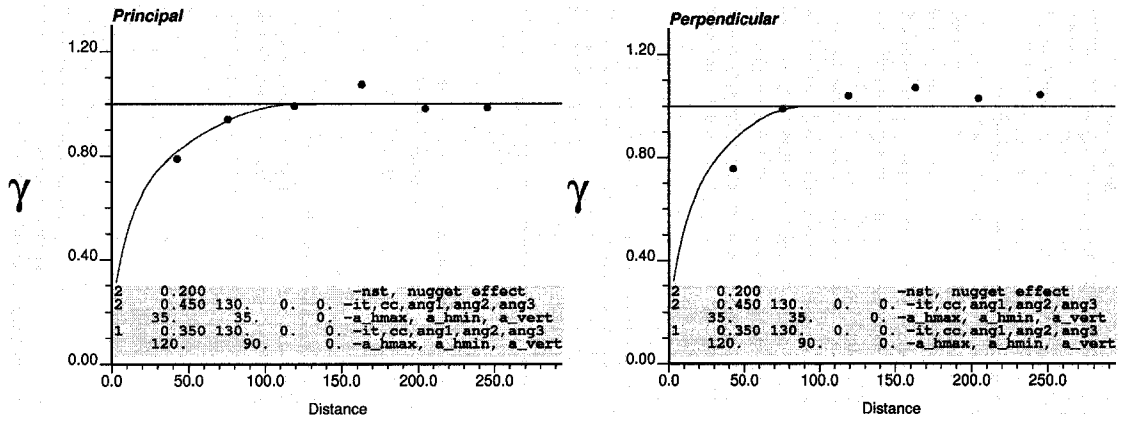


Figure iv: Variogram and fitted model for normal scored exploration data (principal direction is 130° azimuth): Case 1 of simulation.

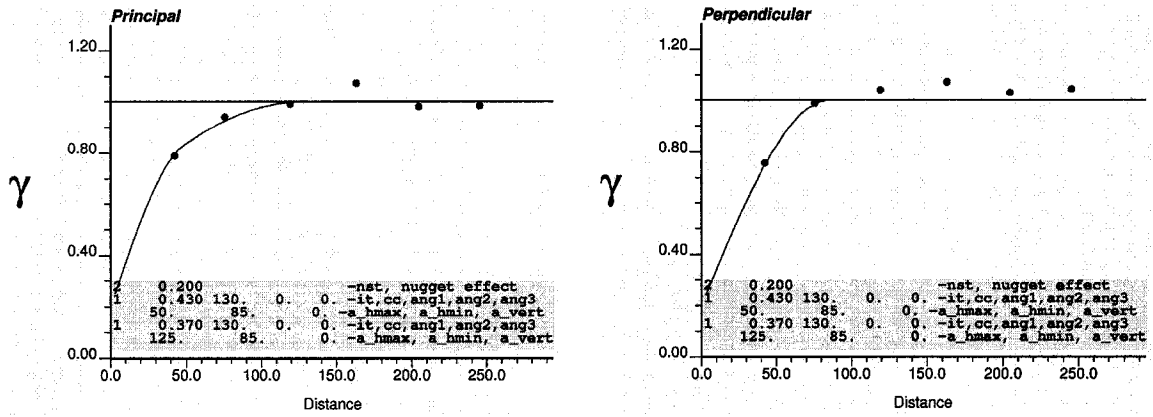
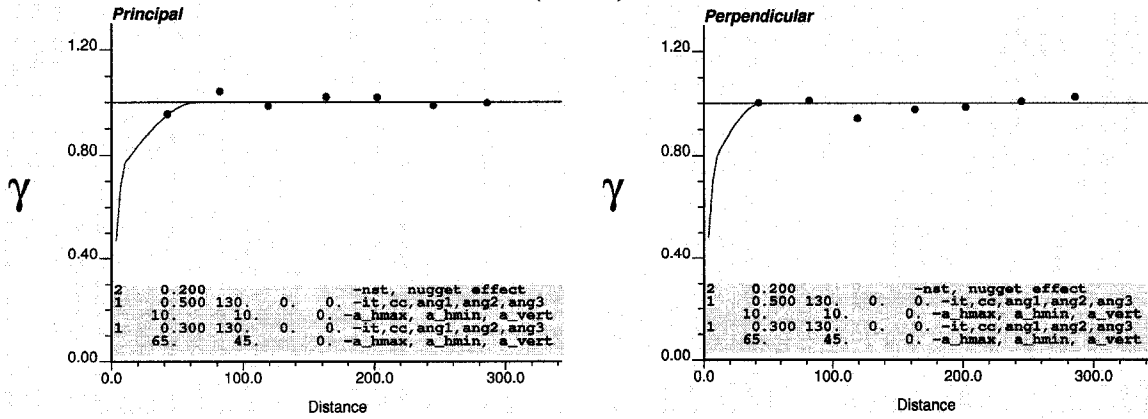


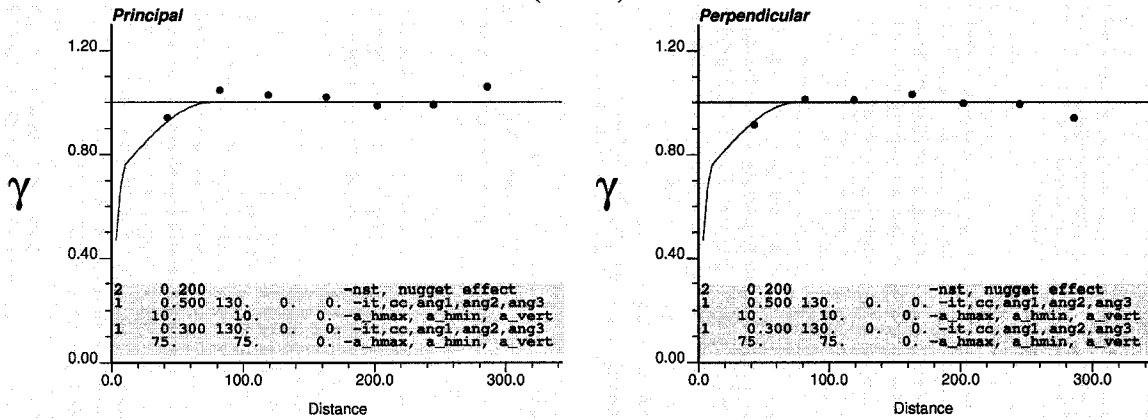
Figure v: Variogram and fitted model for normal scored exploration data (principal direction is 130° azimuth): Case 2 of simulation.

APPENDIX II

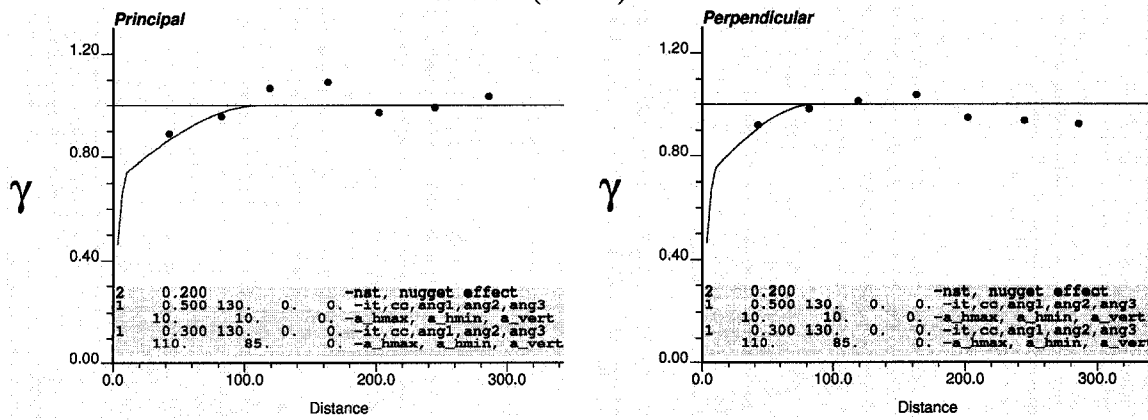
Threshold 1 (0.0805) at 0.1 decile



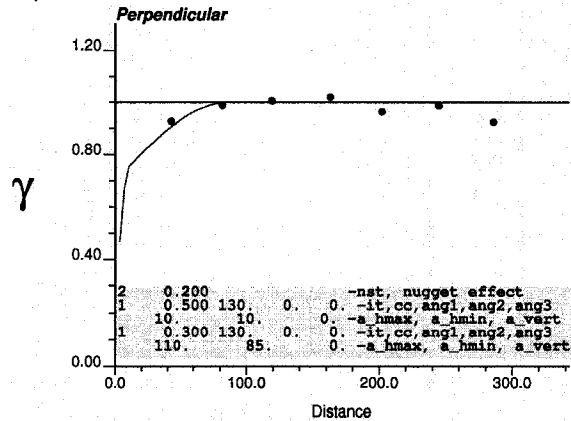
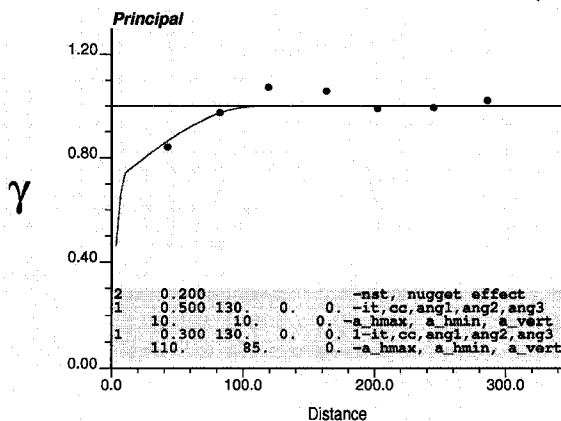
Threshold 2 (0.1194) at 0.2 decile



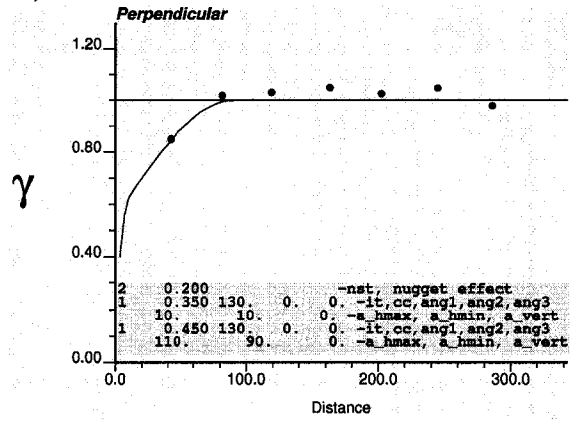
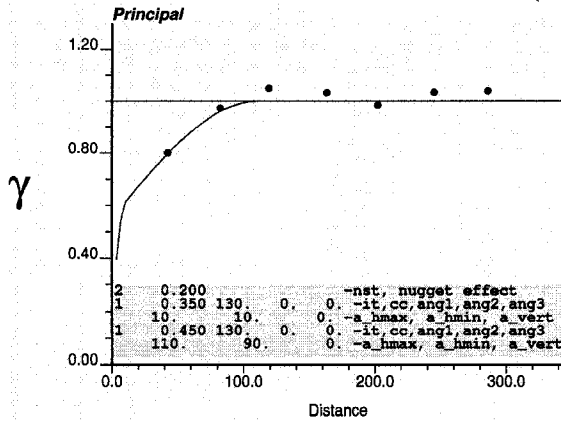
Threshold 3 (0.1805) at 0.3 decile



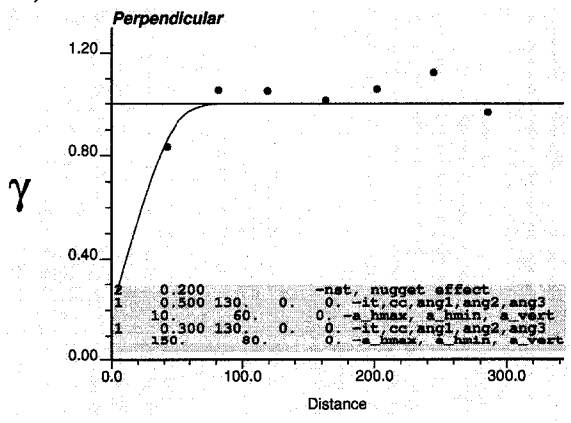
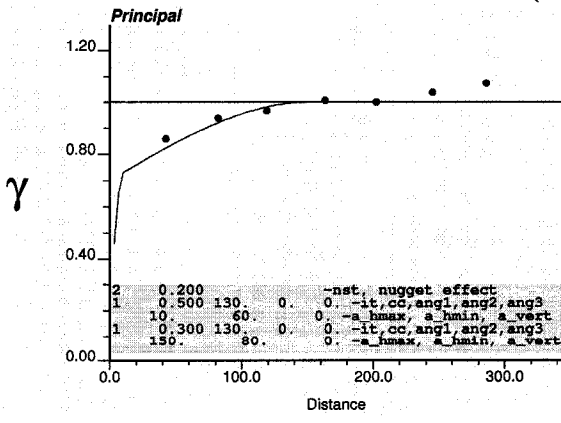
Threshold 4 (0.2598) at 0.4 decile



Threshold 5 (0.3850) at 0.5 decile



Threshold 6 (0.5084) at 0.6 decile



APPENDIX III

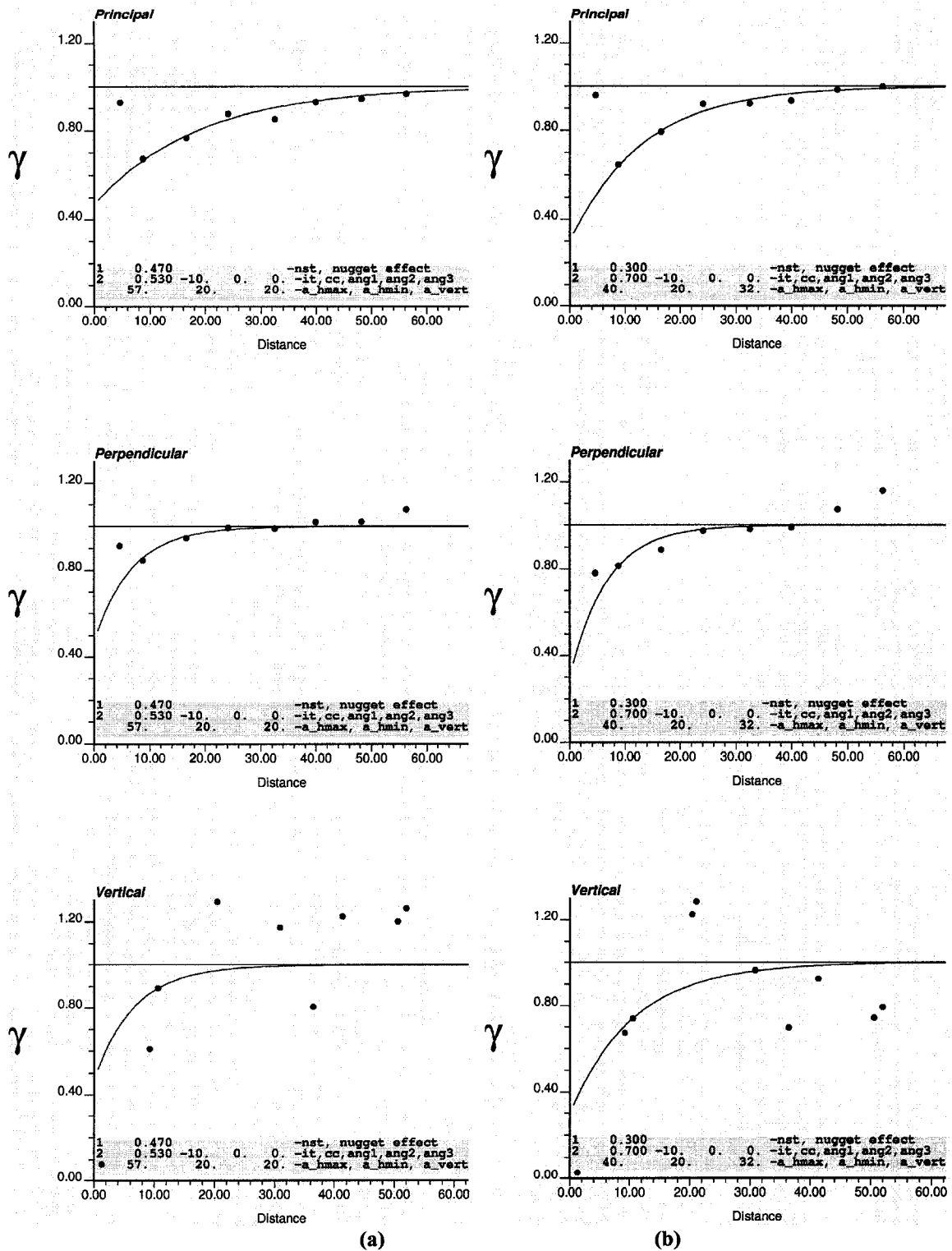


Figure i: Variogram and fitted model to original blasthole data (a) gold data (b) silver data. (-10° azimuth direction as principal (major) direction, 80° azimuth direction as perpendicular (minor) and 90° dip as vertical direction).

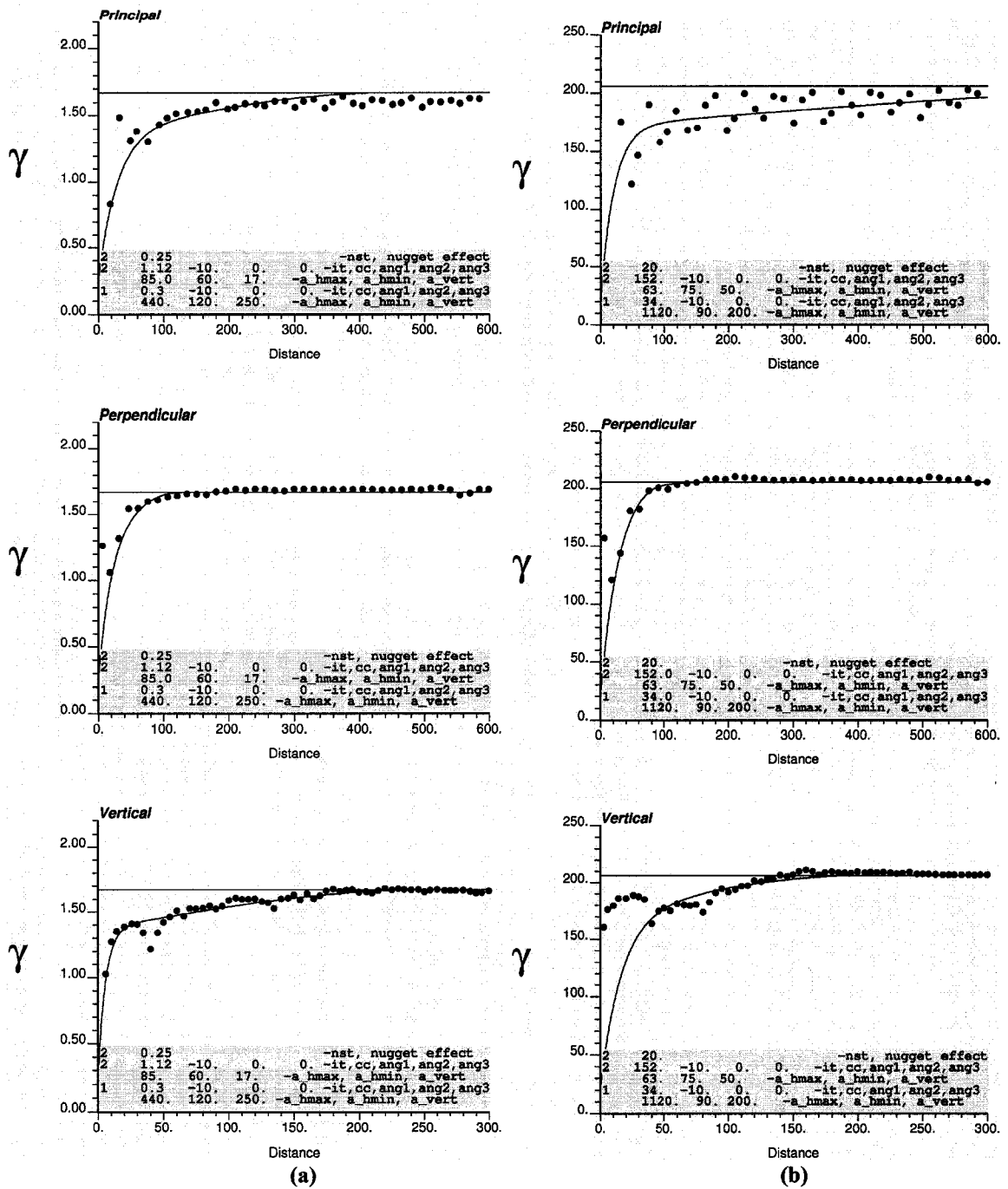


Figure ii: Variogram and fitted model to original exploration data (a) gold data (b) silver data. (-10° azimuth direction as principal (major) direction, 80° azimuth direction as perpendicular (minor) and 90° dip as vertical direction) [3].

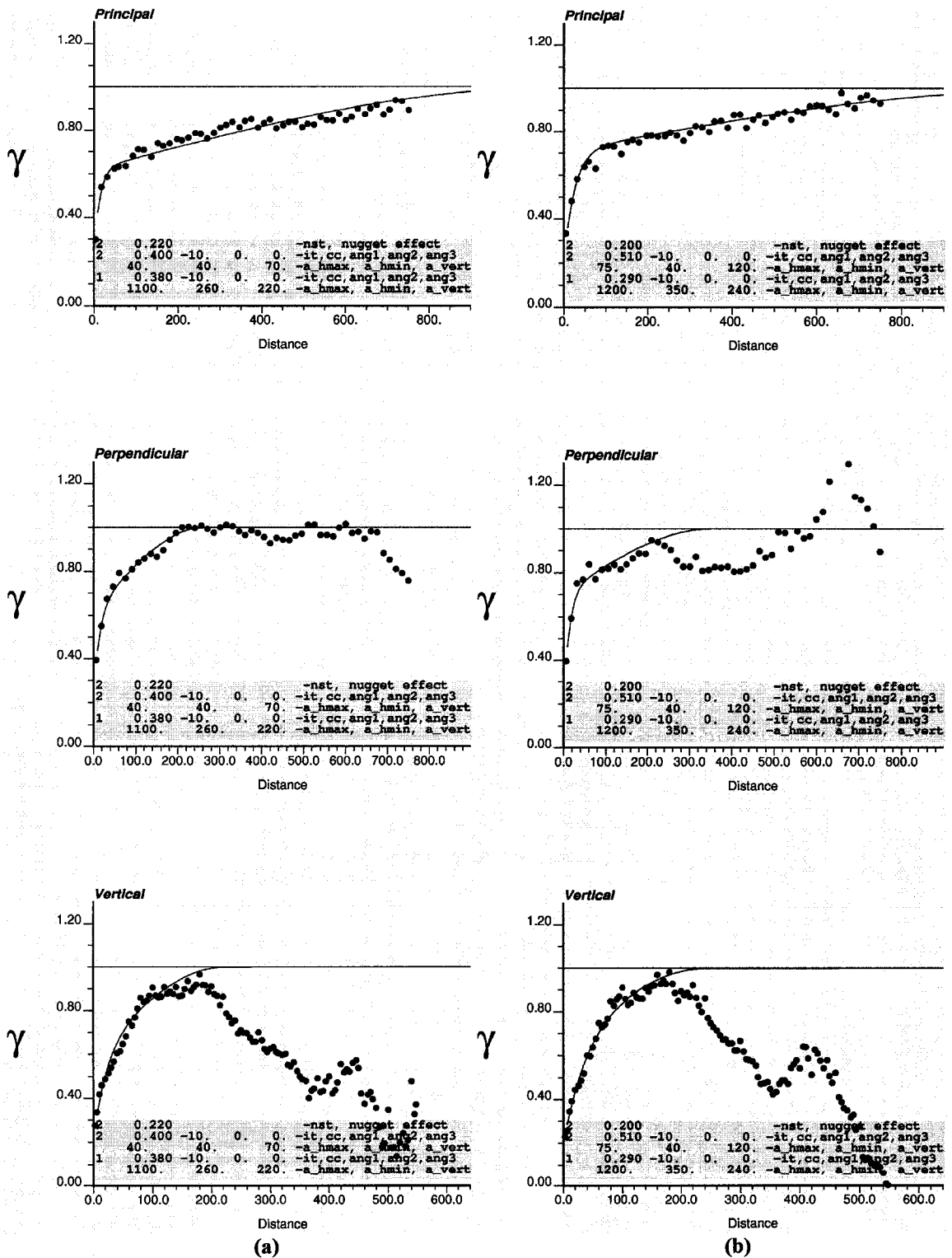


Figure iii: Variogram and fitted model to normal scored exploration data (a) gold data (b) silver data. (-10° azimuth direction as principal (major) direction, 80° azimuth direction as perpendicular (minor) and 90° dip as vertical direction).

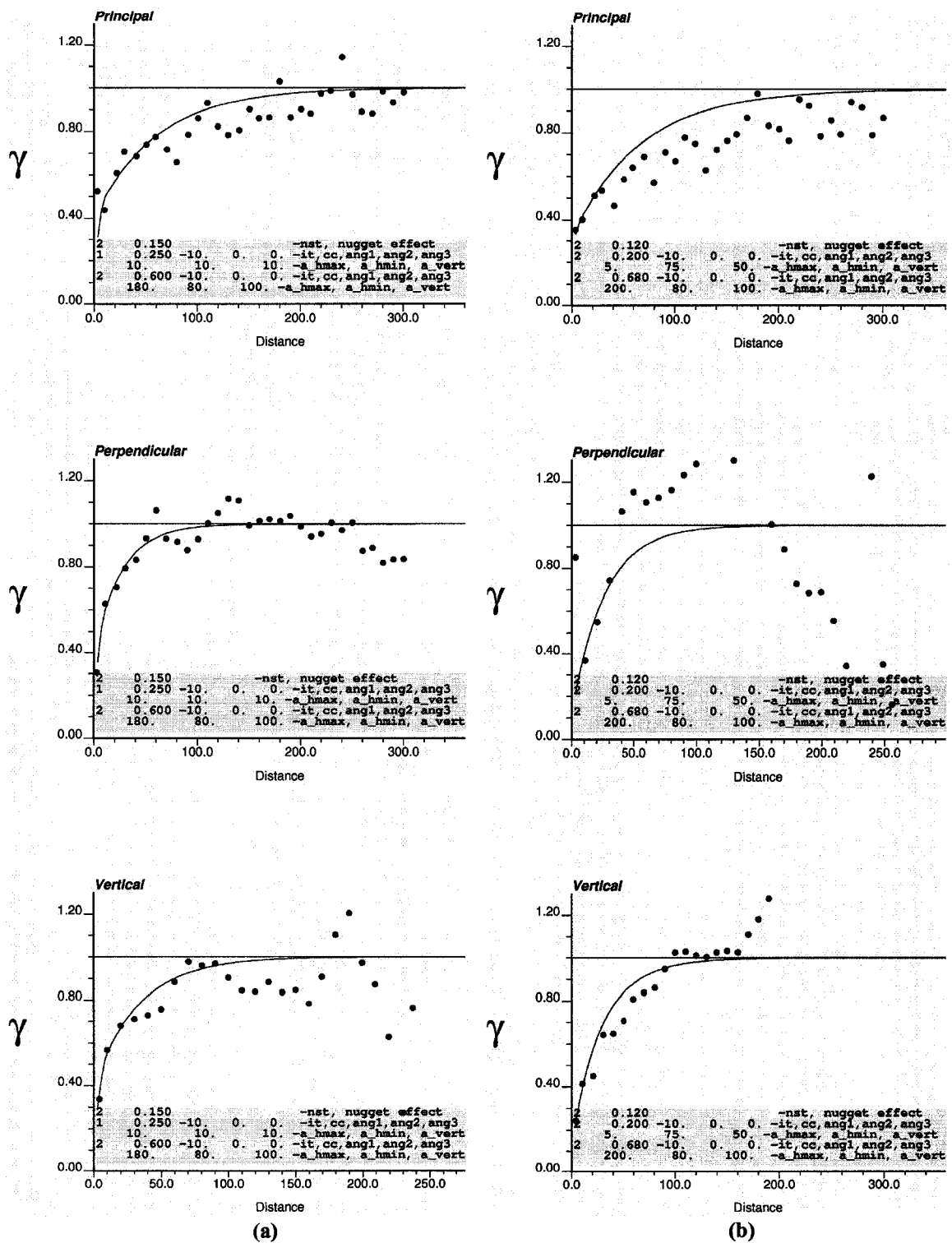


Figure iv: Normal scored variogram and fitted model to exploration data existing within 7m search radius of blasthole data (a) gold data (b) silver data. (-10° azimuth direction as principal (major) direction, 80° azimuth direction as perpendicular (minor) and 90° dip as vertical direction).

APPENDIX IV

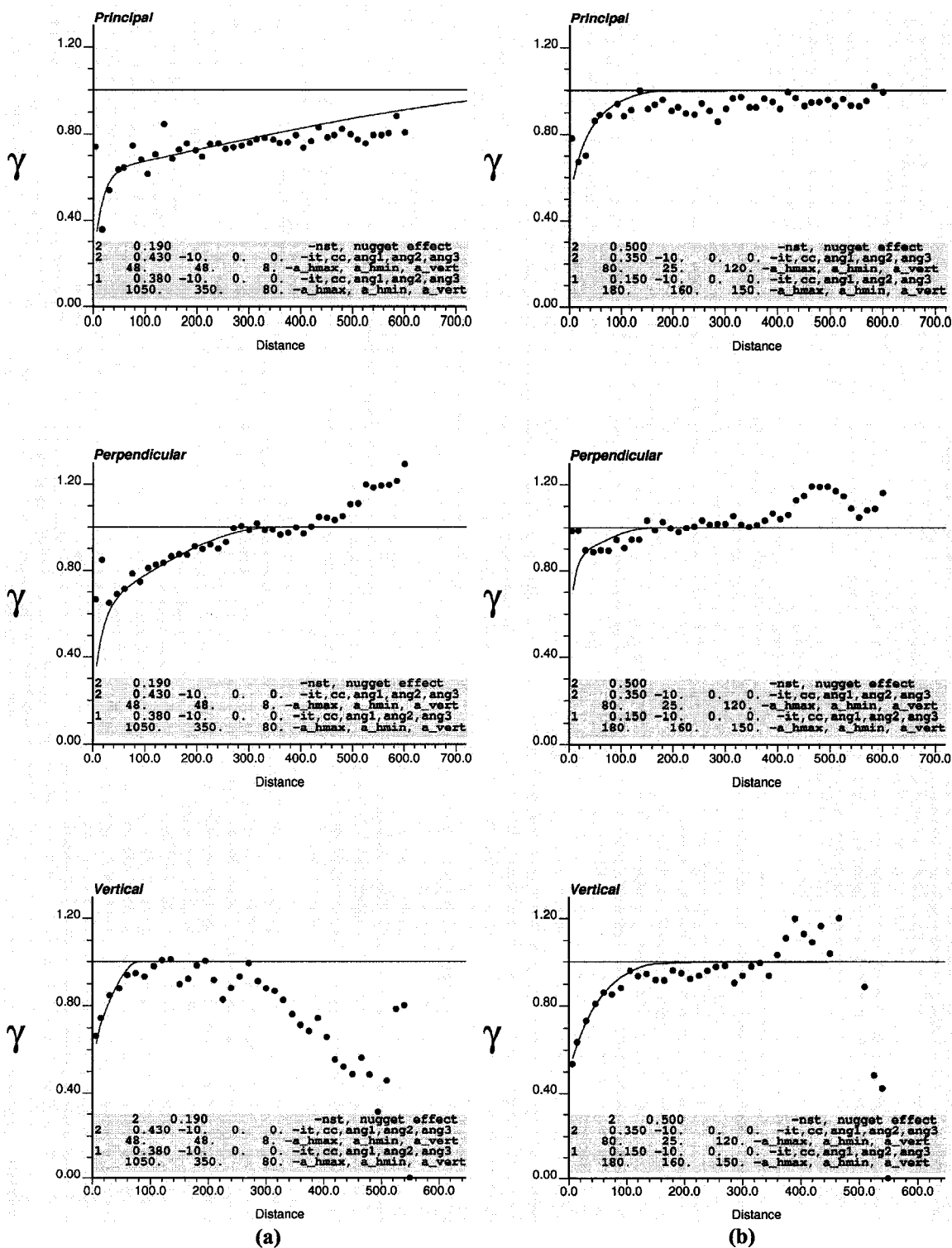


Figure i: Variogram and fitted model to threshold 1 of exploration data (a) gold data (b) silver data. (-10° azimuth direction as principal (major) direction, 80° azimuth direction as perpendicular (minor) and 90° dip as vertical direction).

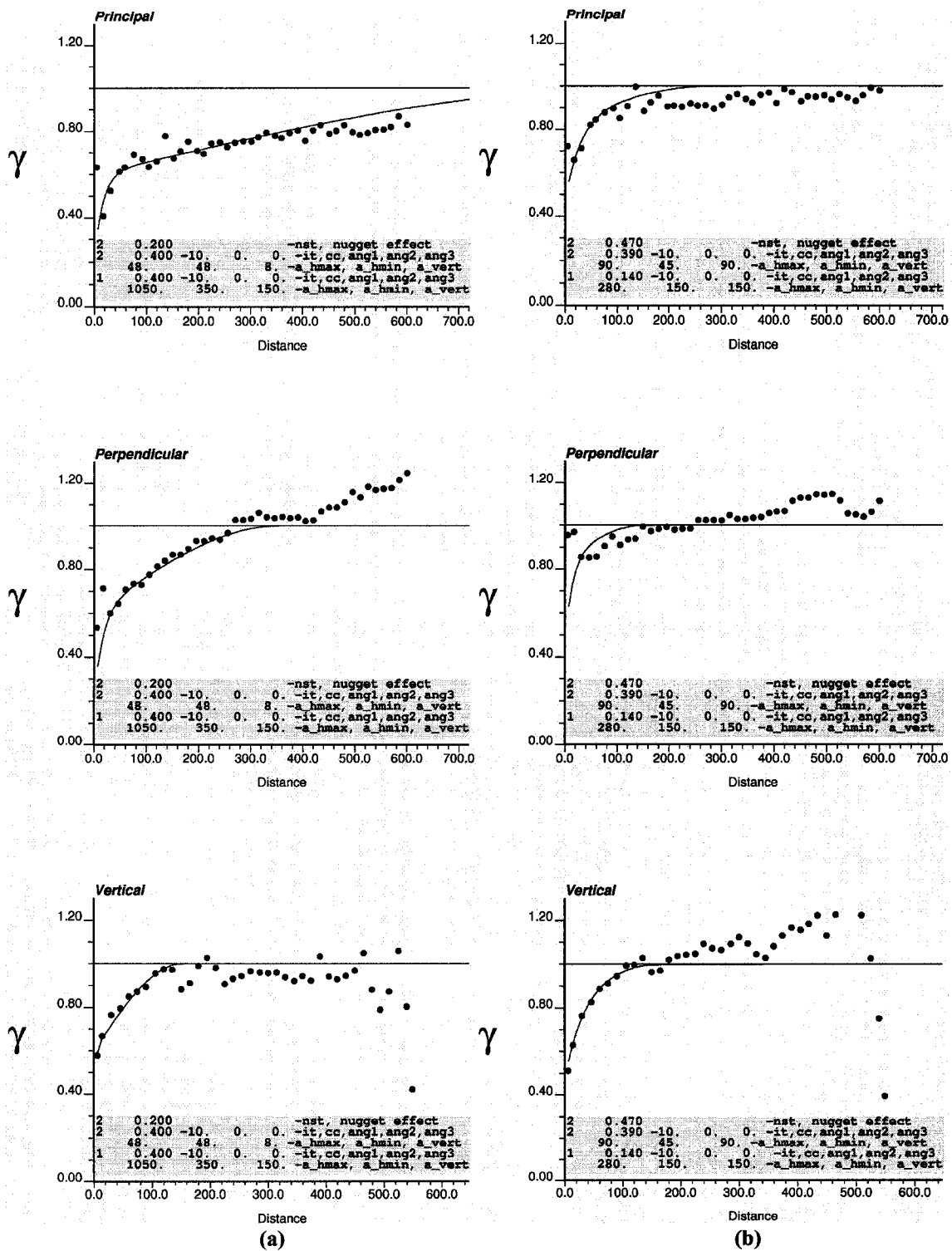


Figure ii: Variogram and fitted model to threshold 2 of exploration data (a) gold data (b) silver data. (-10° azimuth direction as principal (major) direction, 80° azimuth direction as perpendicular (minor) and 90° dip as vertical direction).

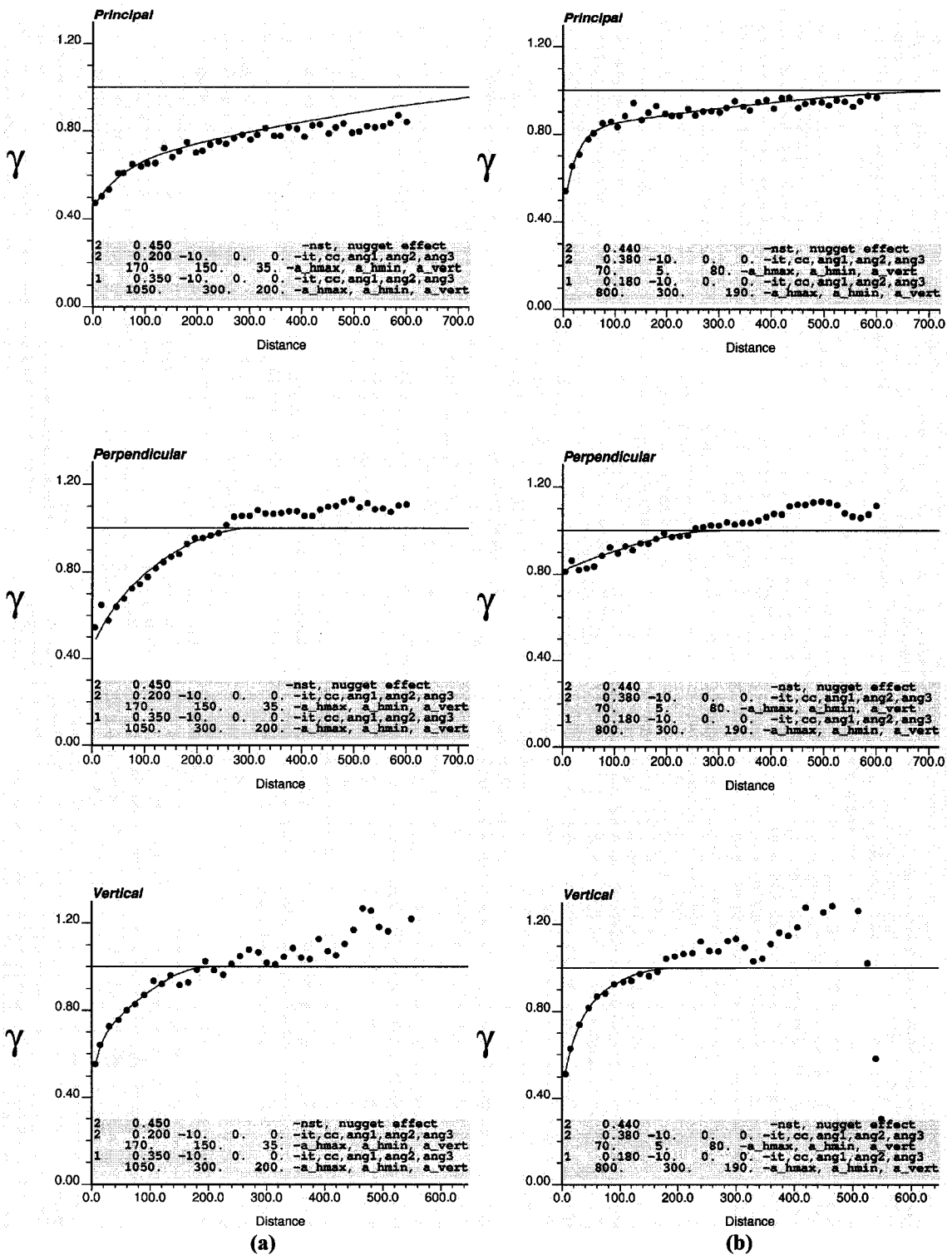


Figure iii: Fitted variogram model to threshold 3 of exploration data (a) gold data (b) silver data. (-10° azimuth direction as principal (major) direction, 80° azimuth direction as perpendicular (minor) and 90° dip as vertical direction).

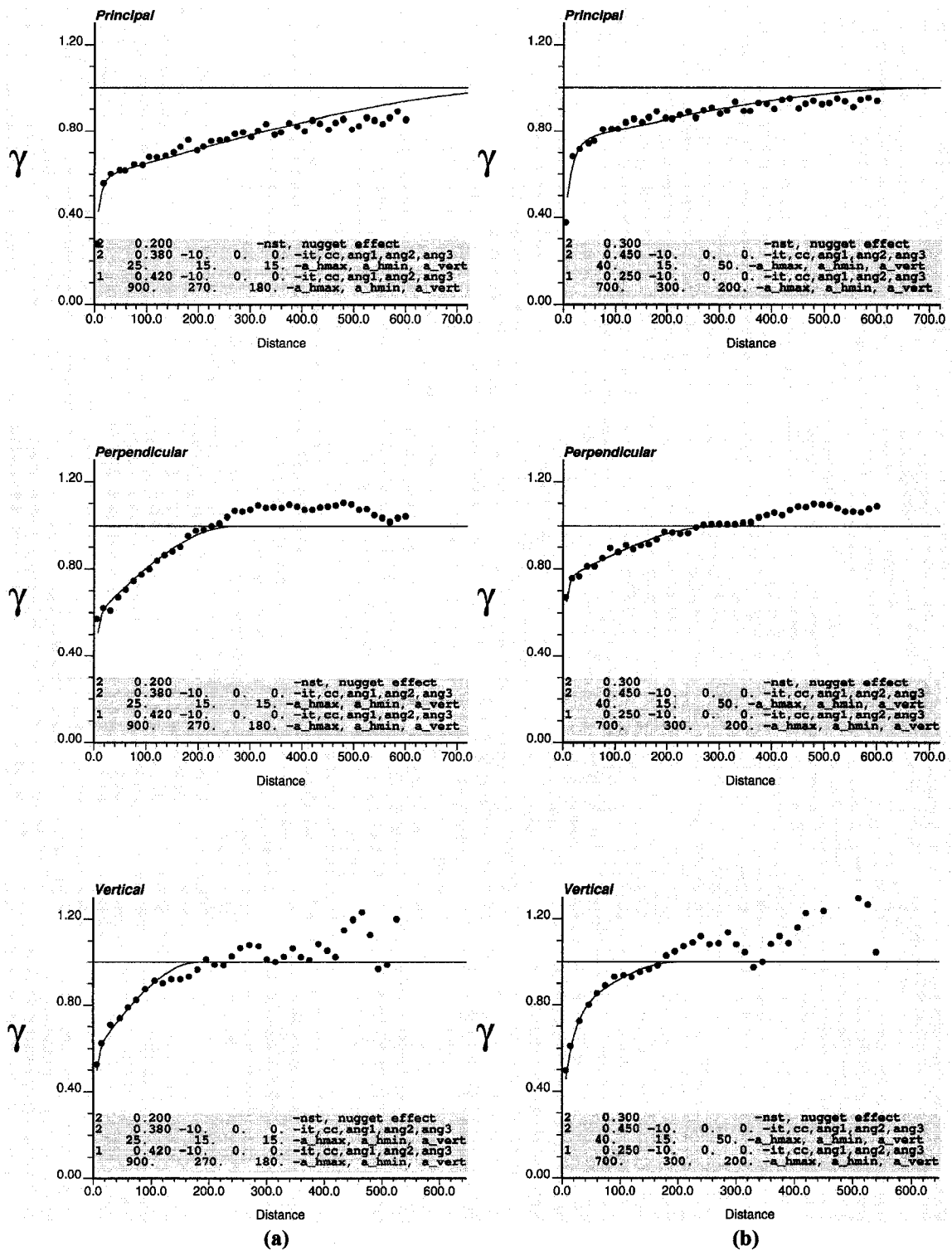


Figure iv: Fitted variogram model to threshold 4 of exploration data (a) gold data (b) silver data. (-10° azimuth direction as principal (major) direction, 80° azimuth direction as perpendicular (minor) and 90° dip as vertical direction).

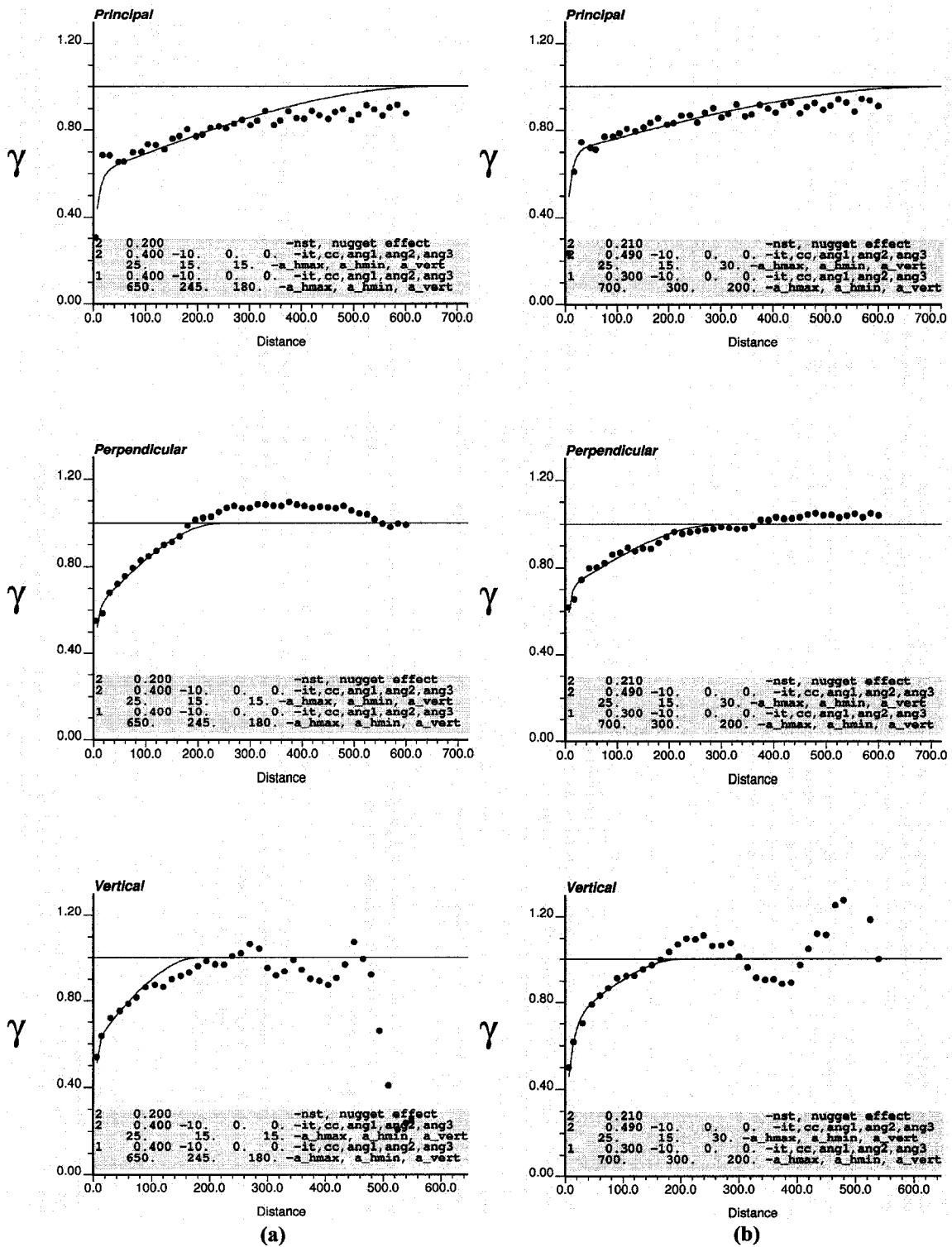


Figure v: Variogram and fitted model to threshold 5 of exploration data (a) gold data (b) silver data. (-10° azimuth direction as principal (major) direction, 80° azimuth direction as perpendicular (minor) and 90° dip as vertical direction).

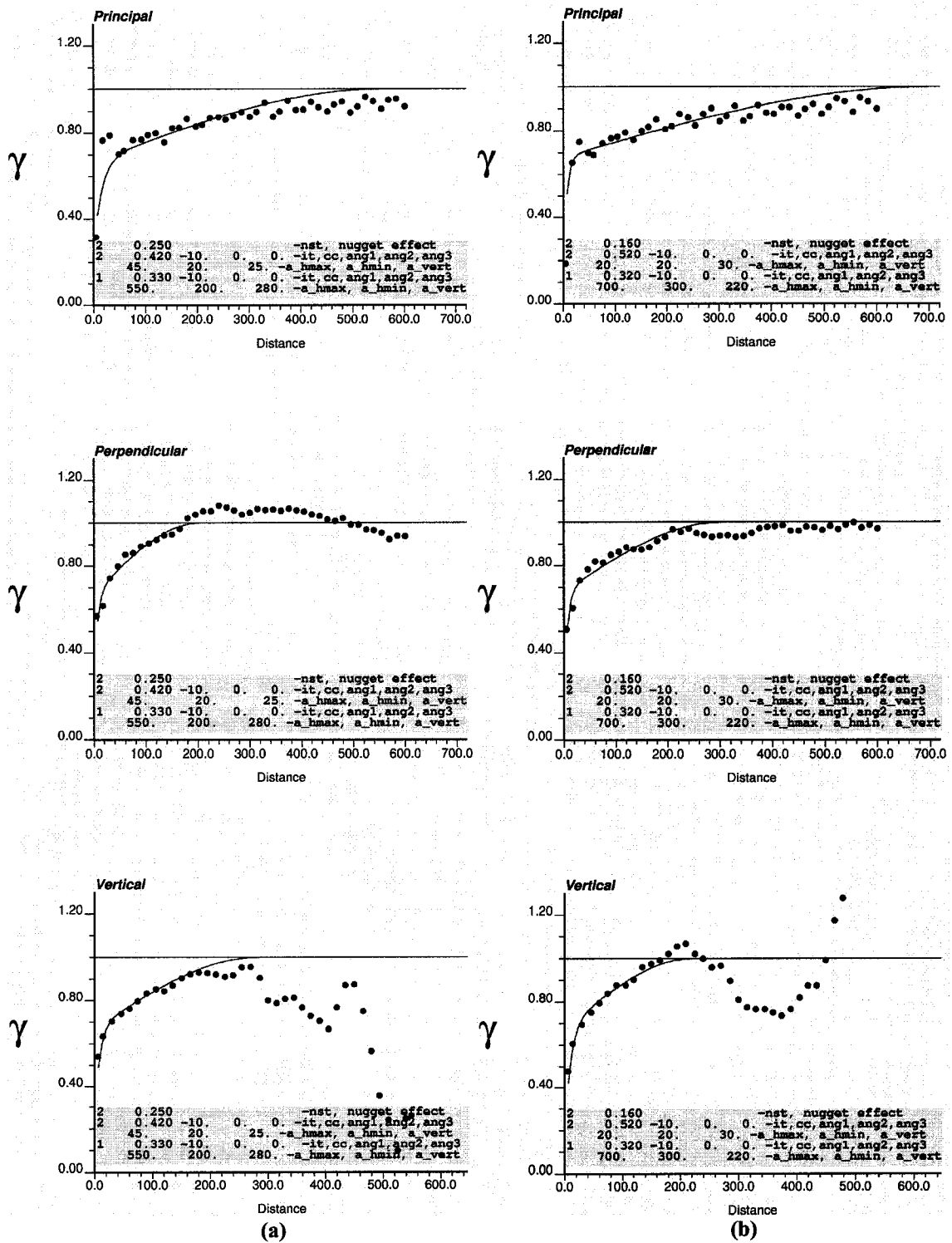


Figure vi: Variogram and fitted model to threshold 6 of exploration data (a) gold data (b) silver data. (-10° azimuth direction as principal (major) direction, 80° azimuth direction as perpendicular (minor) and 90° dip as vertical direction).

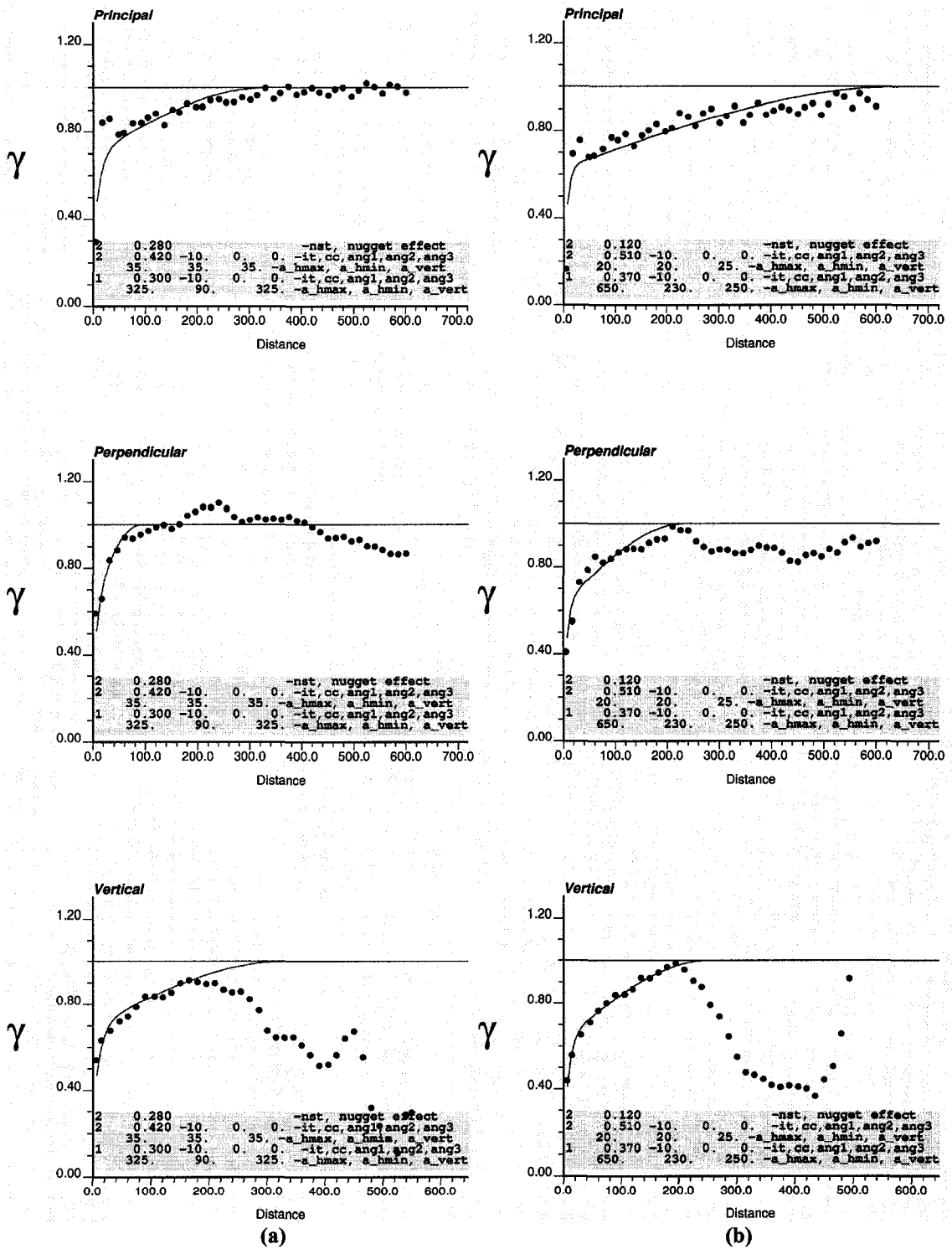
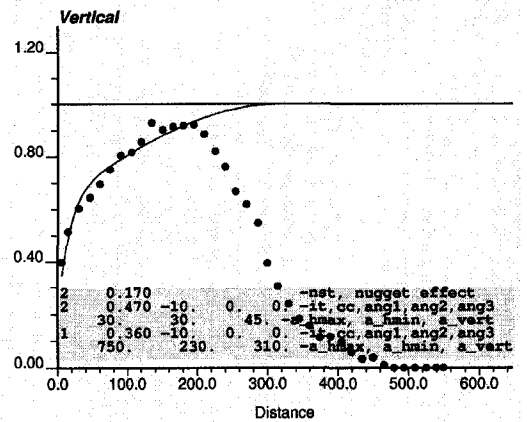
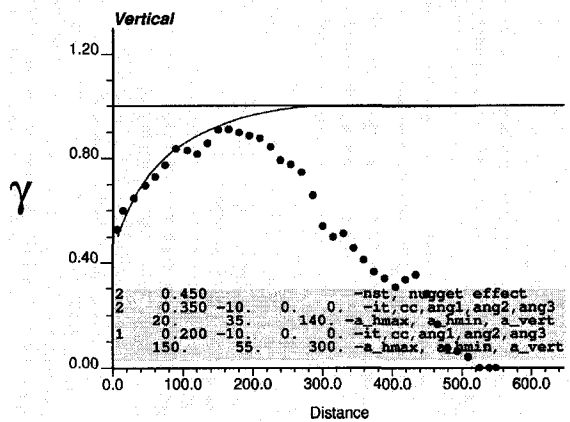
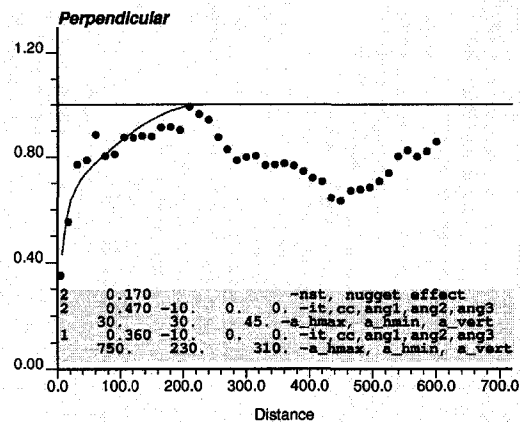
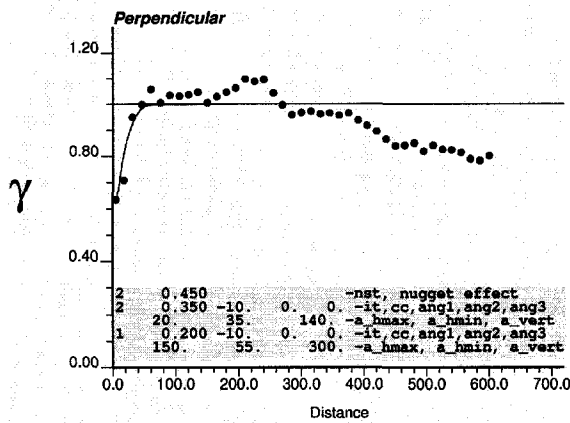
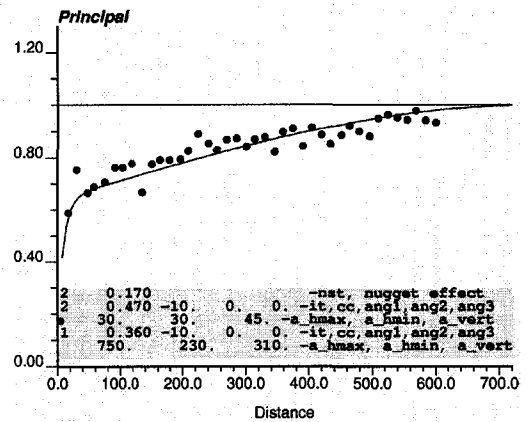
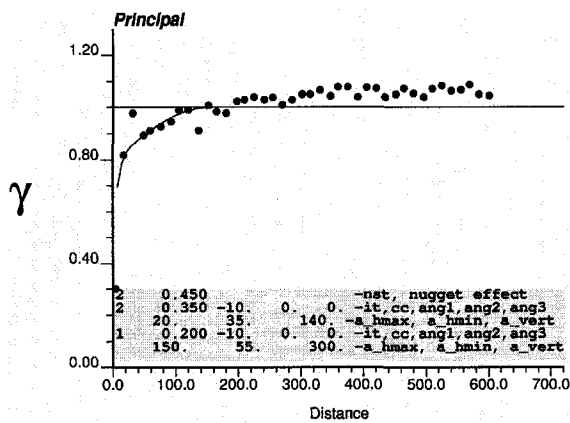


Figure vii: Fitted variogram model to threshold 7 of exploration data (a) gold data (b) silver data. (-10° azimuth direction as principal (major) direction, 80° azimuth direction as perpendicular (minor) and 90° dip as vertical direction).



(a)

(b)

Figure viii: Variogram and fitted model to threshold 8 of exploration data (a) gold data (b) silver data. (-10° azimuth direction as principal (major) direction, 80° azimuth direction as perpendicular (minor) and 90° dip as vertical direction).

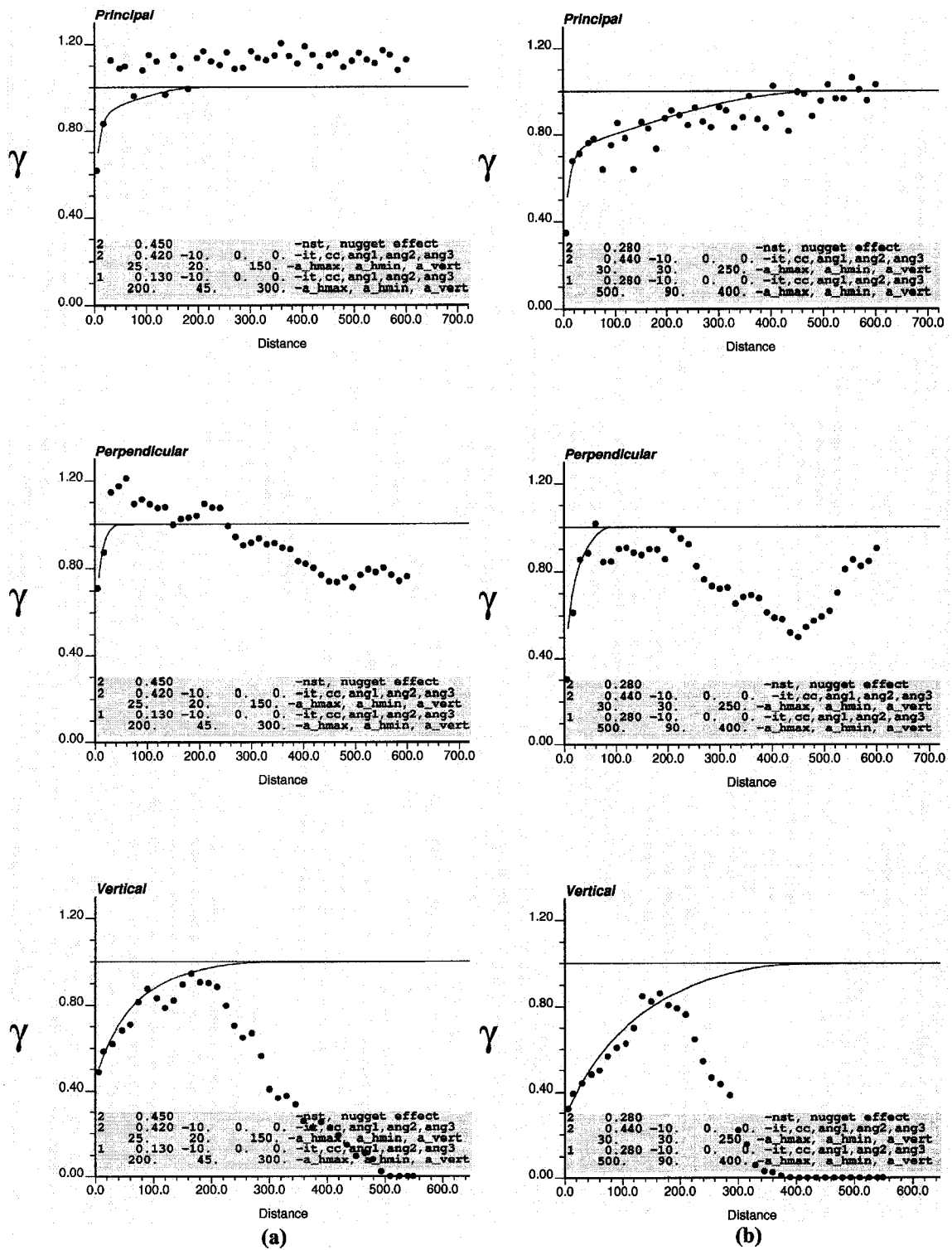


Figure ix: Variogram and fitted model to threshold 9 of exploration data (a) gold data (b) silver data. (-10° azimuth direction as principal (major) direction, 80° azimuth direction as perpendicular (minor) and 90° dip as vertical direction).